PRELIMINARY STUDY OF SECRETOME ANALYSIS FROM *Helicobacter pylori* DUAL RESISTANCE TO CLARITHROMYCIN AND METRONIDAZOLE STRAIN

BY

MISS SUTHATHIP KITTISENACHAI

A THESIS SUBMITTED IN PARTIAL FULFILLMENT OF
THE REQUIREMENTS FOR THE DEGREE OF MASTER OF SCIENCE
(BIOCHEMISTRY AND MOLECULAR BIOLOGY)
FACULTY OF MEDICINE
THAMMASAT UNIVERSITY
ACADEMIC YEAR 2020

PRELIMINARY STUDY OF SECRETOME ANALYSIS FROM *Helicobacter pylori* DUAL RESISTANCE TO CLARITHROMYCIN AND METRONIDAZOLE STRAIN

BY

MISS SUTHATHIP KITTISENACHAI

A THESIS SUBMITTED IN PARTIAL FULFILLMENT OF
THE REQUIREMENTS FOR THE DEGREE OF MASTER OF SCIENCE
(BIOCHEMISTRY AND MOLECULAR BIOLOGY)
FACULTY OF MEDICINE
THAMMASAT UNIVERSITY
ACADEMIC YEAR 2020

THAMMASAT UNIVERSITY

FACULTY OF MEDICINE

THESIS

BY

MISS SUTHATHIP KITTISENACHAI

ENTITLED

PRELIMINARY STUDY OF SECRETOME ANALYSIS FROM *Helicobacter pylori* DUAL RESISTANCE TO CLARITHROMYCIN AND METRONIDAZOLE STRAIN

was approved as partial fulfillment of the requirements for
the degree of Master of Science (Biochemistry and Molecular Biology)

on June 18, 2021

Chairman — Sittiruk Roytrakul
(Sittiruk Roytrakul, Ph.D.)

Member and Advisor — P. Rojpibulstit
(Associate Professor Panadda Rojpibulstit)

Member — Teerakul Arpornsuwan
(Associate Professor Teerakul Arpornsuwan, Ph.D.)

Dean — Dilok Piy
(Associate Professor Dilok Piyayotai, M.D.)

Thesis Title	PRELIMINARY STUDY OF SECRETOME ANALYSIS FROM *Helicobacter pylori* DUAL RESISTANCE TO CLARITHROMYCIN AND METRONIDAZOLE STRAIN
Author	Miss Suthathip Kittisenachai
Degree	Master of Science (Biochemistry and Molecular Biology)
Major Field/Faculty/University	Biochemistry and Molecular Biology Faculty of Medicine Thammasat University
Thesis Advisor	Associate Professor Panadda Rojpibulstit
Academic Years	2020

ABSTRACT

An untreated *Helicobacter pylori* (*H. pylori*) infection is the major cause of gastritis which can develop into stomach cancer. Eradication of *H. pylori* with antibiotics is a simple, non-invasive, inexpensive method that makes it an accessible treatment for the public. Therefore, in the current gastric cancer prevention, this treatment is an effective treatment for gastritis that has been proven to be associated with *H. pylori*. An up-to-date standard treatment for *H. pylori* eradication is in the form of triple therapy: two antibiotics (clarithromycin and metronidazole) and a proton pump inhibitor. However, current antibiotic treatments for *H. pylori* infection are less effective due to increased rates of drug resistance. This occurs due to an unnecessary overuse of antibiotics, antibiotics abuse of patients, and taking unnecessary medications for too long. To date, the prevalence of drug resistance from clarithromycin, metronidazole, as well as concomitant resistance to clarithromycin and metronidazole (Cla-R, Mtz-R, Cla/Mtz-R, respectively) in the eradication of *H. pylori* remains high worldwide. For a better understanding and exploration of a new protein relevant to treatment options for *H. pylori* bacteria, this research, hence, aimed to study proteins secreted from Cla/Mtz-R, Cla-R, Mtz-R, *H. pylori*-associated gastritis strains. By working with proteomic

study (in-solution digestion combined with nanoLC-MS/MS), 592 expression proteins were detected, of which 590, 583, 582, and 578 proteins were identified from Cla/Mtz-R, Cla-R, Mtz-R, and Sensitive strains (Sen-S), respectively. After identifying the biological activity of proteins through protein database searches (PANTHER software version 15.0), These proteins are responsible for the cellular processes such as the metabolic process (41%), cellular process (27%), process localization (10%), etc. Based on the Venn diagram, there are 23 different proteins that overlap between the four strains. In addition, by analyzing the heat maps of these overlapping proteins, the results showed that the Cla/Mtz-R strains exhibited the most differentiated protein expressions, while the less different expressions were found in the Sen-S strains. When considering the overlapped proteins based on the Sen-S strains, nine proteins were identified. In addition, the prediction between proteins- proteins and proteins- antibiotics (metronidazole and clarithromycin) interaction through the STITCH database has been studied. The results revealed two possible central role proteins: rpoBC (found in Cla/Mtz-R, Cla-R, and Sen-S strains, but not found in Mtz-R strains) and FBPAII (found in Sen-S strains only). To quantitatively determine the mRNA expression level of *rpoB* and *fba* genes, quantitative reverse transcription PCR analysis was then performed. Their primers were designed from *H. pylori* 26695 template DNA by Primer 3 web version 4.1.0. Compare with the Sen-S strain, the result showed a down-regulation of *rpoB* from all three antibiotics strains, though its secreted protein was identified in Cla/Mtz-R, Cla-R, and Sen-S strains, but not in Mtz-R strains. This suggests the relationship between *rpoB* expression and metronidazole sensitivity. On the other hand, an up-regulation of *fba* gene mRNA expression level was observed from all three strains used in this study. This suggests inconsistent expression levels between protein (FBPAII) and mRNA (*fba*) that may be involved in the mechanism of antibiotic susceptibility and resistance to *H. pylori*. In conclusion, this is the first report that demonstrates the secretome analysis from clarithromycin, metronidazole, and dual resistance *H. pylori*-associated gastritis compared to the sensitive strain. Moreover, it also shows the association of rpoBC and FBPAII with antibiotic susceptible *H. pylori*-

associated gastritis. However, the exact mechanisms of the two proteins involved in keeping the pathogens susceptible to antibiotics remain to be studied in the future.

Keywords: *Helicobacter pylori*- associated gastritis, antibiotic- sensitive, antibiotic resistance, clarithromycin, metronidazole, dual resistance to metronidazole and clarithromycin, in-solution digestion, proteomic study

ACKNOWLEDGEMENTS

This thesis will never be successful without the valuable helps from these people.

Firstly, I wish to thank you my advisor. Associate Professor Panadda Rojpibulstit, who provided the great opportunity to study in this field, give me many valuable advice and push me forward to successful in Master study. Next, I would like to thank you Dr. Sittiruk Roytrakul at National Center for Genetic Engineering and Biotechnology (BIOTEC), National Science and Technology Development Agency (NSTDA) who gave on opportunity to me in this study and advised many valuable in the part of proteomics and others. I deeply appreciated to Function Proteomics Technology lab, National Center for Genetic Engineering and Biotechnology (BIOTEC), National Science and Technology Development Agency (NSTDA) and all staffs for bearing laboratory and all facilities to do this thesis.

In addition, I grateful acknowledge to Associate Professor Teerakul Arpornsuwan, committee in the thesis for good advice and make a recommendation about my work. I deeply appreciated to Faculty of Medicine, Biochemistry and Molecular Biology, Thammasat University, Thailand and all staffs for bearing laboratory and all facilities to do this thesis.

Beside above, I wish to thank you Prof. Dr. Ratha-korn Vilaichone, who supports the clinical culture and all facilities to do this thesis. I thankful appreciate Miss Pornpen Gamnarai for all helping with advice and operate in the part of cell culture.

Along my study life, I must thank you all teachers who improved my skill and knowledge since I was child until today. I would like to thanks all friends that help and take care during my study. Most of all, I would like to deep appreciate to my beloved family for all their supports in my life.

Miss Suthathip Kittisenachai

TABLE OF CONTENTS

LIST OF TABLES

LIST OF FIGURES

LIST OF ABBREVIATIONS

Symbols/Abbreviations	Terms
°C	Degree Celsius
ACN	Acetonitrile
Bp	Base pair
cDNA	Complementary deoxyribonucleic acid
Ct	Threshold cycle
DNA	Deoxyribonucleic acid
DTT	Dithiothreitol
IAA	Iodoacetamide
Kb	Kilobase
kDa	Kilo Dalton
mg	Milligram
ml	Milliliter
mM	Millimolar
mRNA	Messenger ribonucleic acid
MS	Mass spectrometry
PCR	Polymerase chain reaction
pH	Power of Hydrogen ion concentration
RNA	Ribonucleic acid
rRNA	Ribosomal ribonucleic acid
TOF	Time of Flight
µg	Microgram
µl	Microliter

CHAPTER 1
INTRODUCTION

1.1 Introduction

A gram-negative spiral bacterium *Helicobacter pylori* (*H. pylori*) is discovered by Barry Marshall and Robin Warren in 1983 (1), (2), (3). It is a major cause of gastritis and, if chronically infected, can induce gastric cancer or MALT lymphoma. Therefore, when an infection is detected, the treatment with a specific antibiotic can reduce the incidence of such serious diseases. Currently, the regimen that regularly uses for *H. pylori* eradication is triple therapy which is consisting of proton-pump inhibitors in combination with clarithromycin (Cla) and metronidazole (Mtz) or amoxicillin. This regimen relieves stomach ulcers and also helps prevent cancer (4). Though up to 90% of patients have recovered from the infection, the effectiveness of this treatment regimen is reduced due to increased antibiotic resistance of *H. pylori* (5). Over the past 10 years, Kuo (2017) et al. have reported significant increases (from 7% to 21% and 36% to 45%, respectively) of *H. pylori* resistance to Cla (Cla-R) and Mtz (Mtz-R) in the Asia-Pacific region (6). While the prevalence of Cla-R and Mtz-R in ASEAN countries still common (7). However, the prevalence of Cla-R and Mtz-R found in Thailand was 14% and 36% respectively (7). Additionally, for dual resistance (Cla/Mtz-R), Lu et al. have reported a 10% prevalence in 2019 (8). As a result, if the mechanism of drug resistance could be better understood, it would likely lead to better therapeutic development in *H. pylori*-resistant patients.

Clarithromycin has an antimicrobial mechanism by binding to 23S rRNA, thereby disrupting the translocation process and ultimately inhibiting protein synthesis. Cla-R *H. pylori* has been identified as one of a group of antibiotic-resistant bacteria found critical by the World Health Organization (WHO) in 2017. (9). The mechanism of Cla resistance involves (1) mutations A2142G or A2143G in the 23S mRNA (domain V) and (2) the intracellular decrease of Cla concentrations via the outflow of *H. pylori* RND efflux (10), (11), (12), (13). While metronidazole is a derivative of nitroimidazole,

commonly used in the treatment of both anaerobic bacteria and parasites. Its mechanism of action relies on the generation of toxic free radicals on Mtz-prodrug (at the nitro group), resulting in the Mtz-active drug. The enzyme that helps to convert it into an active form is NAD(P)H-flavin oxidoreductase (encoded by the *frxA* gene) or NADPH nitroreductase (encoded by the *rdxA* gene) (14), (15), (16). The active drug Mtz can induce the production of several strong oxidizing agents, including hydrogen peroxide (H_2O_2), superoxide radical ($O_2^{\cdot-}$), and a hydroxyl radical ($OH^{\cdot}$). These strong oxidizers eventually destroy the bacterial DNA, resulting in the inhibited synthesis of nucleic acids. The two most common Mtz mechanism are (1) the mutations (missense or frameshift) in the *rdxA* and *frxA* gene and (2) the mutation of the gene *HP1027* which is encoding ferric (Fur) uptake regulator protein (C78Y, P114S; *Fur* mutant) (17), (18), (19), (20). The latter mutation decreases Fur protein expression, resulting in increased expression of the superoxide dismutase enzyme. This event leads to a reduction in the number of reactive oxygen species (ROS), thus makes *H. pylori* resistant to the action of Mtz (21). From all of the above, most of the knowledge gained from studies through the molecular techniques (22), (23). In addition, the use of proteomics techniques to examine the comparison of protein expression between interested samples is another effective method. To date, according to a review of the literature, proteomics study is popular in the study of proteins involving in antibiotic resistance of *H. pylori* (24), (25), (26), (27), (28).

Protein analysis using proteomic techniques is a study to identify and quantify proteins under specific conditions by using mass spectrometry (29), (30). The framework of a common procedure for protein identification through mass spectrometry is (1) cell fractionation (according to the needs of which proteins part are studied), (2) 1-dimension or 2-dimension gel electrophoresis, and (3) enzymatic protein digestion. The peptides were then separated by their chemical and physical properties by LC-MS/MS. This was followed by peptide identification and peptide analysis and comparison with a standard database. (31), (32). This technique has two main approaches: top-down and bottom-up proteomic analysis. For the first approach, the advantage is to achieve a more complete protein sequence. However, it is not

suitable for studying large protein fractions due to detection and isolation limitations (33). In contrast, a bottom-up approach is easier for high throughput analysis. It is the most popular approach today (34). In addition, two of the most popular methods of protein digestion in preparation for mass spectrometry are: in-gel digestion (after 1 or 2-dimension gel electrophoresis) and in-solution trypsin digestion, both have different advantages. (30), (35). The advantages of the pre-fractionation of samples performed in the in-gel digestion method are efficiency and reproducibility. While the pros of in-solution digestion is that it has a simpler sample preparation procedure, less time working and need fewer samples (36), (37). Therefore, the experiments in this study were designed using the proteomics approaches with an in-solution digestion protocol.

From the literature review, *H. pylori* proteome analytical studies were conducted exploring proteins under various conditions, for example, under spiral and coccoid patterns, under oxidative stress or from *H. pylori* strains that cause the disease (clinical strain) (38), (39). Diseases caused by *Helicobacter pylori* can range from superficial gastritis to gastric atrophy, intestinal metaplasia, dysplasia, and eventually develop into gastric adenocarcinoma or mucosal-associated lymphoma (MALT) (40), (41). Therefore, gastritis is the earliest lesion that promotes tissue changes, cell remodeling, and morphological modifications. So, the study of the secreted protein from *H. pylori*-associated with gastritis strains are of particular interest. However, limited studies have been performed to analyze protein profile via proteomic study of *H. pylori* strains that are associated with gastritis (42), (43), (44). In addition, a smaller number of studies were also found in comparative proteome analyzes comparing the secreted proteins from antibiotic-susceptible and antibiotic-resistant clinical strains (45), (26), (25). While no proteomic studies were found in *H. pylori*-associated gastritis strains of antibiotic-susceptible, Cla-resistant, Mtz-resistant, and both Cla and Mtz dual resistant. Therefore, this research aims to study the protein secreted by Cla/Mtz-R, Cla-R, and Mtz-R of *H. pylori*-associated gastritis strains compare to the secreted proteins from Sen-S of *H. pylori*-associated with gastritis strains.

The proteomic techniques performed in this study including in-solution digestion and protein quantitation and identification through nanoLC-MS/MS. Data analysis via bioinformatics tools such as DeCyder™, Mascot, MeV, PANTHER, Venn diagram, and STITCH software. Proteins of interest were subsequently quantitated mRNA level by quantitative realtime-PCR analysis. All of these data will provide evidence of secreted proteins from Cla/Mtz-R, Cla-R, Mtz-R, and Sen-S of *H. pylori*-associated with gastritis strains. A prominent benefit of this work seems to be the recognition of new proteins that result in other mechanisms involved in drug resistance. This is the first study to reveal the proteomic profiles of secreted proteins from Cla/Mtz-R, Cla-R, and Mtz-R compare to Sen-S, of *H. pylori*-associated gastritis strains.

1.2 Objectives

This study aimed to

1. clarify amount and type of proteins secreted from clarithromycin and metronidazole dual resistance *H. pylori* strains (Cla/Mtz-R dual resistance *H. pylori*-associated with gastritis strains)

2. compare amount and type of proteins secreted from Cla/Mtz-R dual resistance *H. pylori* strains with those from clarithromycin resistance *H. pylori* strains (Cla-R *H. pylori*-associated with gastritis strains)

3. compare amount and type of proteins secreted from Cla/Mtz-R resistance *H. pylori* strains with those from metronidazole resistance *H. pylori* strains (Mtz-R *H. pylori*-associated with gastritis strains)

4. compare amount and type of proteins secreted from Cla/Mtz-R dual resistance *H. pylori* strains with those from antibiotic sensitive *H. pylori* strains (Sen-S *H. pylori*-associated with gastritis strains)

1.3 Beneficiaries

This is the first study about the quality and quantity of secreted protein from clarithromycin and metronidazole dual resistance, clarithromycin resistance, metronidazole resistance and sensitive *H. pylori*-associated with gastritis strains (Cla/Mtz-R, Cla-R, Mtz-R, Sen-S). The results obtain from this study may provide information to understand the differential expressed proteins in each strain.

Conceptual Framework

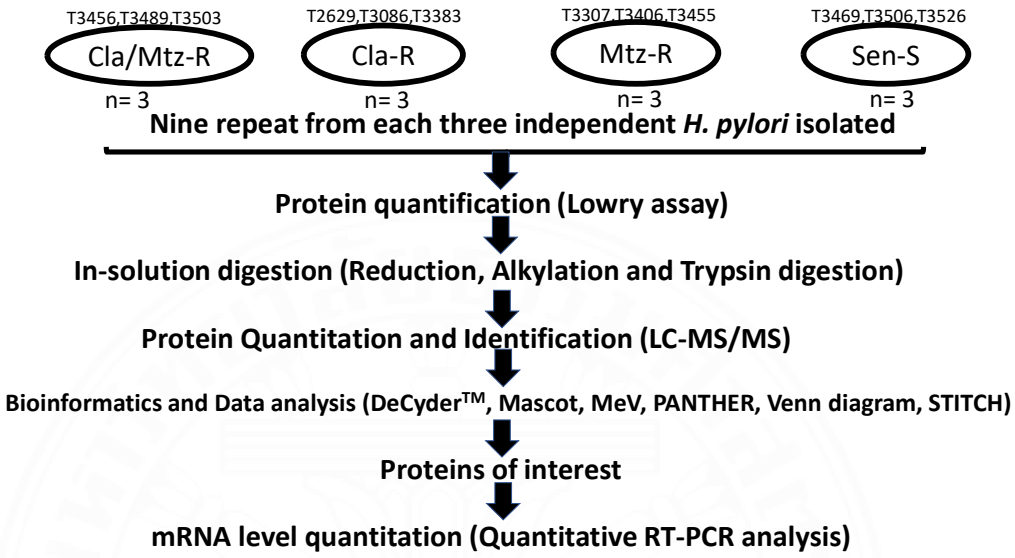

Figure1.1 A conceptual framework of this study

CHAPTER 2
REVIEW OF LITERATURE

2.1 An overview of *Helicobacter pylori*

H. pylori was first reported as a spiral bacterial species from human stomach by Barry J. Marshall and J. Robin Warren for 20 years ago (46). Subsequent studies have shown that bacteria can colonize the human gut, causing inflammation of the gastric mucosa and play the major role in gastritis, peptic ulcer, gastric adenocarcinomas, and gastric mucosa-associated lymphoid tissue (MALT) lymphomas. These provide insights into the pathogenesis of chronic gastritis and contribute to important clinical changes in the management of *H. Pylori*-associated diseases. As a result of these pioneering contributions, Prof. Barry Marshall and Robin Warren were awarded the 2005 Nobel Prize in Physiology and Medicine for "their discovery of *Helicobacter pylori* and their role in gastritis and peptic ulcer disease".

H. pylori is a spiral shaped Gram-negative, microaerophilic bacterial pathogen. Due to the morphology of these organisms similar to those of *Campylobacter*, they were therefore initially considered to be *Campylobacter*-like organisms or *Campylobacter pylori*. Subsequently, with scientific reports published in leading research journals identifying morphological, biochemical and genetic differences, *Campylobacter pylori* was assigned a new genus and species name, *Helicobacter pylori* (47). In addition to the helical shape, *H. pylori* contains 4 to 7 flagella, which are essential for the motility of the bacterium and penetrate the mucous layer of the stomach and thereby cause infection (48). After bacterial infection, *H. pylori* induces inflammation of the gastric mucosa. Without the successfully treated for *H. pylori* infection, the chronic infection will cause atrophy of the mucous membranes (atrophic gastritis), resulting in intestinal metaplasia which are considered to be precursors of gastric cancer (49), (50). Therefore, *H. pylori* has been classified by International Agency for Research on Cancer (IARC), a subordinate organization of the World Health Organization (WHO) as a group 1 carcinogen (definite carcinogen) in 1994

for its association with gastric cancer (51). However, several evidences suggest that the transition from intestinal metaplasia to gastric cancer is the result of *H. pylori* infection combined with environmental risk factors (such as diet) and genetic factors (52), (53), (54), (55). Therefore, identifying which proteins that are secreted by the *H. pylori* in the early stages after infection, i. e. in gastritis, can help to better understand the mechanisms of infection and pathogenesis. This could provide valuable information for the development of new antibiotics to better eradicate *H. pylori* bacteria in the near future.

2.2 Risk factors and prevalence of *H. pylori* infection

As *H. pylori* infection is a global public health problem, in order to reduce the prevalence of infection, a number of scientific studies reported data on the infection risk factors. Factors reported for *H. pylori* infection included lower socioeconomic status, poor hygiene, inadequate sanitation, congested living conditions, smoking, food consumption and family history of gastric disease (56), (57), (58), (59), (60), (61). The main routes of transmission are oral-to-oral and fecal-to-oral intrafamilial transmission (62). The prevalence of *H. pylori* infection varies by country and geographic region, geographic area, age, race, socioeconomic status, and ethnic group. According to a meta-analysis study on the global prevalence of *H. pylori* infection in 2017, the region with the highest reported HP prevalence was Africa and Western Asia (70.1% and 66.6%, respectively) (63). Meanwhile, regions with low reported prevalence of *H. pylori* infection are North America, Oceania, and Western Europe. (37.1%, 34.3% and 24.4%, respectively). Although *H. pylori* prevalence has generally decreased in recent years in developed countries such as the United States and Australia. But it is found to be high among indigenous population of both countries (63), (64). In Thailand, the prevalence of *H. pylori* infection is 45.9%, mainly in the northeastern and northern regions (65), (66), but less common in the south. This could be explained both by the lower socioeconomic status and poor hygiene (as mentioned above). Moreover, it also seems to be related to the spiciness of the local cuisine

consuming regularly, which varies from region to region. For example, in the South, people are more likely to eat spicy food (with Southern curry paste that is very spicy) than in the North. This spicy regional cuisine is correlated well with the previously reported that a diet of spicy chili and garlic play a protective role against *H. pylori* infection (67). In addition, the infection rates in Thailand are also related with ages. It has been found that infection rates of the age range of 5-9 years are 17.5% and increased to 55% over the age of 30 years and up to 75% in the age range 30-49 years (68), (69).

2.3 Pathogenesis of *H. pylori* infection

Though, the majority of *H. pylori* infected patients are asymptomatic, but infection with this bacterial pathogen is associated with an acute or chronic gastritis. The primary site of infection is usually the mucous layer of the antrum, which is the less acidic part of the human stomach. After infection, it causes a local inflammation of the stomach known as gastritis. However, only 10-20% of those infected patients develop peptic ulcer disease, while only 0.5-2% result in gastric adenocarcinoma (70). The varying severity of the disease following bacterial infection mentioned herein depends on three factors: (a) the virulence of the infecting *H. pylori* strains, (b) the host genetics variant, and (c) coexisting factors such as smoking and diet. In addition, a diagram of the pathogenetic process of *H. pylori* infection has been clarified which is described in detail below.

2.3.1 Penetration of gastric mucus

The initial stage of *H. pylori* colonization process after its infection in the host gut begins with *H. pylori* penetration through the gastric mucus. In the normal acid-secreting stomach, *H. pylori* uses multiple sheathed unipolar flagella, with a movement like a corkscrew, to pass through the mucous barrier to reach the underneath epithelial surface of the stomach. The way *H. pylori* can descend to adhere the gastric surface is based on a number of factors such as through the function of the thioredoxin system, which specifically reduces the disulfide bond of the mucin and therefore disrupt the oligomeric structure of mucin. The process results in the mucin loosening, so the bacteria can swim through it. The other one is the urea utilization system through the function of ureases enzyme to increase the local pH (71), (72). The urease enzyme, an essential colonization factor of *H. pylori*, is expressed in both the cytoplasmic part and the surface area of the bacteria (73), (74). During the penetration processes, the surface-expose urease of *H. pylori* catalyzes the hydrolysis of urea (which is abundant in gastric juices) to carbon dioxide and ammonia, therefore, pH in the microenvironment is increased. As a result, the viscosity of the gastric mucosa decreases due to its viscosity property increases at strongly acidic pH (75), (76), (72), (77). This modifies the mucus to be less gel-like properties, which enables the bacteria to use multiple sheathed unipolar flagella to propel itself through the gastric mucus to colonize at the epithelial surface more quickly as shown in the figure 2.3.1 (78).

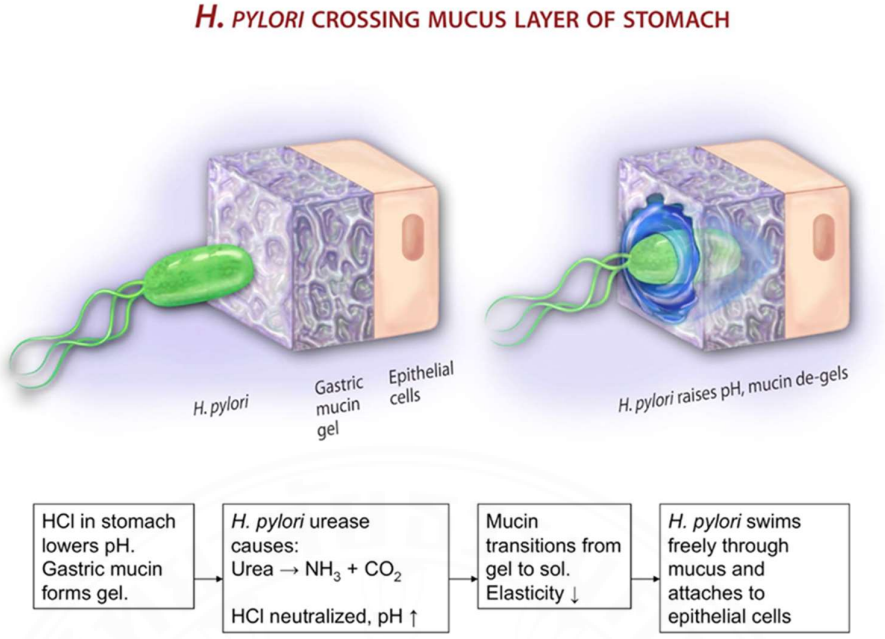

Figure 2.3.1 Illustration of a possible mechanism by which *H. pylori* moves through gastric mucosa to colonize the epithelial surface via exogenous urea secretion that results in gel to sol transition of mucin. It is therefore easier for the *H. pylori* to be able to pass through the mucus in the stomach to colonize at the epithelial surface [(76)].

2.3.2 Acid acclimation

After successfully penetration through the gastric mucosa and then reach the gastric epithelial surface, *H. pylori* colonization process is continued by neutralizing the acidic pH in the gastric environment through an acid acclimation mechanism. Acid acclimation is *H. pylori*'s unique ability to survive in an acidic environment by keeping the periplasmic pH close to neutral and maintaining the cytoplasm's pH within a not too low range (high cytoplasmic pH enough for its metabolism). That will allow bacteria to continuously metabolize nutrients, which is critical to survive and colonize the host gut while the environmental pH is acidic. Effective neutralization of the acidic pH of host stomach by acid acclimatization is a multifactorial mechanism including the urease system (via cytoplasmic urease), carbonic anhydrases enzyme and other ammonia-producing enzymes for example, aliphatic amidases E, F (AmiE, AmiF), aspartate ammonia lyase (AspA) (79), (80), (81).

2.3.2.1 The urease system

H. pylori's cytoplasmic urease is a multi-subunit (hexameric heterodimer, UreA-B+UreE/G+UreF/H) nickel-containing enzyme complex. Its activity is to catalyze the hydrolysis of urea to carbon dioxide and ammonia (82). Regulation of urease synthesis is encoded by *urease gene cluster*. This set of genes is composed of seven genes, including a cytoplasmic catalytic unit (*ureA/B*), an integral inner membrane acid-activated urea channel (*ureI)*, and an accessory assembly protein (*ureE-H*) (83), (84), (85). The size of the structural subunits UreA and UreB estimated to be approximately 30 and 62 kDa, respectively (84), (86). It is initially produced in the form of an apoenzyme. An apoenzyme form of urease is activated to be in an active form via the Ni^{2+} insertion as its cofactor and the assemble of four accessory proteins at its catalytic site. The cytoplasmic accessory proteins UreE, UreF, UreG, and UreH work together as heterodimers, in the form of UreE/G and UreF/H. However, the regulation of urease activity occurs at various levels, including at the level of (1) biosynthesis of the structural genes, (2) transformation into an active form by insertion of Ni^{2+} into the apoenzyme, and (3) regulation of urea access mechanisms to urease enzymes (80).

- Considering at the biosynthesis level control, up regulated of the structural genes *UreA* and *UreB* biosynthesis are regulated by both inner membranes and cytoplasmic localized of bacterial two-component systems. Two-component systems (TCSs) are the signal transduction systems generally found in bacteria. They play a role in the signaling pathways in response to stimuli by inducing changes in the expression of the involved genes (87), (88), (89). The TCSs in the inner membranes and the cytoplasm of *H. pylori* are the acid-responsive signaling system (ArsRS) and the flagellum-responsive signaling system. (FlgRs), respectively. Both respond directly to the low pH, as found in the stomach (90), (91). Its result leads to the induction of the transcription level of urease enzyme (UreA/UreB, UreE/UreG and UreF/UreH) as demonstrated in Figure 2.3.2.1-step a (92). However, without the incorporation of nickel as a cofactor, UreA and UreB would remain in the form of an

apoenzyme. Therefore, the next level of the regulation of urease activity in *H. pylori* is the nickel incorporation.

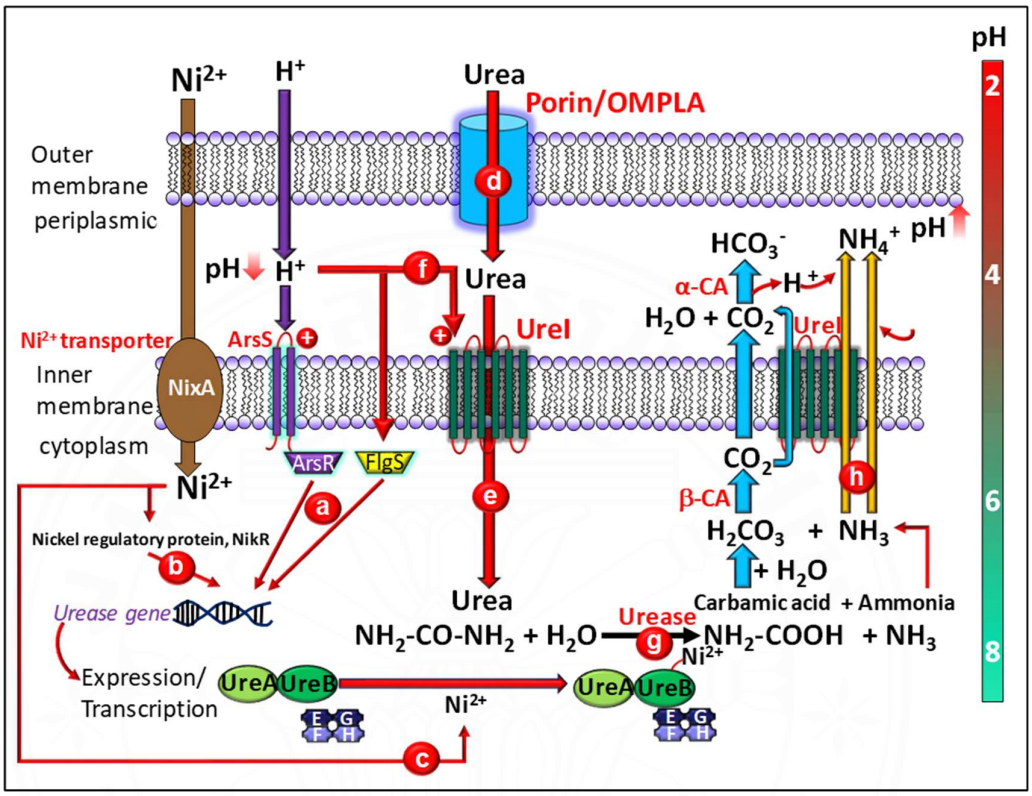

Figure 2.3.2.1 A Model for the acid acclimation processes through the urease system. Step a represents acid activation of the two-component signaling in *H. pylori*, ArsR, and FlgRS. Step b represents Ni^{2+} activation of urease gene expression. The c step refers to the full enzyme activated by subsequent insertion of Ni^{2+} on the urease enzyme. Steps d and e-f demonstrate urea transport into the cytoplasm and the inner membranes through the outer porin/OMPLA membrane transporter and an acid-dependent inner membrane urea channel, UreI, respectively. Step g shows the reaction catalyzed by the urease enzyme complex in the cytoplasmic part of *H. pylori*. Step h shows the diffusion of ammonia gas, a product of urea breakdown by urease complexes, out to the periplasmic fraction, resulting in an increase in pH, which is ideal for the metabolism of *H. pylori*.

- Nickel is transport to the cytoplasmic part through a nickel transporter (NixA) which is located in the inner membrane of *H. pylori*. Ni^{2+} plays a role in the activation of urease enzyme systems at various levels, either by stimulating urease synthesis through nickel-dependent transcriptional regulator (NikR) (Figure 2.3.2.1-step b) or by activating the urease into a fully active form (Figure 2.3.2.1-step c) (93, 94). In the activation process, Ni^{2+} insertion is available in two ways: through direct insertion in UreA/UreB and mediated by UreE/UreG and UreF/UreH accessory proteins (84). The crystal structure of *H. pylori* urease complex was studied in detail 20 years ago (95). It is a huge spherical dodecameric complex (four trimers of UreA-B heterodimers) with two Ni^{2+} needed for each active site. For this reason, the insertion of 24 nickel ions into the enzyme is required for the complete activation of the protein, as shown in figure 2.3.2.1(1). Although the urease enzyme is now fully activated by the activation through the responsive signaling system and Ni^{2+} insertion as described above. But if only a small amount of urea can diffuse across the bacterial inner membranes, effective acid acclimation from urease system will not be able to do perfectly. Hence, the last level of urease regulation is at the influx of stomach urea into the cytoplasmic part of *H. pylori* through the UreI channel (regulation of urea access mechanisms to urease enzymes).

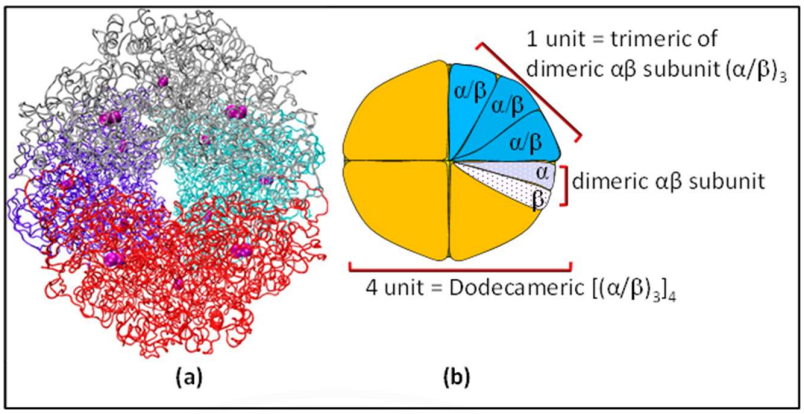

Figure 2.3.2.1(1) The tetrahedral structure of *H. pylori* urease. **(a)** the structural determination from the crystallization and X-ray diffraction of each tetramer trimeric subunit is colored separately to represent the overall assembly. The purple spherical shape represents the insertion of 24 Ni^{2+} ions (Data taken from [95]). **(b)** Cartoon structure of Supramolecular complex of the tetramer of the $(\alpha/\beta)_3$. Dodecameric (12) of each α and β subunit give the 12 active sites (two Ni^{2+} ions per active sites), resulting in the need of a 24 total of Ni^{2+} insertion for activation.

- The regulation of urea access mechanisms to urease enzymes begins with the urea transportation system to the cytoplasm of *H. pylori*. Urea entrance into the periplasmic part of *H. pylori* from its concentration-dependent diffusion through the outer membrane protein (OMPs; including porins and outer membrane phospholipase A, OMPLA). (Figure 2.3.2.1-step d) (96), (97). Urea then transports across the inner membrane of *H. pylori* to its cytoplasm portion through the proton-dependent inner membrane urea channel, UreI, as shown in Figure 2.3.2.1 step e. UreI is a six-transmembrane polytopic integral protein located at the inner membrane of *H. pylori* (98). The regulation of urea uptake through UreI and UreI's activation is pH-dependent. This means that within an acidic pH, a proton-gated channel, UreI, is open (fully open at pH 5.0), allowing the fast entry of urea from the periplasmic part into the cytoplasmic part of *H. pylori* (Figure 2.3.2.1-step f) (99). After urea is transported to the cytoplasm of the *H. pylori*, urea molecules are hydrolyzed by urease which is induced to be upregulation and self-assembly from the trigger of

ArsRS and FlgRs, an important acid-response two-component systems in *H. pylori* as mentioned above. A catalytic unit UreA/B with its accessory proteins UreE/UreG and UreF/UreH is then incorporated with Ni^{2+} to be a fully active enzyme. Fully active urease enzyme, therefore, hydrolyze urea (which comes across from the host gut into cytoplasmic side via porin and UreI channel, individually). This results in the production of ammonia (NH_3) and carbamic acid (NH_2COOH) which is further hydrolyzed to carbonic acid (H_2CO_3) and NH_3 (Figure 2.3.2.1-step g). However, although the host's normal gastric urea concentration remains in the same range as in the blood, that is, between 1-3 mM. This is a very low concentration for enzymes with low affinity to catalyze (for example the enzyme with high Km). But due to the very low Km for urea (0.8 mmol/L) of this enzyme, it thus enables the utilization of the urea which present in limited amounts in the host gut (100), (101). After the reaction is completely catalyzed, the resulting ammonia gas then diffuses from the cytoplasm out to the periplasmic part through the membrane and the UreI channel and then binds with proton (H^+) that catalyzed from the reaction of **α**-carbonic anhydrase enzyme (Figure 2.3.2.1-step h). The products from **α**-carbonic anhydrase are an ammonium ion (NH_4^+) which leads to an increase in the periplasmic pH suitable for various metabolism so that the bacteria survive in a critical acid condition.

2.3.2.2 carbonic anhydrases enzyme system

Carbonic anhydrases (CA) are also a metalloenzymes as urease but containing zinc instead of Ni^{2+} (102). It catalyzes the interconversion reaction of $CO_2 + H_2O \rightarrow HCO_3^- + H^+$ which help to maintain acidic pH of *H. pylori* periplasmic and cytoplasmic part to close to neutral in the highly acidic medium of the stomach. This thus facilitates both survival and growth of the bacteria in the host gust. *H. pylori* contains **β**-CA and **α**-CA, which are located in different subcellular localization i.e. at cytoplasmic and periplasmic part, respectively (103). From the complete genome sequence of *Helicobacter pylori* published in 1997 (104), it has been shown that *H. pylori*'s **β**-CA composed of 221 amino acid residues and shares amino acid sequence identity both with *E. coli* CynT (the *cynT* gene is the one part from those three genes on *Escherichia coli cyn* operon) and **β**-CA of *Helicobacter hepaticus* (30% and 48.5%

identity, respectively) (105), (106). Its zinc-binding core residues include the amino acids Cys42, Asp44, His98 and Cys101 (107). In contrast, *H. pylori*'s **α**-CA composed of 247 amino acid residues and shares amino acid sequence identity both with *Neisseria gonorrhoeae* and *H. hepaticus* (24% and 28% identity, respectively) (106), (108). Its zinc-binding core residues is at the three-His residues (His_{94}, His_{96} and His_{119}) (109). Beyond theses, cytoplasmic **β**-CA catalyzes bicarbonate conversion, a product of the complex urase enzyme (Figure 2.3.2.2-step a) to CO_2 and ammonia (Figure 2.3.2.2-step b). CO_2 gases then diffuse to the periplasmic portion through the inner membrane and UreI transporter (Figure 2.3.2.2-step c). Periplasmic CO_2 is converted back to bicarbonate and H^+ by the functions of **α**-CA (Figure 2.3.2.2-step d). All of these processes help the periplasm reach an optimal pH at which *H. pylori* can still metabolize nutrients and survive in the acidic pH. Of these essential functions, both **β**-CA and **α**-CA are promising drug targets for the eradication of *H. pylori*. Due to the high rate of antibiotic resistance in the current treatment of *H. pylori*, the use of various enzymes inhibition, including sulfonamides, sulfomates, acetazolamides, have been of interest in clinical applications (110), (107), (111), (112).

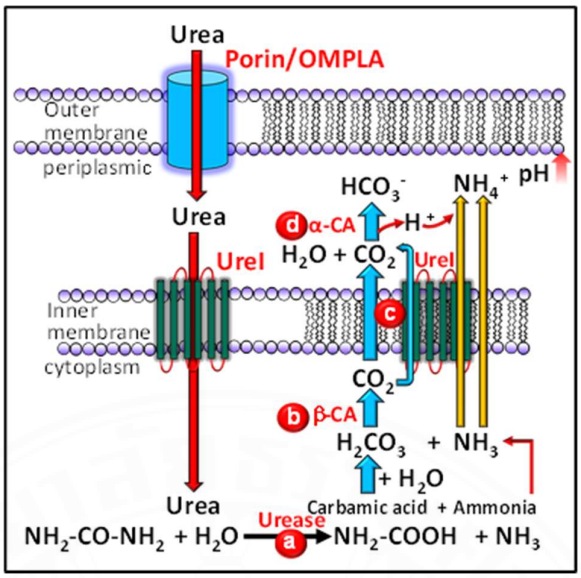

Figure 2.3.2.2 Model of *H. pylori* acid acclimation by carbonic anhydrases enzyme system. Step a-b represents the breakdown of urea into carbamic acid, which is then spontaneously converted to H_2CO_3 which then further catalyzes to CO_2 by cytoplasmic β-CA. Step c shows the diffusion of CO_2 gas from the cytoplasm to periplasm via the inner membrane and UreI channel. Step d refers to an action of periplasmic **α**-CA which catalyzed the conversion of CO_2 to HCO_3^- and H^+.

2.3.2.3 ammonia-producing enzymes (aliphatic amidases E, F (AmiE, AmiF), aspartate ammonia lyase, AspA)

Aliphatic amidase (EC 3.5.1.4), AmiE, and AmiF are cytoplasmic enzymes that produce ammonia and the corresponding organic acid by hydrolyzing short-chain amides. Both are homotetrameric structures but are different in substrate specificity. The substrates for AmiE catalysis include acrylamide (CH_2=CH-$CONH_2$), acetamide (CH_3-$CONH_2$), and propionamide (CH_3-CH_2-$CONH_2$), but not formamide (H-$CONH_2$), which is the specific substrate for AmiF (113). From activity analysis of these two enzymes in *H. pylori*, (114) demonstrated the cysteine residues active-site of AmiE and AmiF is Cys-165 and Cys-166, respectively (114). The next ammonia-producing enzyme found in *H. pylori* is aspartate ammonia lyase, AspA. catalyze the reversible deamination of l-aspartate into fumarate and ammonia. In addition, acid transcriptome

analysis revealed that aspA changes 1.5-2 times as the acidity increases (85), (115). This evidence supports the role of AspA as one of the pH-homeostatic mechanisms in helping *H. pylori* survive in acidic conditions.

2.3.3 Acid resistance

Acid resistance mechanism is the other important mechanism that help *H. pylori* to survive and colonize in an acidic environment such as in the hot gut. Unlike an acid acclimation, which is the mechanism to maintain periplasmic pH near neutral in an acidic region. Acid resistance defines as the mechanism that allows bacteria to survive in the stomach by keeping the pH in the cytoplasm close to 5. In order to survive and colonize in the gastric host, *Helicobacter pylori* is able to neutralize gastric acidity through the major acid resistance mechanism, i.e., surface located urease.

2.3.3.1 surface located urease

In addition to having the cytoplasmic urease as mentioned above, a large amount of surface located urease is also found in the wild-type *H. pylori* strain. Previously, it was believed that surface-bound or extracellular urease, is urease derived from bacterial autolysis (116). But this idea has been shifted from the evidence of Hong et al. (117). From immunoelectron photomicrographs technique, the researchers demonstrated that the urease gold particles are distributed more in the outer part than in the inner part of the wild-type *H. pylori* strain incubated at acidic pH as shown in the figure 2.3.3.1. Based on this fact, it is widely accepted that, at acidic pH as in the gastric host, the surface located urease comes from the redistribution of cytoplasmic urease to the membrane via outer membrane vesicle (OMV) (118), (119). This process, however, depends on the UreI activation (the processes as mention above). In conclusion, after the activation of pH-gating urea transporter from acidic pH (UreI), urea quickly accesses to the cytoplasmic portion and is then hydrolyzed by cytoplasmic urease. As a result, NH_3 and CO_2 are formed and then diffuses into the periplasmic portion. Thus, urease moves from the cytoplasm to the membrane through the OMV processes and then hydrolyzes urea in the lumen of the stomach

into ammonia gas, increasing intestinal pH. This event resulted in the bacterial cells being buffered to a pH suitable for bacterial survival.

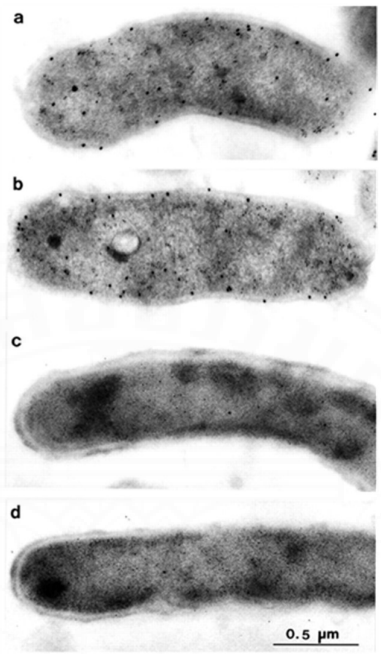

Figure 2.3.3.1 Immunoelectron photomicrographs (immunogold particles) of *H. pylori*. The distribution of the urease gold particles incubated in the *H. pylori* wild type strain.at neutral pH (a) and at acidic pH (b). Comparatively, at acidic pH (b) the more distribution in the outer part is than in the inner part of the *H. pylori* wild type strain. (c) and (d) show result from the same technique in the *H. pylori urel*-deletion mutant strain.at neutral pH and at acidic pH, respectively [(117)].

2.3.4 motility

As *Helicobacter pylori* is a flagellated gram-negative bacterium, its flagellar thus play an important role both in traversing the mucus layer and colonizing the host's intestinal epithelial surface. *H. pylori* possess 3-8 unipolar flagellar. The flagellar structure consists of three components, a base or basal body, a hook, and a filament, as shown in figure 2. 3. 4. Each compartment has a different protein composition according to the review reports by Gu (120). In brief, the major proteins found in the flagellar filament are FlaA and FlaB. FlaA is localized in the outer region, while FlaB lies in the base of the flagellum. Both of them play roles in bacterial motility. Flagellar hook protein, FlgE, is the protein connecting the filament with the flagellar basal body. It forms an arc structure that translates the torque generated by the motor into the flagellum movement (121). The basal body is a complex structure consisting of various protein compositions, including C rings, MS ring, flagellar rod, motor, a specialized type III secretion system (T3SS), and an export structure (122). Each protein has different functions, for example, the C ring protein is involved in (1) transferring and coordinating proteins to the export apparatus and (2) controlling the direction of flagellar rotation from regulating the flagellum motor. While FliF, a MS ring flagellar body protein, in addition to its main function in anchoring flagella to cell membranes, is also involved in the synthesis of flagellar filament (FlaA and FlaB) and flagellar hook protein (FlgE). The flagellar rod protein is a protein that is laid across the cell membrane. In addition, the function of motor flagellar basal body proteins (MotA and MotB) is related to fixation and rotations of the flagellar. Whereas type III secretory protein (T3SS) is a specialized group of various proteins responsible for the transport of flagellar proteins across the cell membrane to the protein exporting apparatus for secretion. From the specific gene mutation techniques, some studies report the importance of some of the flagellar proteins (for example MotB, FlaA, FlaB, FlgE, and FliD) in the colonization of *H. pylori* (123), (124), (125). Therefore, it is known that, in addition to the urease system, another important factor in the colonization of *H. pylori* is its flagella.

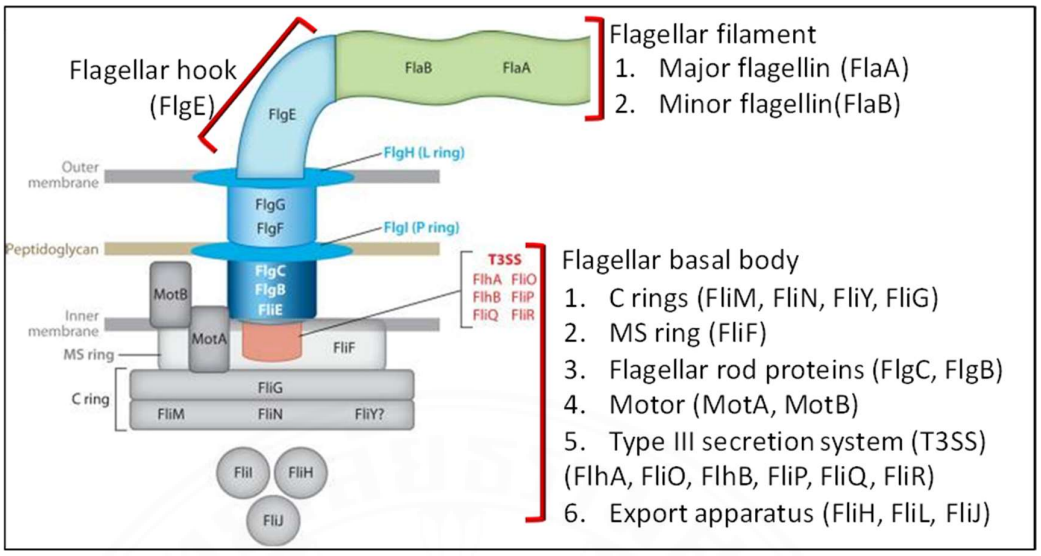

Figure 2.3.4 A model of *H. pylori* flagellum's structure. It composes of three part, i.e. a basal body, hook and filament [120), (121)].

2.3.5 adhesions

After the motile *H. pylori* penetrate the gastric mucosa, the bacteria can form micro- colonies with the MUC5AC, gel- forming mucin secreted by the epithelium of the gastric mucosa (126). The binding is between bacterium's surface (a) blood group antigen-binding adhesin (BabA) to Lewis b (Le^b) motifs and/or fucopresent on the stomach mucin MUC5AC, (b) the sialic acid- binding adhesin (SabA) to sialyl-Lewis x (SLe^x) and sialyl-Lewis a (SLe^a) as shown in figure 2.3.5 (126), (127), (128).

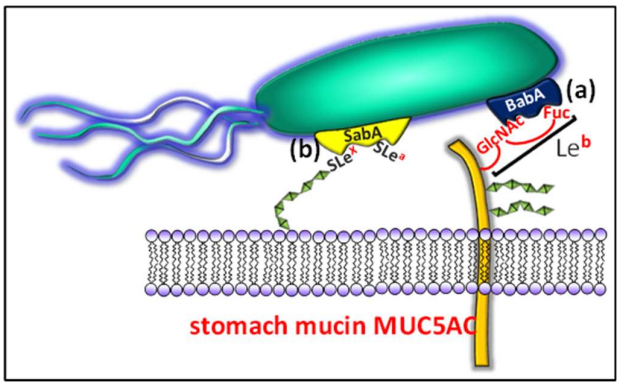

Figure 2.3.5 The model demonstrates example of adhesion molecules of *H. pylori.* (a) adhesion protein BabA adheres to Lewis b (Le^b) motifs and/or fucopresent on the stomach mucin MUC5AC. (b) SabA links to sialyl-Lewis x (SLe^x) and sialyl-Lewis a (SLe^a)

Bab A is a 78 kDa outer membrane adhesion protein. Genes encode for a BabA protein are *babA1* and *babA2*. Only the protein encoded by *babA2* is active, due to the insertion of a 10 bp in the initiation codon (129). Another adhesin protein is the sialic-acid binding adhesin (SabA), a 66 kDa outer membrane protein. It mediates the binding to sialyl-$Lewis^x$ and sialyl-$Lewis^a$ antigen of gastric epithelium in humans (130). Furthermore, SabA also binds to sialylated receptors on neutrophils, which leads to non-opsonic phagocytosis activation of the neutrophils, and induction of the oxidative damage in the gastric epithelium (131). In addition, the outer membrane (OM) proteins are also involved with the adhesion of the bacteria. An example of adhesion OM proteins includes the adherence-associated lipoproteins A and B (AlpA and AlpB). AlpA and AlpB contain 518 amino acids. There is a piece of evidence that both are derived from homologous genes (132).

2.3.6 cytotoxin

A cytotoxin is the group of secretion substances released by *H. pylori* to damage the host cell. For example, VacA (Vacuolating toxin A) is a cytotoxin secreted from bacteria as a large 140-kDa pro-toxin form consisting of an N-terminal signal peptide, N-terminal Hydrophobic region, the secreted VacA p88, a 12-kDa small, secreted peptide with unknown function (SAP), and the C-terminal autotransporter β-

barrel shape (33 kDa) subunits as shown in figure 2.3.6(1) (a) (133). The last domain is responsible for the transport of VacA to the outside of the bacterial cells via a type V autotransporter secretion system (133). During the secretion process, the pro-toxin form of VacA is cleaved to produce a mature toxin 88-kDa, which is subsequently broken down to the N-terminal p33 and the C-terminal p55 domain (known as subunits A and B, respectively). These two subunits have different functions. The N-terminal p33 domain is responsible for the formation of the anion-selective channels in the lipid bilayer of the host organelles. Whereas the right-handed parallel β-helix of the C-terminal p55 domain makes this structure-function as toxin-binding or a cell-binding domain as shown in figure 2.3.6(1) (b) (134). When *H. pylori* secrete VacA, its monomer then binds to the receptors on the host cell membrane. Examples of VacA receptors on epithelial cells include receptor protein tyrosine phosphatase α and β (RPTPα and RPTPβ) and low-density lipoprotein receptor-related protein-1 (LRP1) and other glycosylate-containing transmembrane proteins on the host cell surface (135), (136) (137). Most importantly, when it binds to its receptor on the host plasma membrane and associates with lipid rafts, the VacA monomer undergoes oligomerization to a hexameric structure which is then internalized into host cells, as shown in figure 2.3.6(1) (c) (138), (139). After internalization into the cells, VacA targets the late endosome membrane and forms an anion-selective channel. This channel allows the transport of chloride ions (Cl^-) into the cell, resulting in an increase in the chloride concentration in the intra-luminal compartment. This activates the V-ATPase proton-pumping activity and thus increases the ATP-dependent acidification of endosomes. The consequence of this is an increased diffusion of membrane-permeable weak bases and hence accumulate within the organelle. This eventually results in the osmotic swelling of the late endosomes and results in vacuolation as shown in figure 2.3.6(2) (a)-(e) (140), (141), (142), (143), (144).

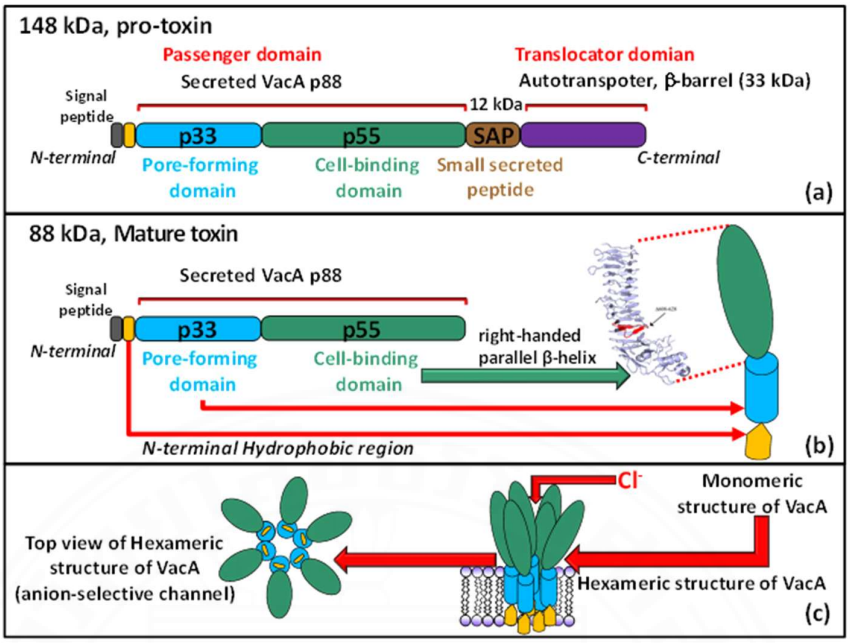

Figure 2.3.6(1) A model of VacA protein and its subunit. (a) pro-toxin form of VacA , (b) mature toxin form of VacA (right-handle β-helix conformation of p55 from [138]) (c) hexameric structure of VacA

In addition, to induce cytoplasmic vacuolation, a number of VacA effects have been reported. VacA induces apoptosis by stimulating the release of cytochrome *c* from the induction of mitochondrial transmembrane potential reduction as well as activation of Bax/Bak (figure 2.3.6(2) (f) and (g)). It has also been reported that VacA can alter the cell signaling pathway. For example, Vac A induces the activation of the PI3K/ Akt signaling pathway resulting in inactivate GSK3β by phosphorylation at Ser9 of GSK3β. This phosphorylation leads to trigger the liberation of β-catenin from the GSK3β/β-catenin complex (Figure 2.3.6(2) (h) and (i)). The free β- catenin then translocates from the cytoplasm to the nucleus and induces the expression of protooncogene, the cyclin-D1. Finally, expression of this protooncogene thus lead to abnormal cell proliferation as shown in figure 2.3.6(2) (j) (145), (146), (147).

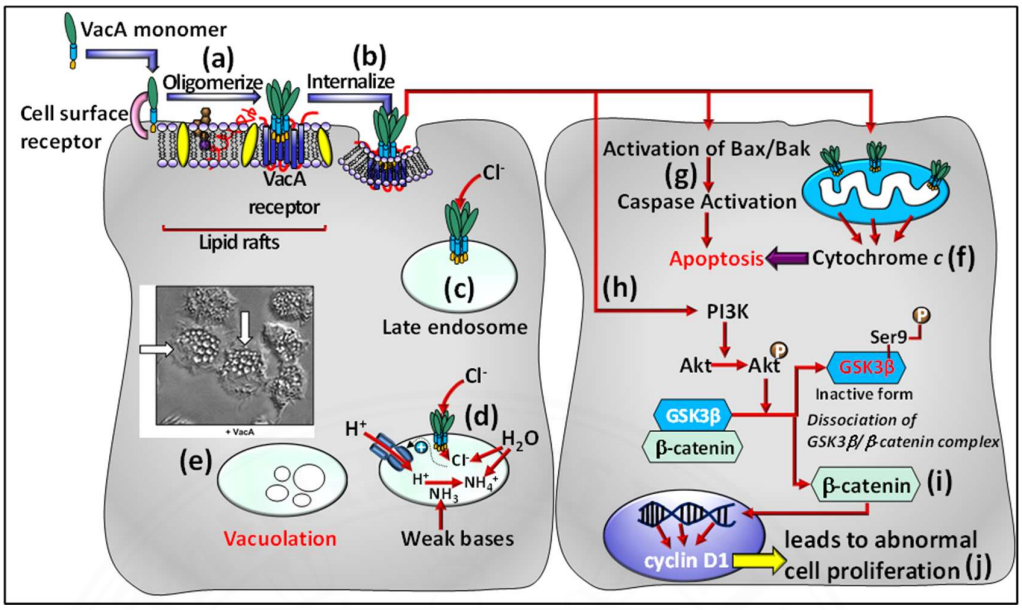

Figure 2.3.6(2) A multifunctional model of VacA after *H. pylori* infection. Step (a)-(e) represent the generation of vacuolation in the late endosome of the epithelial cells of the host gut. Step (microscopic data from reference [136] (f)-(g) demonstrate the induction of cell apoptosis through stimulating the releasing of mitochondria cytochrome c and caspase activation via the activation of Bax/BaK protein. Step (h)-(j) shows the effect of VacA on the activation of the PI3K/Akt signaling pathway, which ultimately promotes an expression of cyclin D1 and then leads to abnormal cell proliferation [145), (146), (147)].

Another virulence factor evidenced for enhancing gastric cancer from *H. pylori* infection is CagA. CagA is a 120– 140 kDa protein encoded by a *cag* pathogenicity island (*cag*PAI). It is translocated from the cytoplasm of *H. pylori* to the host's gastric epithelial cells through the pilus of the type IV secretory system (T4SS), shown as arrows from a photograph of a scanning electron micrograph in figure 2.3.6 (3)(a). T4SS is a multi-protein complex that lies across both the inner and outer membranes and is also encoded from the cagPAI (148), (149), (150), (151). T4SS proteins are composed of proteins that act as (1) the core main structural protein complex, (2) the active component, (3) the translocation-related factor, and (4) the pilus

component, as shown in figure 2.3.6(3)(b). During CagA^{+}*H. pylori* infection, the delivery of CagA to the host cell is initiated by the binding of the transmembrane receptor integrin ($\alpha5\beta1$ integrin) with the RGD (Arg-Gly-Asp) motif of CagL located on the surface of the pilus component, as shown in figure 2.3.6(3)(c) (152). Additionally, other T4SS proteins, including CagY and CagI, can bind to the $\alpha5\beta1$ integrin, which is beneficially helping stabilize the T4SS-host cell interactions (153). This, therefore, activates the delivery of CagA from the pilus into the cytoplasm of the host cell, as shown in figure 2.3.6(3)(d) (152). In addition to injecting CagA through the pilus, there is evidence that CagA can enter the host cell by inducing the phosphatidylserine externalization process. This occurs after the binding of *H. pylori* to epithelial cells that results in surface-exposed CagA internalization into the host cell (154). After the formation of a protein complex of T4SS to the host cell, and CagA has entered the host cells, it then localizes to the inner surface of the plasma membrane of the host, as shown in figure 2.3.6(3)(e). This, therefore, activates a number of pathogenic events include CagA phosphorylation-independent pathway and CagA phosphorylation-dependent pathway. An example of the CagA phosphorylation-independent pathway is its interaction with E-cadherin leading to disrupt E-cadherin-β-catenin complex. This results in the accumulation of deregulated β-catenin, which is a protein that promotes carcinogenesis, as shown in figure 2.3.6(3)(f) (155). On the other hand, the CagA phosphorylation-dependent pathway involves two intracellular tyrosine kinases, a focal adhesion kinase (FAK) and a steroid receptor coactivator (Src) (156), (157). Subsequently, FAK-Src cluster activation initiates a cascade of downstream phosphorylation of several proteins including EPIYA (glutamate-proline-isoleucine-tyrosine-alanine) motifs presented on CagA itself. An example of the results from the CagA phosphorylation-dependent pathway includes the dysregulation of various cell functions, cytoskeletal changes, enhanced cell motility (all of these events occur through c-Abl tyrosine kinase pathway), as well as activates a number of mitogenic and proinflammatory genes via Erk1/2MAP kinase signaling pathway, etc. as shown in figure 2.3.6(3) (g). These promote the induction of gastric pathologies from *H. pylori* infection, including gastritis, duodenal ulcers, and gastric cancer (158). However, the disease

worsens if the patient is infected with the *H. pylori*- expressing strain of CagA in combination with VacA or BabA.

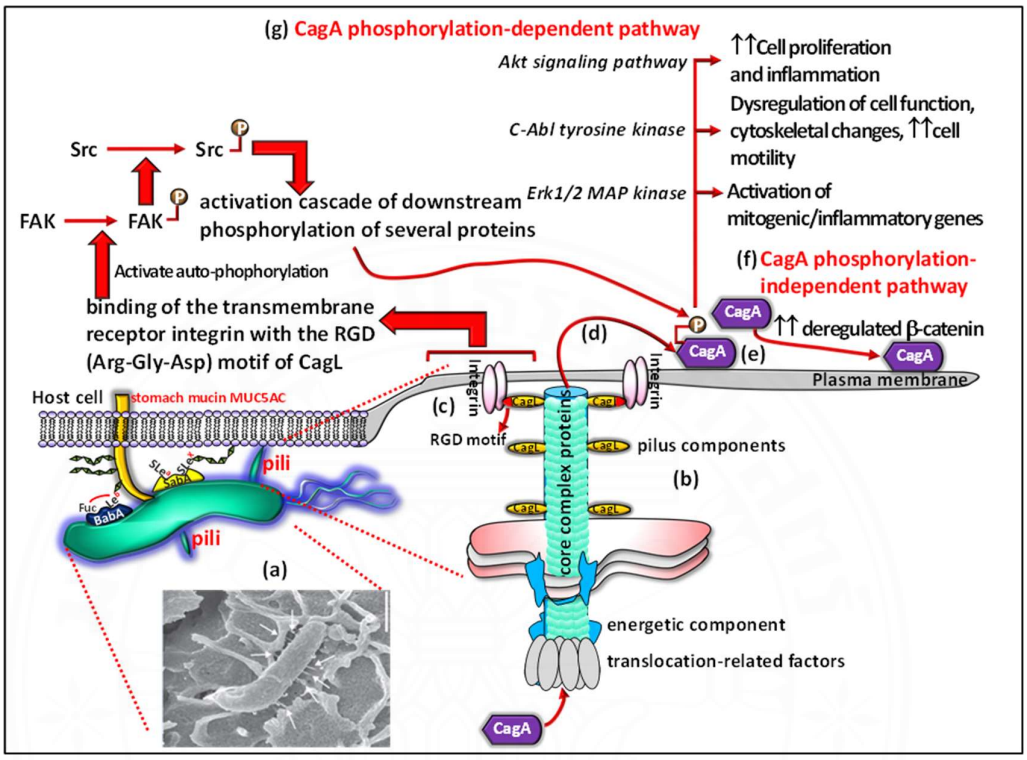

Figure 2.3.6(3) The representation model of CagA pathogenesis (scanning electron micrograph from reference Backert, S, 2015) [(149)].

2.4 Treatment of *H. pylori* infection

Once the patient is diagnosed with *H. pylori* infection, the goal of treatment is to eradicate the bacteria by at least two antibiotics with a combination of a proton pump inhibitor (PPI) therapy. In the PPI-based triple therapy regimens, antibiotics of choice are often chosen in different groups to help eliminate *H. pylori*, such as macrolides, particularly clarithromycin, and nitroimidazoles, or amoxicillin (159), (160). The preferred PPIs used with combination therapy are omeprazole or

lansoprazole. The advantage of this drug primarily increases the intragastric pH and enhances the activity of the antibiotics (161).

2.4.1 Clarithromycin

Clarithromycin (Cla) is a new generation macrolide antibiotic. It is the derivative of erythromycin (6-O-methylerythromycin) (Figure 2.4.1(1)). By adding the C6 methoxyl group to the macrocyclic lactone ring, thereby promotes both the stability of Cla in the acidic environment and its absorption in the small intestine. In addition, the add-on group resulted in Cla having a longer half-life than erythromycin (3 to 4 hours (162), (163). Its antimicrobial mechanism is based on inhibiting bacterial protein synthesis by binding to the bacterial 23S rRNA in the large (50S) subunit of the bacterial ribosome. It thus inhibits protein synthesis during the translocation process. So, the mechanism of action of clarithromycin is bacteriostatic. The target site of clarithromycin is the large (50S) subunit of the bacterial ribosome. In bacteria, active ribosomes are composed of two subunits called the large and small subunits. The small subunit (30S subunit) consists of 21 proteins and 16S RNA (164) (Figure 2.4.1(2)). While the large subunit (50S subunit) consists of 31 proteins and two RNA molecules, a 23S RNA and 5S RNA (165). The Cla-binding site is at the domain II (hairpin 35) and domain V (the peptidyl transferase center) of 23S rRNA. Since these drugs are small relative to the ribosome, so interactions would be possible only the rRNA is folded after hairpin 35 and the peptidyl transferase loop are adjacent (166), (167), (168), (169), (170), (171). This results in the blockade of transpeptidation and translocation of peptidyl tRNA from the A site to the P site, which effectively stops chain elongation and inhibits RNA-dependent protein synthesis. (172), (173) (Figure 2.4.1(3)). For *H. pylori* eradication, standard triple therapy consists of 7-14-day of clarithromycin 500 mg, twice a day (bid) with amoxicillin 1 g, bid plus PPI standard dose (174), (175).

.

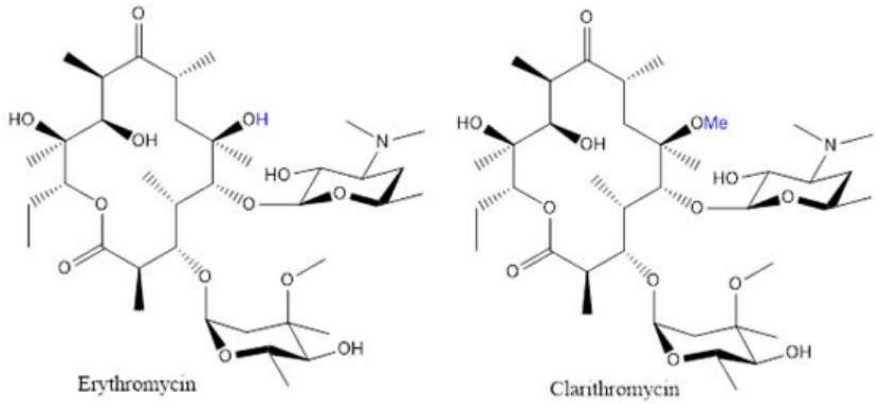

Figure 2.4.1(1) Structure of clarithromycin compared with erythromycin. Retrieved from https://pharmafactz.com/medicinal-chemistry-of-macrolides/

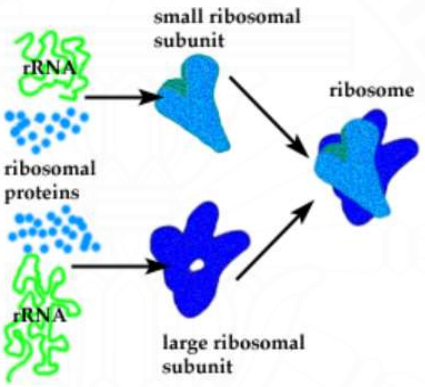

Figure 2.4.1(2) The structure of ribosomal RNA and their compounds. Retrieved from http://www.brooklyn.cuny.edu.

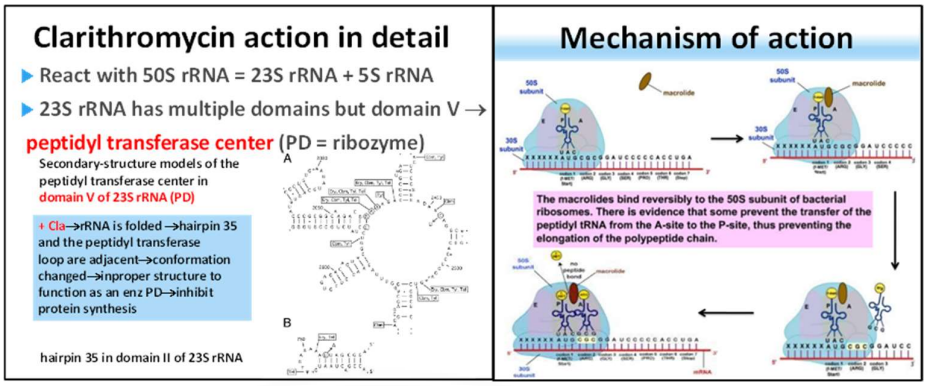

Figure 2.4.1(3) The mechanism of action of clarithromycin and inhibition of protein synthesis process [171].

2.4.2 Metronidazole

Metronidazole (Mtz) and other nitroheterocyclic drugs are a nitroimidazole derivative drug that is mainly used to treat anaerobic and parasitic infections (Figure 2.4.2(1)). Its mechanism of action relies on its ability to generate toxic free radicals in bacterial cells that damage the bacterial DNA. Therefore, metronidazole is classified as a bactericidal agent. The mechanism of action of Mtz in the eradication of *H. pylori* is based on an oxidation-reduction reaction. Through the action of the Oxygen-insensitive NADPH nitroreductase (coding by *rdxA* gene), it converts the oxidized form of ferredoxin into the reduced form, with NADH/NADPH being the coenzyme. Whereas ferredoxin in the reduced form is converted back to its oxidized form by the enzyme NAD(P)H-flavin oxidoreductase (coding by *frxA* gene), which contains $FADH_2$ as a coenzyme (15), (16), (14), (176), (177), (17). The reduced form ferredoxin binds electrons to the prodrug-formed metronidazole ($R\text{-}NO_2$), resulting in metronidazole being the active drug of the nitro-free radicle ($R\text{-}NO_2^{\bullet -}$) form as shown in figure 2.4.2(2) (left). Additionally, it can be further reacted by incorporating O_2 to form superoxide ($O_2^{\cdot -}$), hydrogen peroxide (H_2O_2), and a hydroxyl radical ($OH^{\cdot}$). These free radicals are produced in large numbers in the system resulting in DNA damage and eventual bacterial cell death (178) (Figure 2.4.2(2) (right)). In the past decade,

metronidazole has become an essential treatment of *H pylori* infection. In Western countries, more than 70% of metronidazole is used. However, *H pylori* eradication is rarely successful when used as a single drug (179). In contrast, in developing countries where metronidazole is frequently used, more than 80% of *H. pylori* isolates have been found to be resistant to metronidazole (180), (181), (182). Therefore, treatment using metronidazole is always combined with at least one antibiotic. The current recommendation for the treatment of *H. pylori* infection in areas of high metronidazole resistance is proton pump inhibitor-clarithromycin-amoxicillin (160).

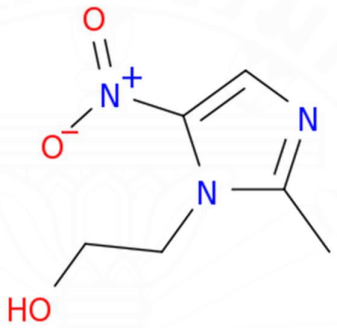

Figure 2.4.2(1) The structure of metronidazole (1-(2-hydroxyethyl)-2-methyl-5-nitroi-midazole).

Retrieved from https: / / www. molinstincts. com/ structure/ metronidazole- cstr-CT1000897687.html

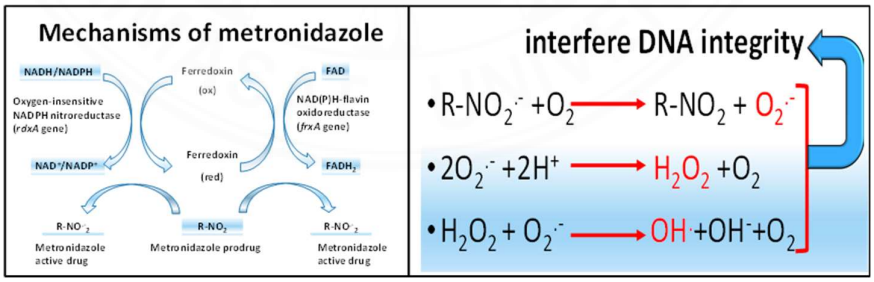

Figure 2.4.2(2) The futile cycling process of metronidazole mechanism of action in cell.

2.4.3 Amoxicillin

Amoxicillin is an antibiotic commonly used in the case of metronidazole resistance. It is aminopenicillin, generated by adding an extra amino group to penicillin (Figure 2.4.3(1)). Amoxicillin is a beta-lactam antimicrobial agent. Its mechanism of action is that amoxicillin binds to penicillin-binding proteins (PBPs) at transpeptidase's active site, interfering with the action of the enzyme transpeptidase, which is the enzyme used to form cross-linkage of the peptidoglycan. So, it acts through the inhibition of cell wall biosynthesis that leads to the death of the bacteria. It is thus classified in the group of bactericidal antibiotics (183), (184), (185) (Figure 2.4.3(2)). Amoxicillin as monotherapy achieves only less than a 20% eradication rate of *H. pylori* (186), (187).

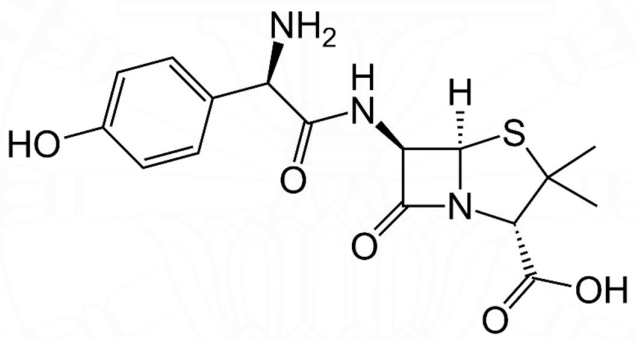

Figure 2.4.3(1) The structure of amoxicillin [188].

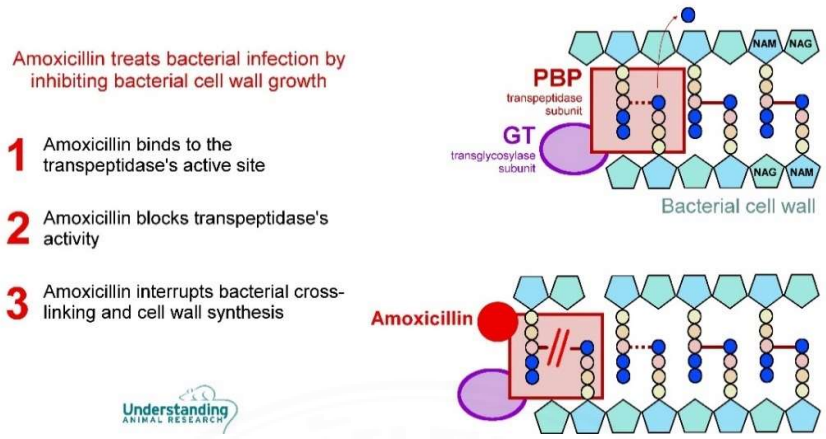

Figure 2.4.3(2) The mechanism of action of amoxicillin.
Retrieved from https: / / www. animalresearch. info/ en/ drug- development/ drug-prescriptions/amoxicillin/

2.5 Antibiotic resistance

The prevalence of antibiotic resistance of *H. pylori* has been found to increase steadily worldwide. The latest report from Savoldi A. et al. (2018) (5) demonstrated that both primary and secondary resistance rates to clarithromycin and metronidazole were ≥15% in all WHO regions. Considering the prevalence of primary clarithromycin resistance (Cla-R) in regions with prevalence rates ≥ of 15%, it was found to be lowest in the European (EUR) region (18%), highest in the Western Pacific region. (WPR) (34%). Whereas the 10% of primary Cla-R prevalence rate was found in the Americas region (AMR) and the Southeast Asia regions (SEAR). However, although the prevalence of primary metronidazole resistance (Mtz-R) was >15%, the highest and lowest resistance rates were all higher than the highest and lowest prevalence rates of Cla-R, i.e. 56% (in the Eastern Mediterranean region; EMR) and 23% (in the AMR region). In addition, the prevalence of primary clarithromycin and metronidazole resistance rates (dual resistance; Cla/Mtz-R) in almost all regions was detected at <10% except in the EMR region where the rate was high at 19% (Table 2.5).

Besides, Savoldi A. et al. (2018) also reported that the prevalence of secondary Cla-R and MTZ-R was above 15% in all regions. The highest prevalence of Cla-R and Mtz-R was observed in WPR and EMR (67% and 65%, respectively). While the lowest prevalence of Cla-R and Mtz-R was recorded in SEAR and AMR (15% and 30%, respectively). The prevalence of secondary dual resistance to clarithromycin and metronidazole was 18%, the highest prevalence rate in EUR (Table 2.5). However, if we look at the 10-year trend between 2006 and 2016, the prevalence of antibiotic resistance rates tends to increase in almost all regions. In particular, the trend in the prevalence of Cla-R in SEAR increased significantly (from 13% to 21% from 2006 to 2015). On the other hand, a trend in the prevalence of Mtz-R in SEAR was lower over 10 years (from 99% to 53% from 2006 to 2015). In Thailand, the prevalence of Cla-R in large cities is at a similar rate to the reported of Savoldi A. (14%), which is higher than in rural areas (~3.7%). While the prevalence of Mtz-R and dual resistance was found at 36% and 10%, respectively (7), (189), (190), (191). Therefore, the investigation for protein secretion from antibiotic-resistant strains compared to antibiotic-susceptible of *H. pylori* strains would be highly helpful in the development of the new drugs to treat *H. pylori*-resistance strains.

Table 2.5 Prevalence of clarithromycin, metronidazole and dual resistance stratified by WHO region.

Regions	Clarithromycin resistance (Cla-R)		Metronidazole resistance (Mtz-R)		dual resistance (Cla/Mtz-R)	
	Primary Cla-R	Secondary Cla-R	Primary Mtz-R	Secondary Mtz-R	Primary Cla/Mtz-R	Secondary Cla/Mtz-R
Western Pacific region. (WPR)	**34%**	**67%**	47%	62%	8%	13%
Eastern Mediterranean region (EMR)	33%	17%	**56%**	**65%**	**19%**	*11%*
European (EUR) region	18%	48%	32%	48%	*1%*	**18%**
America's region (AMR)	*10%*	18%	*23%*	*30%*	Not specified	
Southeast Asia region (SEAR)	*10%*	*15%*	51%	44%	Not specified	

Bold and *italic* percentage numbers indicate the highest and the *lowest* prevalence rates, respectively. Arrows show an increase or decrease in antibiotic prevalence when comparing primary and secondary resistance in each region.

2.5.1 Mechanism of antibiotic resistance in *H. pylori* infection

The molecular mechanisms by which bacteria become resistant are manifold, but in general these can be characterized as involving either the drug inactivation, alterations in the drug target site, or drug efflux. The most common clarithromycin resistance mechanism is due to point mutations within the peptidyl transferase center encoding region of the 23S rRNA associated with three major point mutations. The A2142G, A2142C mutation at the V domain of 23S rRNA is the most common point mutation to induce clarithromycin resistance. Whereas the A2143G mutation of the previously mentioned domain also results in drug resistance, although this mechanism is less common (166), (192), (193), (194), (195), (196). When this

mutation is present, the formation of a 3D structure that influences the bending of the domain V loop of 23S rRNA and the hairpin 35 of domain II cannot occur. Clarithromycin, therefore, unable to bind properly to the ribosome. As a result, the drug is unable to inhibit the protein synthesis of *H. pylori* bacteria (197) (Figure 2.5.1). Another suggestive mechanism of clarithromycin resistance is the reducing potential of intracellular antimicrobial through *H. pylori* restriction-nodulation-division (RND) efflux of antimicrobial compounds, resulting in reducing intracellular antimicrobial concentration (11), (198), (199). The presence of a 23S rRNA mutation in combination with an efflux pump is a synergistic effect that resulted in *H. pylori* resistance to clarithromycin. This is because the first mechanism results in a reduction in the affinity of clarithromycin with the ribosomes, while the latter mechanism drives the antibiotic out of the cell (13).

On the other hand, the most reported mutations in metronidazole resistance *H. pylori* are from insertions and deletions of transposons or missense and frameshift mutations in the *rdxA* (Oxygen-insensitive NADPH nitroreductase) and the *frxA* (NAD(P)H-flavin oxidoreductase) gene, resulting in inactivation of these genes (14), (177) (17), (18), (19), (20), (200). In addition, the other metronidazole resistance mechanism is related to the mutation of the ferric (Fur) uptake regulator (C78Y, P114S; *Fur* mutant), which is a direct suppressor of the superoxide dismutase; SodB. This enzyme is essential for protection against superoxide attacks. As mentioned above, the active form of metronidazole eliminates *H. pylori* bacteria by producing large amounts of superoxide radicals that cause intracellular oxidative stress. Therefore, this mutation significantly reduces the generation of superoxide radicals compared with that in the metronidazole-susceptible strains (21).

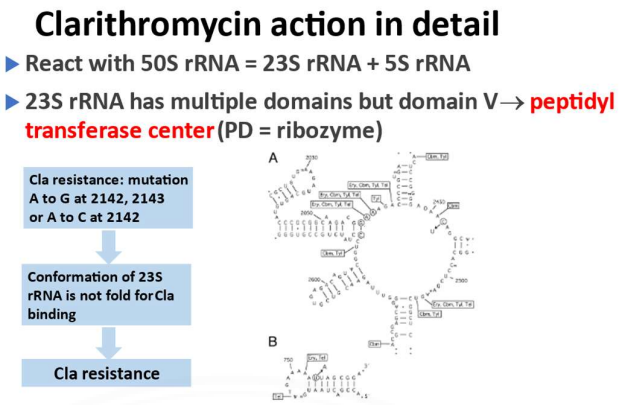

Figure 2.5.1 The point mutation in 23S rRNA and led to resistance with clarithromycin in *H. pylori* infection [171].

2.5.2 Dual resistance

Uncontrolled use of antibiotics may lead to the emergence of dual resistance to clarithromycin and metronidazole in *H. pylori* strains. The prevalence of combined resistance rates to clarithromycin and metronidazole (Cla/Mtz-R) to *H. pylori* isolates has increased over the past two decades. In Asia, the prevalence of dual antibiotic resistance has doubled over the past 20 years (1998 to 2018), i.e. from 6.9% to 12.2%. In Thailand, data collected from 2015-2019, reported by Vilaichon RK et al., found that the prevalence of dual resistance rate (clarithromycin and metronidazole, Cla/Mtz-R) in *H. pylori* increased from 12% to 25% (7). In addition, data from the Center of Excellence in Gastrointestinal Diseases of Thammasat University (an unpublished data of Vilaichon RK. et al.) shows that the prevalence of Cla/Mtz-R is 5.6-15%. The results differ by region to region in Thailand, for example, the prevalence of Cla/Mtz-R from Northeastern (Isan), Southern Thailand, North, and Central Thailand was 5.6%, 5.9%, 6.7%, and 15%, respectively. This is probably due to the differences in the spiciness of the local food, genetic diversity, and socioeconomic status of the people in each region.

2.6 Proteomics Study

Proteomics is the study of peptides and proteins within a biological system. The term "proteomics" was first created in 1995 and defined as the large-scale characterization of the entire protein complement of a cell line, tissue, or organism. It is well known that proteins are responsible for an endless number of tasks within the cell. The complete set of proteins in a cell can be referred to as its proteome and the study of protein structure and function and what every protein in the cell is doing is known as proteomics. The proteome is highly dynamic, and it changes from time to time in response to different environmental stimuli. The goal of proteomics is to understand function of proteins, what allow them to do, what they do, what they interact with, and how they contribute to life processes. It can also be applied to map the difference between a wild type and a genetically modified organism.

Proteomics was supported by the introduction of the two-dimensional gel, the improvement in mass spectrometry, and the development of computer algorithms for database searching. Proteins are extracted from cells, tissues, body fluids or other organisms and then fractionated using various methods such as 1D or 2D gel electrophoresis. The proteins are digested in-gel or in solution with a proteolytic enzyme (such as trypsin). These peptides are analyzed by LC-MS/MS to thousands of spectra. Data analysis of the mass spectra involving database searching and statistical approaches are performed to quantitate and identified the proteins (Figure 2.6.1) (201).

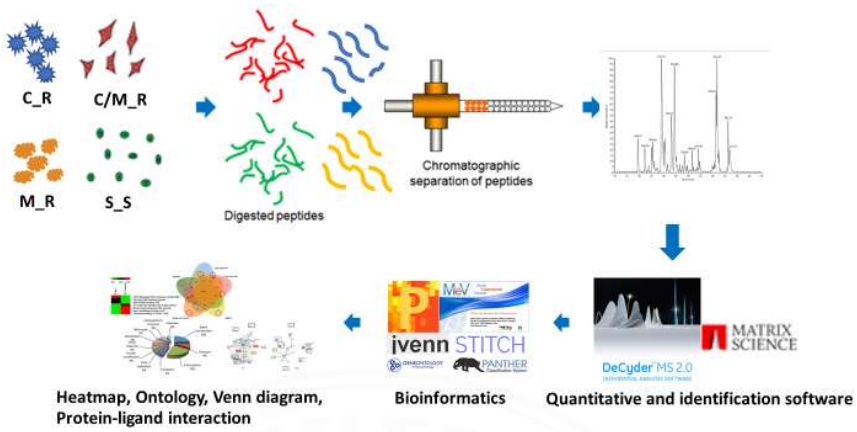

Figure 2.6.1 The typical workflow of a tandem MS/MS based shotgun proteomics [202].

Proteins can be separated by polyacrylamide gel electrophoresis that included SDS-PAGE (sodium dodecyl sulfate–polyacrylamide gel electrophoresis) and 2D-PAGE (Two-dimensional gel electrophoresis) (201). Due to its resolution and sensitivity, this technique is a powerful tool for the analysis and detection of proteins in complex biological sources (203). First, 2D-PAGE (Two-dimensional gel electrophoresis) separated proteins according to isoelectric point by isoelectric focusing in the first dimension, and according to molecular weight by sodium dodecyl sulfate electrophoresis in the second dimension. Sodium dodecyl sulfate–polyacrylamide gel electrophoresis (SDS-PAGE) separated proteins based on their molecular size (204), (205). However, SDS-PAGE has resolved proteins only range 10-130 kDa of molecular weight protein while Isoelectric focusing (IEF) separated only hydrophilic proteins at pI of 3-10 (206).

Liquid chromatography (LC) is the most important and widely used technique for the recovery and isolation of proteins, peptides, and other biomolecules. This separation occurs according to the interaction of the sample with the mobile and stationary phases. The stationary phase in most column chromatography is highly absorbent solid. On the other hand, the proper mobile phase is solvent with polarity that relative to the sample and the stationary phase. General types of chromatography are normal phase chromatography, reverse phase chromatography and flash

chromatography. In normal phase chromatography, the stationary phase is polar, and the more polar solutes were separated by adhere to the stationary phase. When the solvent or gradient of solvents is passed through the column, the less polar components will be flow through faster than the more polar ones. In reverse phase chromatography, the polarities of the mobile and stationary phases are opposite to normal phase chromatography. The stationary phase is non-polar, and the most polar solvent was flow first and the least polar solvent was eluted later. Flash chromatography is a specialized and modified method of column chromatography in which the mobile phase was pushed faster through the column with the help of compressed gas (such as nitrogen or air) or a vacuum. Those higher solubility compounds will flow through the column faster than those with less solubility and can be collected individually (207), (208), (209), (210). LC has proven to be not only highly resolution, but also ultimately flexible. This unique combination allows good yield of both mass and biological activity with extremely high purity (211).

The mass spectrometry, the mass analyzers can carry the gas-phase ions to the detector where the m/z ratio is determined. The most common types of mass analyzers used in proteomics are time-of-flight (TOF), quadrupole, and ion trap.

A quadrupole also known as a transmission quadrupole mass spectrometer, quadrupole mass filter, or quadrupole mass spectrometer, is consisted with four cylindrical metal rods that oscillated in electric fields and arranged in parallel to which a voltage and radiofrequency (rf). The sample ions are separated based on their mass-to-charge ratio (m/z) (212) (Figure 2.6.2).

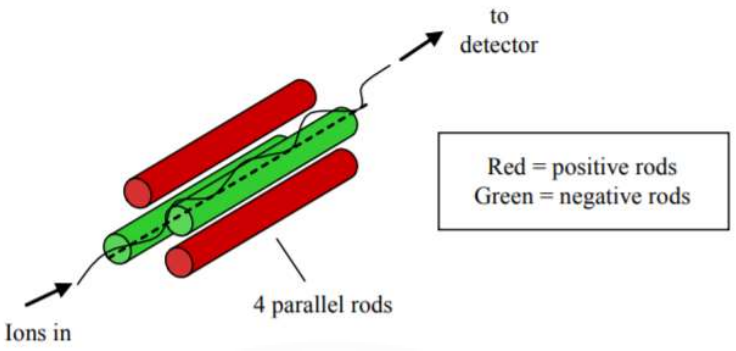

Figure 2.6.2 Diagram of a linear quadrupole [213].

Time-of-Flight (TOF) mass spectrometer measures the m/z ratio of ions based on the time that move through the mass analyzer to the detector (between the emission of a signal and its return to the sensor, after being reflected by an object). The time taken is proportionated to the m/z ratio with smaller ions that reached the detector faster than larger ones. TOF mass analyzers have significant advantages over quadrupoles for many applications (212), (214), (215), (216). TOF is improved speed and resolution, ensures that no important information is lost, and made to easy identify analytes and interpret measurements.

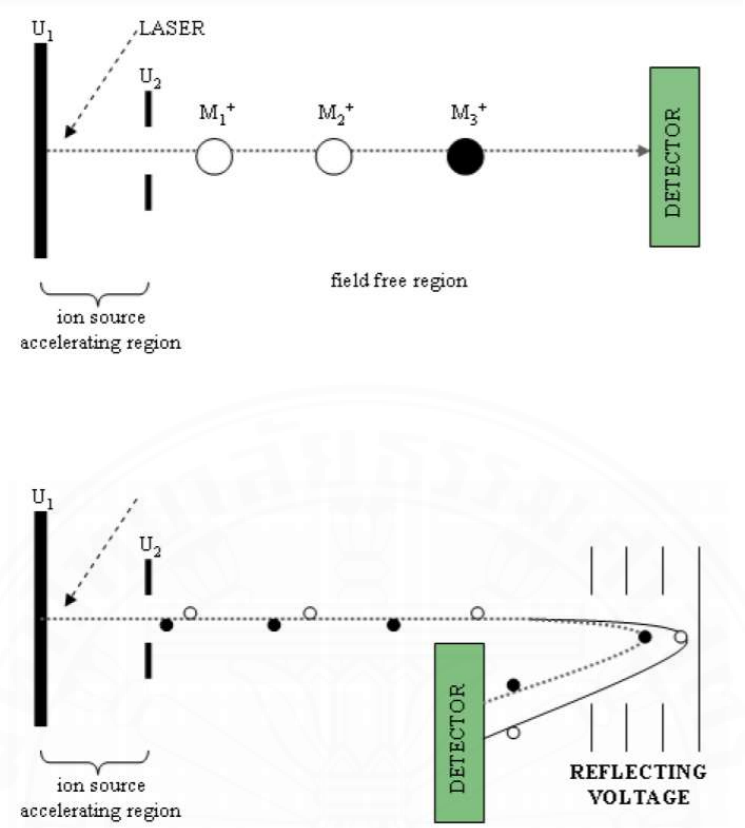

Figure 2.6.3 Schematic diagram illustrates the basic principles of linear and reflector Time-of-Flight mass analyzer (TOF).
Retrieved from https://www.slideshare.net/sadiqrahim2/mass-spectrometry-53829494.

The ion trap analyzer acts as an 'electric-field box' for restrict the ions either positively charge or negatively charge. When the trapping field is changed, the orbit of trapped ions become sequentially unstable, and the ions are ejected the trapping field in order of mass/charge (m/z) ratio and period. Upon ejection from the ion trap, ions are stroked to a detector. Then an output signal is provided. Finally, the ion trap can isolate and fragment peptide ions from complex mixtures (209), (212), (214), (217) (Figure 2.6.4).

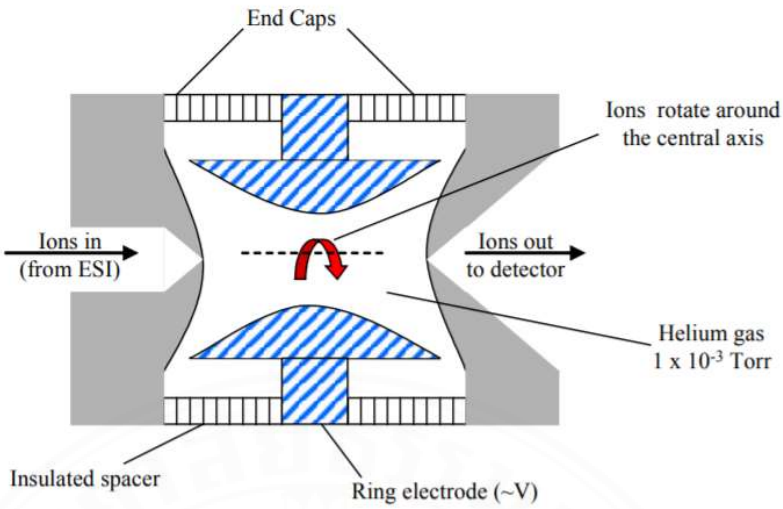

Figure 2.6.4 Diagram of Ion Trap mass analyzer [218].

Proteomics can also be used to develop a protein-network map where interaction among proteins can be determined for a particular living system (Figure 2.6.5, Figure 2.6.6).

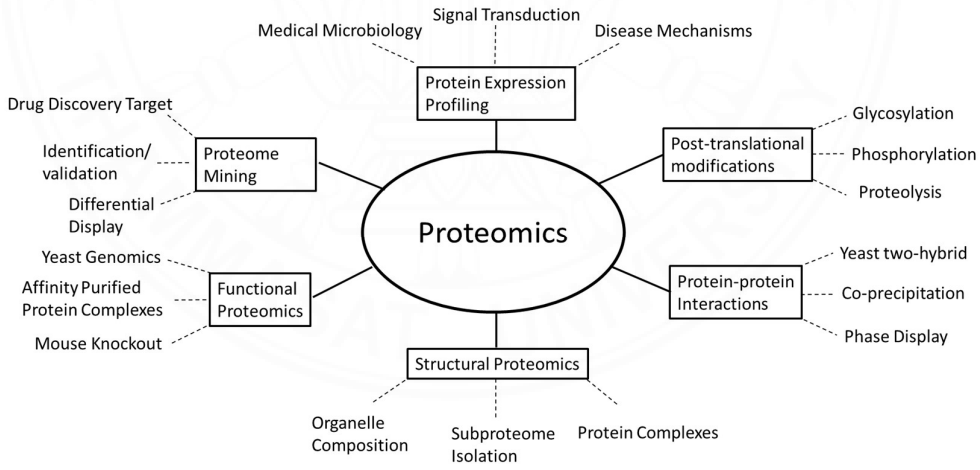

Figure 2.6.5 The protein-network map of proteomics.

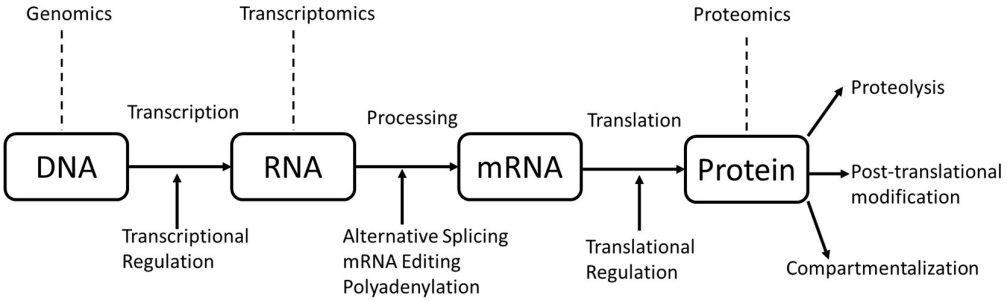

Figure 2.6.6 The relative among omics system.

2.7 Secreted protein involving in antibiotic resistance in *H. pylori* infection.

Previously, Jungblut et al. identified 152 secreted proteins, including 9 virulence factors (such as CagA, UreA, UreB) and 28 antigens in *H. pylori* strain 26695 and J99 (219). While 33 extracellular proteins of *H. pylori* strains 26695 and J99 were detected, 6 of them are oxidoreductases and the others are virulence factors (such as VacA, FlgE) (220). After coculture of *H. pylori* and monocytes (THP-1 cells), elongation factor-Tu (EF-Tu) was detected in culture media (221). Smiley et al. reported the comparative proteomics analyses of isolated sarcosine-insoluble OMP fractions from clarithromycin-susceptible and-resistant *H. pylori* strains. The elongation factor Tu was downregulated, whereas transmembrane protein HopT was upregulated in clarithromycin-resistant *H. pylori* strains (25).

CHAPTER 3
RESEARCH METHODOLOGY

3.1 *H. pylori* clinical strain

The *H. pylori* strains were obtained from the *H. pylori* stock culture of the Center of Excellence in Digestive Diseases, Thammasat University, which was courtesy of Prof. Dr. Ratakorn Wilaichon (222), (223). The bacteria were responsible for cultivation by Ms. Pornpen Ngamnarai (under approval to research by the Ethics Committee Faculty of Medicine MTU-E-1-009/51). Each strain was randomly isolated from three excised stomach biopsies from patients as previously reported (222), (223). All of them were isolated from gastritis patients (8 females and 4 males). The mean ages of the patient in the Cla/Mtz-R, Cla-R, Mtz-R, and Sen-S sample were 45.7, 50.7, 56, and 51.3 years, respectively.

3.2 Sample Size

The samples used in this study were the samples from clinical stock culture, which are obtained from gastritis patients. They were divided into four groups (Cla-R, Mtz-R, C/Mtz-R, and Sen-S strains) and there were 3 samples in each group as shown in Table 3.2.

Table 3.2 Sample code, gender, and age, of the patient samples according to *H. pylori* stock culture.

Antibiotic susceptibility	Sample code	Gender	Age
Cla/Mtz-R	T3456	F	51
	T3489	M	33
	T3503	F	53
Cla-R	T2629	F	61
	T3086	F	49
	T3383	M	42
Mtz-R	T3307	F	68
	T3406	F	50
	T3455	M	50
Sen-S	T3469	F	58
	T3506	F	56
	T3526	M	40

3.3 Ethical and Biosafety Considering

The biosafety protocol has been approved by the Institute Biosafety Committee of Thammasat University (TU-IBC- 126/2019) and the Institutional Biosafety Committee of National Center for Genetic Engineering and Biotechnology (BT-IBC-19-056). In addition, this research has been ethical approved by the Human Research Ethics Committee No. 1 of Thammasat University (MTU-EC-ES-0-236/19).

3.4 Clinical Stock Culture

After the biopsies specimen were homogenized in saline, *H. pylori* were inoculated onto brain heart infusion (BHI) selective culture medium (Becton, Dickinson, Sparks, MD, USA), and then incubated under microaerophilic conditions (10% CO_2, 5% O_2, and 85% N_2) at 37°C for 5 to 7days. All *H. pylori* colonies were subcultured in 7% horse blood-rich BHI agar (Nippon Biotest, Tokyo, Japan) without the use of antibiotics. *H. pylori* bacteria was identified by microscopic characterization, gram staining, and confirmed by oxidase, catalase, and urease activity tests. The antibiotic susceptibility of *H. pylori* colonies is carried out through the identification of MICs. Initially, the *H. pylori* suspension was prepared by mixing the viable *H. pylori* strain into 7% horse blood-rich Mueller-Hinton II broth (Becton, Dickinson). A culture suspension equivalent to 2 McFarland standards was used for plate inoculation. Antibiotics susceptibility or antibiotics resistance were classified according to the recommendations of EUCAST, such as Cla (R ≥0.5 mg/mL) and Mtz (R≥8 mg/mL) (224), (225). Then, *H. pylori* strains were collected and stored at -80°C. Triplicate samples of *H. pylori* strains (numbers Cla-R 1-3, Mtz-R 4-6, Cla/Mtz-R 7-9, and Sen-S 10–12) were individually recovered in BHI broth, incubated at 37° C, 3 days (220). This was done after research ethical approve from the Research Ethics Subcommittee in People Thammasat University Series 1 (approval number 236/2019). All bacterial strains were ensured to be *H. pylori* through microscope identification, as well as specific enzyme analysis (oxidase, catalase, and urease activity test) before studying the protein secretion by proteomic study. Moreover, the antibiotic susceptibility test according to EUCAST recommendations was also confirmed. All procedures were performed under the standard guidelines and specific regulations for special microbiological practices (biosafety level II).

3.5 The preparation of secreted protein from *H. pylori* clinical strains for the proteomic study.

Preparation of secreted protein from three samples of each strain (Cla/Mtz-R, Cla-R, Mtz-R, and Sen-S) of *H. pylori* was performed as described previously (220). In brief, each *H. pylori* sample was cultivated in BHI broth in a microaerobic environment at 37°C. When the culture suspension was reached 0.5-1 McFarland units at $OD_{600\ nm}$, the *H. pylori* were collected by centrifugation. The bacterial pellets were then washed with BHI and cultured in a fresh BHI broth (three samples for 20 mL each, independently) until an optical density at 600 nm of 0.01 was reached. Then, all of the three *H. pylori* samples were independently cultivated according to this condition: 37°C, 150 rpm (20 to 24 h till an optical density at 600 nm of 0.3 to 0.5). The cell pellet of *H. pylori*, and its supernatant, were separated by centrifugation at 5,000×g for 10 minutes at 4°C. To remove cell debris, the supernatant was consequently centrifuged at 10,000×g for 10 min at 4°C. Finally, the supernatant from the previous step was then filtered through a membrane filter of 0.2 mm pore size. The cell pellets are used for RNA isolation to perform the reverse transcription for the quantification of the gene of interest by real-time PCR.

3.6 Protein Determination

Protein concentrations were performed according to Lowry method (226) and used bovine serum albumin (BSA) as a standard. It was done on 96-well plate. In brief, pipette 5 µL of diluted sample solution (1:25) or BSA standard solution (2-10 mg/mL) into separate 96-well microtitration plates. Then add 200 µL of freshly prepared reagent A (copper ions in alkali solution, 0.4 % $CuSO_4.7H_20$ in tartaric acid, 5% SDS, 0.8 molar NaOH, and sodium carbonate. 20%) and incubated at room temperature for 30 minutes. At the end of the time, 50 µl of reagent B (20% folin-ciocalteu reagent) was added and incubated in the dark at room temperature for 30

min. Finally, the absorbance was measured at OD_{690} with a microtiterplate reader (Rayto, Rayto Life and Analytical Sciences Co., Ltd., Shenzhen, China) and the concentration of protein samples was determined using standard BSA standard curves.

3.7 In-solution Digestion

50 micrograms of protein are digested by a slightly modified in-solution digestion process (227), (228). In brief, 50mg of protein sample was resuspended in 10µl of solution X (10mM AMBIC solution (Sigma, USA); NH_4HCO_3 in double-distilled water [ddH_2O]). To cleave disulfide bonds, 10µl of solution Y (5mM dithiothreitol, DTT (GE Healthcare, UK) in AMBIC solution) was subsequently pipetted into the sample tubes, and incubated for 1 hour at 60°C. For alkylate proteins, the samples, which were placed back to ambient temperature, were added to the reconstituted iodoacetamide (GE Healthcare, UK) in the AMBIC solution. Then, the samples were incubated at room temperature in the dark for 60 minutes. At the end of time, 20 µL of sequencing-grade trypsin (1:20 wt/wt) (Promega, Walldorf, Germany) was added to perform trypsin digestion and incubated overnight at room temperature. The peptide solution was dried in a high-speed vacuum centrifugal dryer (Savant AES 1010 SpeedVac® concentrator, Thermo Fisher Scientific Ltd, MA, USA) and stored at -20 °C until use.

3.8 Protein Quantitation and Identification (Nano LC/MS/MS Analysis)

The peptide samples from the previous step were protonated with 0.1% formic acid solution (Merck, Germany). Then, the 1 µl sample was injected triplicately into a nano HPLC system (Ultimate 3000 LC System, Thermo Fisher Scientific, Waltham, MA, USA) coupled to an ion trap MS (HCTultra Ion Trap, Bruker Daltonics). Subsequently, fractionation of the samples was performed using a reverse-phase high-efficiency liquid chromatography column (Acclaim PepMapTM 100 Å, 75 µm×5 cm; Thermo Scientific, UK and PepSwift Monolithic Trap Column 200 µm×5 cm; Thermo Scientific, UK) in combination with an ion trap MS (HCTultra Ion Trap, Bruker Daltonics).

The mobile phase was 0.1% formic acid in H_2O (buffer A) (0.1% formic acid/99.9% water (v/v)) and 0.1% formic acid in 80% ACN (buffer B) (0.1% formic acid/ 80% acetonitrile/19.9% water/ (v/v/v)). Peptides were eluted with a 4%-70% linear gradient mobile phase protocol as follows: 0-20 minutes with buffer B, 20-25 minutes with 90% of buffer B, and re-equilibration the column with 5 minutes of 96% buffer A. Finally, mass spectra of gradient eluted peptides were analyzed by Data Dependent Acquisition (DDA) mode with an MS_1 precursor scan (m/z 400–1,500). The top five most abundant multiply charged ions were selected for MS_2 fragmentation from MS_2 scans (m/z 200–2,800).

3.9 Data Analysis

3.9.1 DeCyder™ MS Differential Analysis Software

All MS/MS raw files were converted with CompassXport software (Bruker Daltonics) to mzXML files. Then these files were processed with DeCyder™ MS 2.0 Differential Analysis (DeCyder MS, GE Healthcare, Amersham, UK) (229) (230), for measuring the peptide intensity based on peptide MS signal of the individual LC-MS analyzed data. First, the isotropic peaks were determined to assign the charge states of peptide. The PepDetect module of DeCyder™ MS was used to optimize the Intensity, analyze, and detect peptide ions with the following data set: ion trap, mass resolution, 0.6 u; typical peak width, 0.1 min; charge status, from 1 to 4; and m/z shift tolerance, 0.1 u. Then, detected peptides were transferred to the PepMatch module of DeCyder™ MS. The PepMatch module of DeCyder™ MS was used for matching of peptides from different signal intensity chromatogram. The highest-intensity sample was used as a control, presenting the relative abundance of peptides as log2 intensities with mass tolerance set to 0.5 amu. In alignment intensity map step of the DeCyder™ MS software, the highest-intensity sample should contain all (or most) peptides present in the other intensity sample. An average abundance ratio of more than two-fold was

determined as an over-expressed protein with a significant standard t-test and one-way ANOVA $p < 0.05$.

3.9.2 MASCOT Software Version 2.3.0

All MS/MS spectra analyzed by the Decyder™ MS software was used to search for in silico MS/MS spectra against a *Helicobacter pylori* database (2,306 sequences; downloaded on 19 December 2019) from NCBI (National Center for Biotechnology Information, Bethesda US) (https://www.ncbi.nlm.nih.gov/) using MASCOT software version 2.3.0. (Matrix Science, London, UK) (231). Firstly, the enzyme specificity was set to trypsin with allowing up to 3 missed cleavages. Secondly, the precursor mass tolerance was set to 200 ppm for first search and set respectively such as peptide mass tolerance of 1.2 Da., fragment mass tolerance of ±0.6 Da., peptide charge state of 1+, 2+ and 3+, mass values of monoisotopic. Next, cysteine carbamidomethylation was selected as fixed modification and methionine oxidation was selected as variable modification. Finally, the mascot DAT file were merged with evaluated peptide level by DeCyder™ MS 2.0 Differential Analysis software and the data was exported to Microsoft Excel. Proteins considered as identified proteins was at least one peptide with an individual MASCOT score corresponding to $p<0.05$. Then, identified proteins were filtered with a one-way ANOVA $p<0.05$. In this experiment, the relative quantitation was obtained by normalize based on internal standards of 200 fmol bovine serum albumin (BSA).

In addition, the data were represented by heatmap by using the Multi Experiment Viewer (MEV) software version 4.9.0 (232). Moreover, the Bioinformatics and Evolutionary Genomics tool or Venn diagram (http://bioinformatics.psb.ugent.be/webtools/Venn/) was used to compare interaction of secreted proteins between sensitive and resistant groups. Specially, the PANTHER program 15.0 (The Protein Analysis Through Evolutionary Relationships Classification System-Geneontology Unifying Biology) (http://pantherdb.org/) was used to classify in term cellular component, molecular and biological functions. Furthermore, the Stitch database version 5.0 (http://stitch.embl.de/) was used to analyzed association of chemicals-proteins and protein-protein interacted network.

3.10 Quantitative RT-PCR (qPCR) Analysis

The expression of two genes of interest, the beta-beta subunits (*rpoB* gene) and Fructose-bisphosphate aldolase (*fba* gene), from all *H. pylori* strains used in this study, were performed by a quantitative real-time reverse transcription-PCR (RT-PCR) technique.

3.10.1 Primer Design

All of the reverse and forward primers were designed from *H. pylori* 26695 template DNA by Primer3 software web (https://bioinfo.ut.ee/primer3-0.4.0/) and were listed in Table 3.10.1. The 6 pairs of designed primer were subsequently compared with the GenBank database (https://blast.ncbi.nlm.nih.gov/Blast.cgi).

Table 3.10.1 Primer PCR for Real-time PCR

Name		product size (bp)	5'---------->3'	Length
rpoB	F	190	ATATGCGCTACAGGAGTGGC	20
	R		AACGAGACGGCTTGTTTTGC	20
fba	F	161	GGTGGGGGCGTTTAATTTCG	20
	R		AGCGTTCGCACATGGTTTTC	20
16s	F	152	GCTCTTTACGCCCAGTGATTC	21
	R		GCGTGGAGGATGAAGGTTTT	20

3.10.2 PCR Amplification

Parameters for 40 PCR reaction repetition cycles include: denaturing at 95 ℃ for 30 seconds, annealing at 60℃ for 30 seconds, and extending at 72℃ for 30 seconds. Finally, PCR products were run on 2% agarose gel to estimate their size.

3.10.3 Total RNA Extraction

Total RNA from 10^8 cells/ml of bacterial cell pellet (from Cla-R, Mtz-R, Cla/Mtz-R, and Sen-S strains of *H. pylori*-associated gastritis) from step 3.5 were isolated by a GenUP™ total RNA kit (Biotechrabbit, Germany) according to the manufacturer's protocols. In brief, the cell lysates were transferred to a mini-filtered DNA (blue) placed in a collection tube. After centrifugation at 8,000×g for 2 minutes, the supernatant DNA fraction was then discarded. The filtrate (which is RNA) was added with equal amounts of 70% ethanol and transferred to Mini Filter RNA (purple) placed in new collection tubes. The RNA sample was 2xwashed with buffer wash A and buffer wash B. Finally, the RNA pellet was eluted with DEPC treated water.

3.10.4 qPCR Analysis

9 µg of RNA was converted back to cDNA with the following reagents added: 1 µg of oligo dT, 10 µl of (2x) SuPrimeScript RT-PCR Premix (GeNet Bio, Korea). The mixture was then incubated at 42℃ for 60 minutes. qPCR was subsequently amplified by adding the reaction mixture to a total volume of 10 µl as follows: 1 µl of 100 ng cDNA, 0.4 µl of 10 pmol/ µl forward and reverse primers, 5 µl of 5x Hot Firepol Evagreen qPCR master mix (Solis BioDyne), and 3.2 µl of nuclease-free water. The mixture was then amplified on an Exicycler™ 96 Real-Time PCR Instrument (Bioneer, Korea). Parameters for 40 qPCR repetition cycles are: denaturing at 95℃ for 30s, annealing at 60℃ for 30s, and extending at 72℃ for 30s. The experiment was performed in 3 independently duplicate tubes. qPCR's result was defined as the cycle threshold (Ct) value. However, for internal standardization, 16S RNA Ct values for each sample were used to compare the relative expressions for the qPCR results. In addition, the relative transcript levels were determined by $2^{-\Delta\Delta CT}$ (233). Data were analyzed by a statistically significant student t-test at $p < 0.05$.

3.10.5 Sequencing Analysis The nucleotide sequence of PCR products from 3.10.2 analyzed by U2bio Inc. with the 96-capillary 3730xl DNA Analyzer (Applied Biosystems®). The nucleotide sequences that are the product of PCR of both the *rpoB* gene and the *fba* gene were aligned with forward primer, reverse primer and searched against all gene available in NCBI using NCBI Alignment Search Tool (BLAST) online database program (https://blast.ncbi.nlm.nih.gov/Blast.cgi?PAGE_TYPE=BlastSearch) (blastn). In addition, the nucleotide sequence was in silico translated and compared with other related proteins by blastx.

CHAPTER 4
RESULTS AND DISCUSSION

As a key mediator of host-pathogenic interactions, particular interest is drawn to the study of the secreted proteins of *H. pylori* since they are in direct contact with host tissues (220). However, some of them are still difficult to analyze and require special techniques. Proteomics is another technique popularly used to study protein secretion from *H. pylori* strains by using a protein-free culture medium. Such studies are called secretomics, which are techniques for analyzing all secreted proteins. In this study, proteins secreted from three antibiotic-resistant strains of *H. pylori*-associated with gastritis (Cla-R, Mtz-R, Cla/Mtz-R), were compared with those secreted from antibiotic-susceptible strains by proteomic tools via in-solution digestion and quantitative analysis through nanoLC-MS/MS. The experiment was done with the triplicate of each group. They are therefore studied further by using bioinformatic tools such as Heatmap, Ontology, Venn diagram, Protein-ligand interaction. According to the study, two of the most interesting proteins were found: rpoBC and FBPAII. To study the expression at the genomic level, their mRNA level from all of the 4 strains (Table in Appendix E) was determined by RT-PCR (qPCR) Analysis. The results might be expanding the knowledge of this protein in *H. pylori*-associated with gastritis strains.

4.1 The identification of Differential Expressed Proteins by Proteomics.

4.1.1 Mass Spectrometry via LC-MS/MS

The present study used in-solution digestion and mass spectrometry approach to compare and separate the secreted proteins of clarithromycin-resistance to *H. pylori* (Cla-R), metronidazole-resistance to *H. pylori* (Mtz-R), dual resistant with clarithromycin, and metronidazole to *H. pylori* (Cla/Mtz-R) and sensitive strains (Sen-S). Based on the fact that mass spectrometry is a high sensitivity method for protein quantitation. It is, however, proteins that are abundant in protein mixtures tend to drown out the signals from less abundant proteins. Therefore, the chromatography

technique is often employed to separate proteins from complicated protein mixtures and resolving into individual peptides before mass spectrometry. The decisive parameter was achieved using the intensity of maximum protein represented as log^2 intensities which were indicated by DeCyder™ (DeCyder MS, GE Healthcare, Amersham, UK). The data were filtered to show different expression changes with only a statistically significant value, $p < 0.05$ (one-way ANOVA and standard t-test) as mentioned above. From this criteria, quantitative analysis of LC-MS/MS showed 592 differential expressed proteins (Figure 4.1.1(1) and Table in Appendix E), of which 590, 583, 582, and 578 proteins were identified from Cla/Mtz-R, Cla-R, Mtz-R, and Sen-S samples, respectively (Figure 4.1.1(2)). After that, the data will be shown on a heat map diagram (the Multi Experiment Viewer (MEV) software version 4.9.0) which gave a significant overall picture of the up- and down-regulated proteins in each strain (Figure 4.1.1(1)).

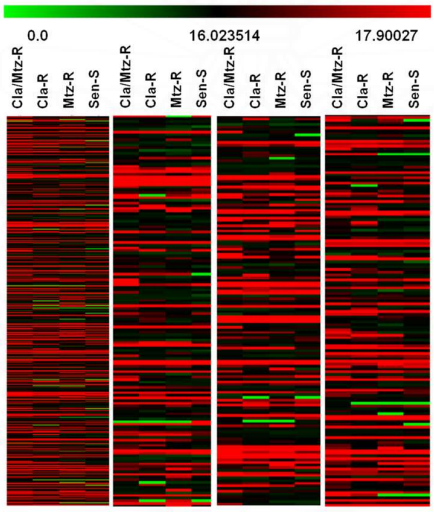

Figure 4.1.1(1) A Heatmap analysis of the 592 secreated proteins differentially expression in Cla-R, Mtz-R, Cla/Mtz-R, and Sen-S *H. pylori*-associated with gastritis (meanings of all abbreviations as shown in the text above). A higher-than-average abundance of a protein (indicated by log^2) is displayed in shades of red, whereas reduced abundance is displayed in shades of green.

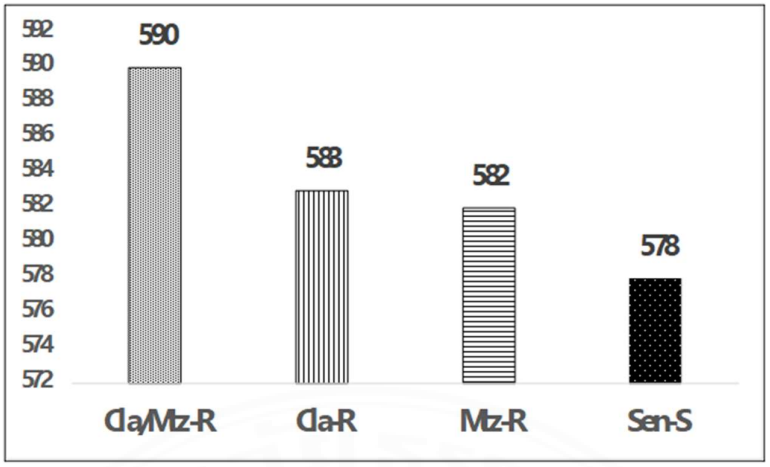

Figure 4.1.1(2) Comparison bar graph of secreted proteins found from Cla/Mtz-R, Cla-R, Mtz-R, and Sen-S *H. pylori*-associated with gastritis strains by LC-MS/MS technique. A protein found on 590, 583, 582, and 578 belonged to the Cla/Mtz-R, Cla-R, Mtz-R, and Sen-S strains, respectively (meanings of all abbreviations as shown in the text above).

When comparing the amount of protein secreted by *H. pylori* with the original article we cited on the separate protein secretion method, the researchers found that the amount of protein secreted by *H. pylori* was different. The results of this study found that the amount of protein secreted was 20 times greater (592 secreted proteins versus 26 secreted proteins from the reference work) (220). This difference is likely due to two main reasons. The first is likely a result of differences in protein preparations (in-solution digestion versus in-gel digests). In-solution digestion, the method used in this study, is a higher throughput method than in-gel digestion. It is also a method that can be used to identify all peptides in the solution (234). Secondly, this is probably due to the result of the genetic diversity of the *H. pylori* clinical strain, which is consistent with the previous report (235). However, this study used only three sample sizes per strain, which may be our limitation. In conclusion, all of these discussions demonstrate that our experimental procedure was carried out to investigate the protein secreted by *H. pylori* bacteria.

4.2 The Classification of the Secreted Proteins by the PANTHER version 15.0 (Protein Analysis Through Evolutionary Relationships Classification System) (http://pantherdb.org/).

4.2.1 Classification based on cellular components.

Total identified secreted proteins were classified by the PANTHER version 15. 0 software (Protein Analysis Through Evolutionary Relationships Classification System) (http://pantherdb.org/) that according to Gene Ontology. The classification group based on cellular components reveal that the majority of the secreted proteins are **(1) cellular anatomical entity** (52%), **(2) protein-containing complex** (39%) **(3) intracellular** (9%) as shown in figure 4.2.1. Example of the proteins in each group shown in the table 4.2.1.

Table 4.2.1 Example of the proteins classified based on cellular components by the PANTHER program. (Search at 200621)

#	Part	Example	%
(1)	**cellular anatomical entity**	Mucin-6, Ferric uptake regulation protein, Glutamine synthetase, Flagellar hook protein FlgE, Enolase, Thiamine- phosphate synthase, 29 kDa ribonucleoprotein, chloroplastic	52
(2)	**protein-containing complex**	Chaperone protein ClpB, Phosphopentomutase, Catalase, Thiamine- phosphate synthase, Flagellum site-determining protein YlxH	39
(3)	**intracellular**	30S ribosomal protein S5, 30S ribosomal protein S9, Protein HP_1247, Enolase, ATP synthase subunit c, DNA gyrase subunit A, Probable iron chelatin transport ATP-binding protein	9

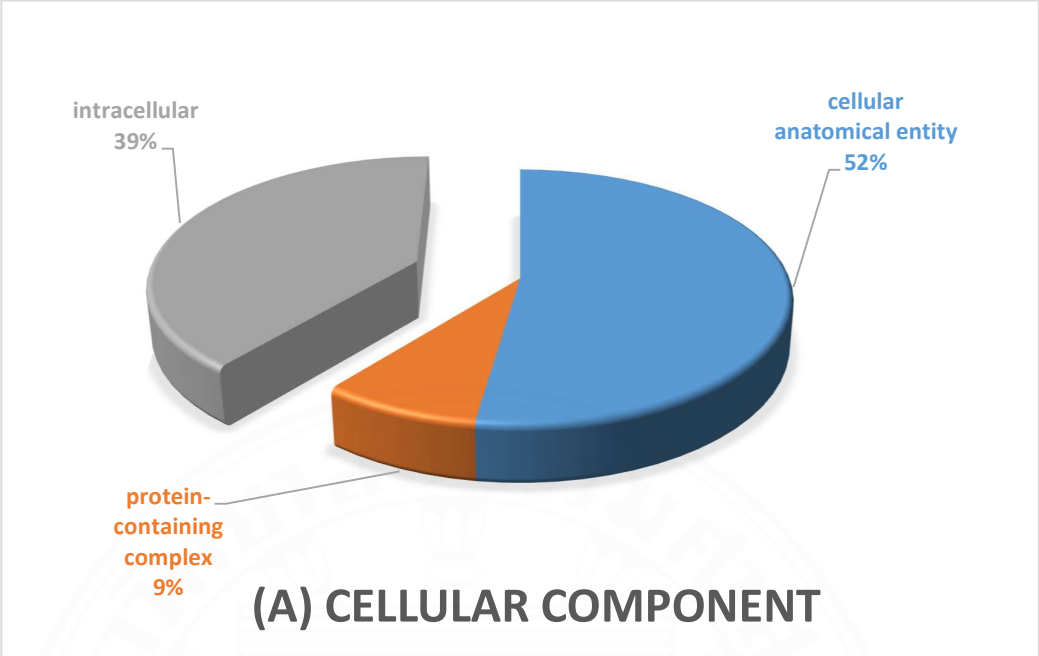

Figure 4.2.1 Pie chart of percentages classified from 592 secreted proteins identified based on cellular component via the PANTHER version 15.0 software.

4.2.2 Classification based on biological process.

When classifying 592 secreted proteins by their biological process via the PANTHER version 15.0 software, most of the proteins are found in the **cellular process** (46%) and **metabolic process** (40%) (Figure 4.2.2). The remainder were distributed in the functional areas of localization (5%), biological regulation (4%), response to stimulus (3%), and signaling (1%). Example of the proteins in each group shown in table 4.2.2.

Table 4.2.2 Example of the proteins classified based on biological process by the PANTHER program. (Search at 200621)

#	Part	Example	%
(1)	**cellular process**	Enolase, Fumarate hydratase class II, Fumarate reductase flavoprotein subunit, Aspartyl/ glutamyl-tRNA (Asn/ Gln) amidotransferase subunit B, GTPase Era, Pantothenate synthetase, Orotate phosphoribosyltransferase	46
(2)	**metabolic process**	Triosephosphate isomerase, Fumarate reductase iron-sulfur subunit, Aconitate hydratase B, Catalase, Hydrogenase/ urease maturation factor HypA, Adenosylmethionine- 8- amino- 7- oxononanoate aminotransferase	40
(3)	**localization**	Flagellar hook protein FlgE, Adhesion G protein-coupled receptor B1, Motility protein A, Nucleoside permease NupC	5
(4)	**biological regulation**	Interferon gamma receptor 1, Nuclear factor erythroid 2-related factor 2, Interferon gamma receptor 1, Ferric uptake regulation protein	4
(5)	**response to stimulus**	Chaperone protein ClpB, Catalase, Adenine DNA glycosylase, Serine/threonine-protein kinase MARK2	3
(6)	**signaling**	Interferon gamma receptor 1, Serine/ threonine-protein kinase MARK2	1

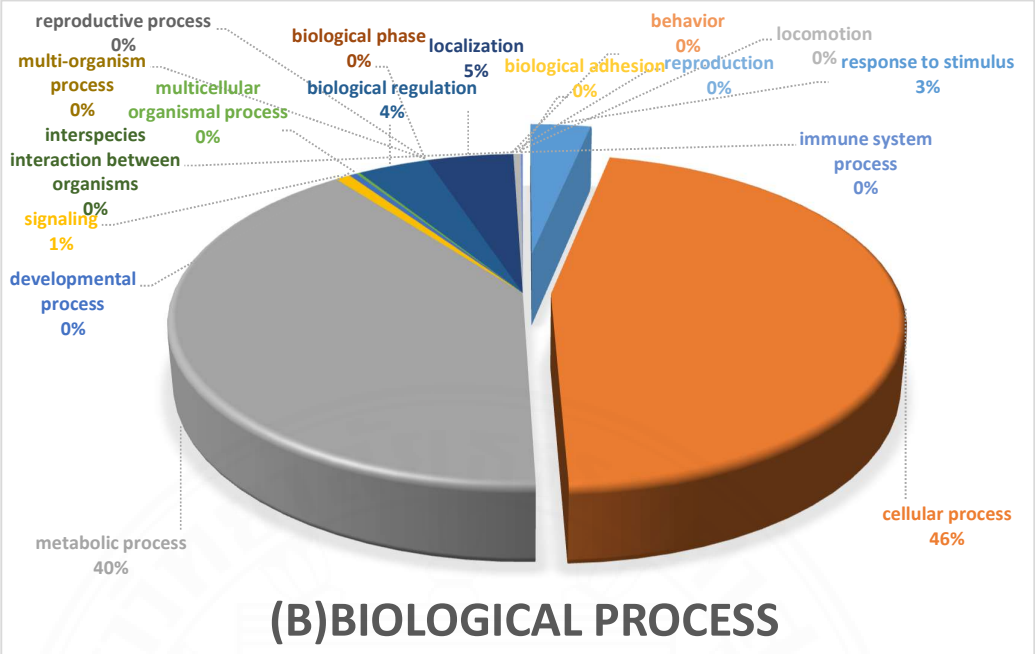

Figure 4.2.2 Pie chart of percentages classified from 592 secreted proteins classified based on the biological process via the PANTHER version 15.0. Two most of the functions found are cellular process (46%), and metabolic process (40%).

4.2.3 Classification based on molecular function.

In addition, 592 proteins were classified according to their molecular functions. Most of these identified proteins are responsible for **catalytic-related activity** (57%), and **binding-related activity** (31%). Few have molecular functions related to transport (5%), regulator (3%), transducer (2%), and structural molecule activity (2%). Example of the proteins in each group shown in table 4.2.3.

Table 4.2.3 Example of the proteins classified based on molecular function by the PANTHER program. (Search at 200621)

#	Part	Example	%
(1)	**catalytic-related activity**	Glutamine synthetase, Hydrogenase/ urease maturation factor HypB, Tyrosine-tRNA ligase, DEAD-box ATP-dependent RNA helicase RhpA, Phospho-N-acetylmuramoyl- pentapeptide- transferase, Serine/ threonine- protein kinase MARK2, Heme oxygenase HugZ, Enolase, Aspartyl/ glutamyl- tRNA (Asn/ Gln) amidotransferase subunit B, ATP-dependent Clp protease adapter protein ClpS	57
(2)	**binding-related activity**	Aconitate hydratase B, Cysteine synthase, Catalase, DNA gyrase subunit A, Adenine DNA glycosylase, Chorismate synthase, ATP-dependent Clp protease adapter protein ClpS, Iron- sulfur cluster carrier protein	31
(3)	**transport activity**	Magnesium transport protein CorA, Fe (2+) transporter FeoB, Probable iron chelatin transport ATP-binding protein HP_0888	5
(4)	**molecular function regulator**	Ferric uptake regulation protein, Nuclear factor erythroid 2-related factor 2, Beta-lactamase HcpA	3
(5)	**molecular transducer activity**	Adhesion G protein-coupled receptor B1, Interferon gamma receptor 1	2
(6)	**structural molecule activity**	30S ribosomal protein S5, and 30S ribosomal protein S9	2

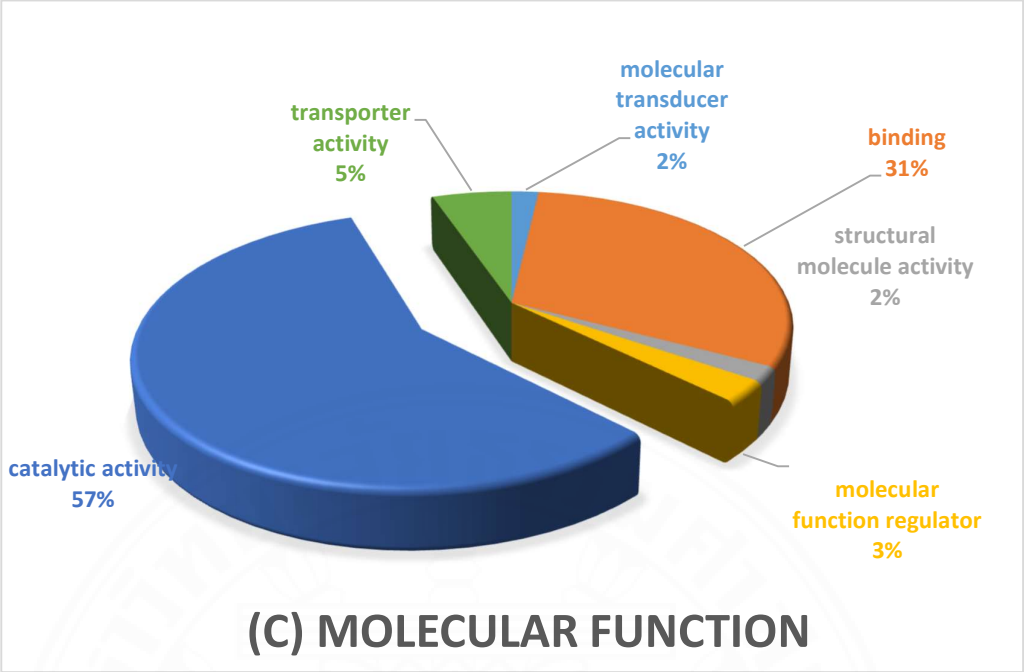

Figure 4.2.3 Pie chart of percentages classified from 592 secreted proteins identified based on molecular function via the PANTHER version 15.0 software. Two most of the functions found are related to the catalytic-related activity (57%), and binding-related activity (31%).

As the results of the study revealed that the main functions of the 592 secreted proteins found in this study are related to cellular processes. and metabolic processes (Figure 4.2.2), these are groups of proteins that are often responsible for the metabolism that occurs in the cytoplasm. The next question is how do proteins that act primarily in cells secrete out of the cell? The answer to that question has been previously studied extensively. These include the mechanism involving in (1) activation of cellular lysis via a protein that acts as adhesion, (2) activation of membrane degrading agents, (3) alteration of environmental osmotic stress. Furthermore, it also includes (4) an increase in membrane permeability and (5) an outer membrane vesicle (OMV) formation resulting from antibiotic-induced channel activation (236), (237). Among these processes, OMVs have recently been described as a release mechanism that plays a role in the transmission of virulence factors in Gram-

negative bacteria, including *H. pylori*. An example of a well-known *H. pylori* protein exported through OMV is vacuolating cytotoxin (VacA) (118). In addition, another well-known release mechanism that plays a role in the transmission of virulence factors in *H. pylori*, CagA, is the type IV secretion system (T4SS) which is described in detail in the review literature section of this thesis (148), (149). From these pieces of information, it may therefore be hypothesized that protein secretion from the *H. pylori*-associated with gastritis strains in this study was likely proceeded through the generation of OMV and/or the secretory system of T4SS. However, to know the exact mechanism, further investigation is required.

4.3 The Identification of Secreted Proteins by the Venn Diagram

Based on the distribution of proteins according to Venn diagrams, 569 overlapping proteins were found from all four groups (Figure 4.3.1). In addition, when considering the intersection of each group, 23 proteins were found to overlap between each group. In particular, if looking at the secreted proteins found only in the Sen-S strains, nine proteins were found (numbered 1 to 9 in Table 4.3). The names of the nine proteins in the order presented in Table 4.3 are as follows: 2,3-bisphosphoglycerate-independent phosphoglycerate mutase, bifunctional DNA-directed RNA polymerase subunit beta-beta9, UDP-3-O-acyl-Nacetylglucosamine deacetylase, iron chelation transport ATP-binding protein HP_0888, chaperone protein HtpG, glycine-tRNA ligase beta subunit, ribosome maturation factor RimP, portal protein, and fructose-1, 6 bisphosphate aldolase II [FBPAII]. Proteins #1-4 in Table 4.3 were found in Cla/Mtz-R, Cla-R, and Sen-S, but not in the secreted protein from Mtz-R. Whereas proteins #5-7 were expressed in Cla/Mtz-R, Mtz-R, and Sen-S, but not in the secreted protein from Cla-R. Proteins #8 was shown in both Cla/Mtz-R and Sen-S. Interestingly, protein #9 (fructose-bisphosphate aldolase, FBPAII), was represented only from the Sen-S strain. In addition to the unique proteins mentioned above, this study also identified two unique proteins specifically expressed in Cla/Mtz-R strains, i.e. GTP-binding protein TypA/BipA homolog and type III pantothenate kinase (protein #22-23

in Table 4.3). On the other hand, we do not find unique protein in the group of secreted proteins from Mtz-R and Cla-R strains.

In addition, 23 overlapping secretory proteins were then analyzed for heat mapping (Figure 4.3.2), the Sen-S strains exhibited less differentiated protein expression. Whereas the Cla/Mtz-R strain expressed the most differentially expressed proteins. This heatmap analysis also clearly demonstrated the unique protein of fructose-bisphosphate aldolase, FBPAII, which was found to be expressed only in the Sen-S strain.

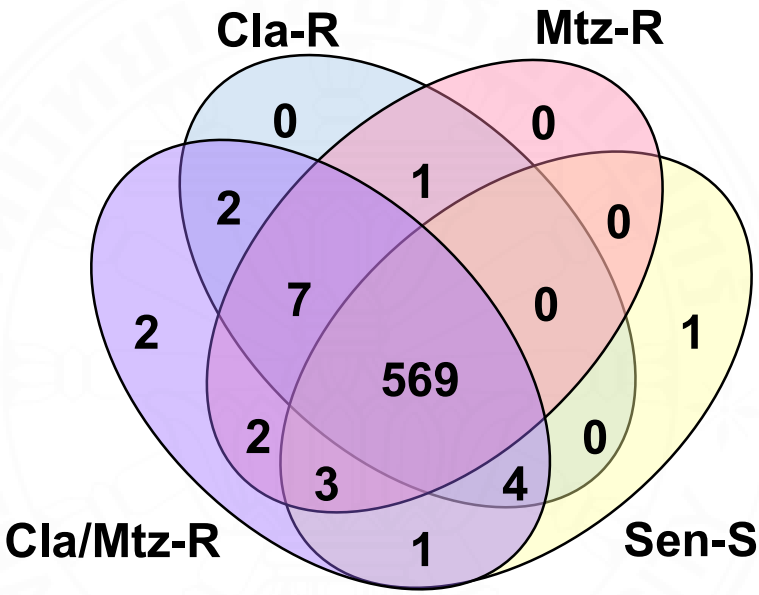

Figure 4.3.1 Venn diagram of 592 differentially expressed proteins identified by nano-LC-MS/MS analysis. 569 overlapping proteins from the four groups were found at the center of the Venn diagram. On the other hand, 23 proteins overlapping between each group were observed at the intersection of each group.

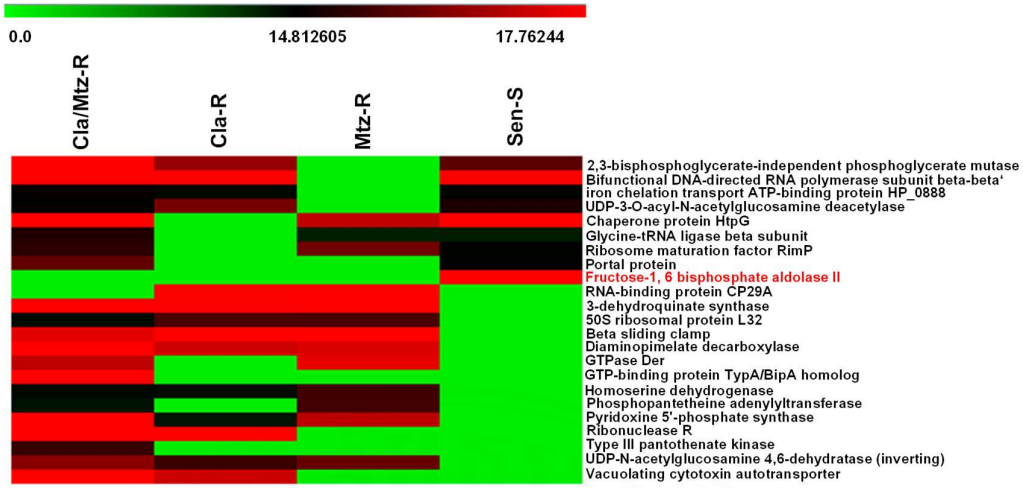

Figure 4.3.2 Heatmap analysis of 23 overlapping proteins among Cla/Mtz-R, Cla-R, Mtz-R, and Sen-S strains. A lower than average abundance of a protein (indicated by $\log^2$) is displayed in shades of green, whereas increased abundance is displayed in shades of red. The heatmap analysis showed that the secretory protein found only in the Sen-S strain was FBPAII (shown in red font).

Table 4.3 23 overlapping protein secretions expressed differently in each group of antibiotic-resistant strains from nano-LC-MS/MS analysis. The functions of proteins are classified according to the UniProt database (http://www.uniprot.org/).

#	GenBank Accession no.	Protein name	Gene name	Function	Peptide sequence	MOWSE score	Log 2 abundance			
							Cla/Mtz-R	Cla-R	Mtz-R	Sen-S
1	gi|123373726	2,3- bisphosphoglycerate- independent phosphoglycerate mutase (2,3 BPGM)	*gpmI*	glucose catabolic process [GO: 0006007] ; glycolytic process [GO:0006096]	VLIPSPK	2.62	18.11	16.56	0	**15.87**
2	gi|41017590	Bifunctional DNA- directed RNA polymerase subunit beta-beta' (rpoBC)	*rpoB*	transcription, DNA-templated [GO:0006351]	VGAGQIIADGPSMDR	4.6	19.98	19.66	0	**18.75**
3	gi|14285572	UDP- 3- O- acyl- N- acetylglucosamine deacetylase	*lpxC*	lipid A biosynthetic process [GO:0009245]	EFALQK	7.23	14.66	16.19	0	**15.14**
4	gi|2492572	iron chelation transport ATP- binding protein HP_0888	*HP_0889*	transmembrane ABC- transporter components FecE, ion transport [GO: 0006811] ; iron ion homeostasis [GO:0055072]	QMVLLAR	4.54	14.89	14.29	0	**14.47**
5	gi|118575192	Chaperone protein HtpG	*htpG*	protein folding [GO:0006457]	KTLELNPNHAILQK	1.24	18.03	0	17.04	**18.08**
6	gi|238064852	Glycine-tRNA ligase beta subunit	*glyS*	glycyl-tRNA aminoacylation [GO:0006426]	YFATFCQK	2.18	15.22	0	13.04	**13.23**
7	gi|6648012	Ribosome maturation factor RimP	*rimP*	ribosomal small subunit biogenesis [GO:0042274]	VEVKLINK	2.08	15.32	0	16.10	**14.67**
8	gi|426021105	Portal protein	*AC1LGJY*	head- to- tail connector in *H. pylori* bacteriophage KHP30 [GO:0099002]	QLLRLLAGLNDESLGMAVNR	2.34	15.95	0	0	**14.74**
9	gi|9789722	Fructose-1, 6 bisphosphate aldolase II (FBPAII)	*fba*	fructose 1,6- bisphosphate metabolic process [GO:0030388]; glycolytic process [GO:0006096]	KFFSPAQLALK	5.23	0	0	0	**22.40**
10	gi|2492962	3-dehydroquinate synthase	*aroB*	aromatic amino acid family biosynthetic process [GO: 0009073] ; chorismate biosynthetic process [GO:0009423]	MQEILIPLKEK	23.44	17.76	17.74	18.26	0
11	gi|2500328	50S ribosomal protein L32	*rpmF*	translation [GO:0006412]	MAVPDRR	3.47	14.12	15.71	15.67	0
12	gi|3913505	Beta sliding clamp	*dnaN*	DNA strand elongation involved in DNA replication [GO:0006271]	RELAGILMQFDQK	2.89	17.44	18.71	18.67	0

#	GenBank Accession no.	Protein name	Gene name	Function	Peptide sequence	MOWSE score	Log 2 abundance			
							Cla/Mtz-R	Cla-R	Mtz-R	Sen-S
13	gi|8134398	Diaminopimelate decarboxylase	*lysA*	lysine biosynthetic process *via* diaminopimelate [GO:0009089]	FGVEEK	1.4	20.33	17.22	17.36	0
14	gi|11132649	Homoserine dehydrogenase	*hom*	isoleucine biosynthetic process [GO: 0009097]; methionine biosynthetic process [GO: 0009086]; threonine biosynthetic process [GO:0009088]	AMLAYHRYELEQIAK	8.18	14.32	14.02	15.55	0
15	gi|226700973	Pyridoxine 5'-phosphate synthase	*pdxJ*	pyridoxine biosynthetic process [GO:0008615]	RHIQNEDVLR	6.69	18.71	13.73	16.99	0
16	gi|81341467	UDP- N- acetylglucosamine 4,6- dehydratase (inverting)*	*pseB*	not previously reported as the biological function	VLDTTNAK	3.65	16.41	15.47	16.01	0
17	gi|7674337	Ribonuclease R*	*rnr*	not previously reported as the biological function	EALQSNKDR	6.11	19.16	20.50	0	0
18	gi|2499107	Vacuolating cytotoxin autotransporter	*vacA*	pathogenesis [GO:0009405]	NDKNESAK	9.96	18.00	17.19	0	0
19	gi|238058975	GTPase Der	*der*	ribosome biogenesis [GO:0042254]	NTSPKTLK	3.29	17.01	0	17.50	0
20	gi|226709008	Phosphopantetheine adenylyltransferase	*coaD*	coenzyme A biosynthetic process [GO:0015937]	MMQLATKSFK	1.25	13.71	0	15.61	0
21	gi|30316379	RNA-binding protein CP29A	*CP29A*	chloroplast rRNA processing [GO: 1901259]; cold acclimation [GO: 0009631]; mRNA processing [GO:0006397]; RNA stabilization [GO:0043489]	SSYGSGSGSGSGSGSGNR	4.11	0	19.37	18.80	0
22	gi|8134781	GTP-binding protein TypA/BipA homolog	*typA*	ribosome biogenesis [GO:0042254]	CEEMGEGK	5.8	22.84	0	0	0
23	gi|81555831	Type III pantothenate kinase	*coaX*	coenzyme A biosynthetic process [GO:0015937]	SAKILEQPFK	4.63	15.47	0	0	0

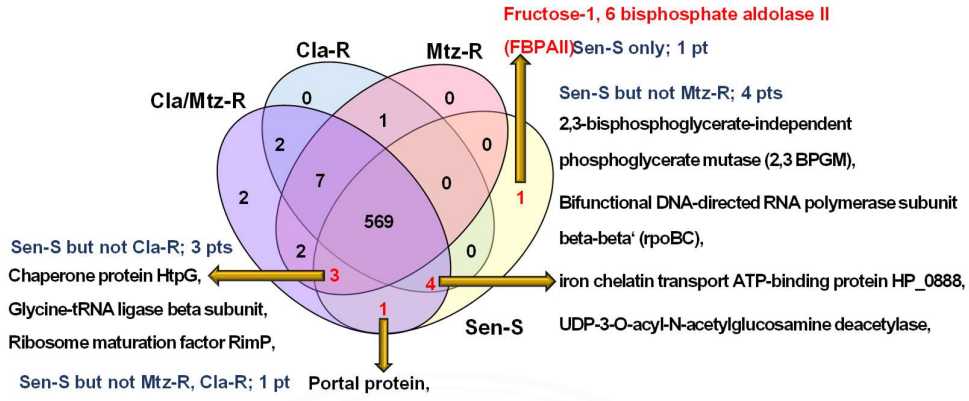

Figure 4.3.3 Venn diagram of 9 overlapped proteins base on the Sen-S strains from nano-LC-MS/MS analysis.

4.4 Protein-protein Interactions by STITCH database.

The protein-protein interaction identification of 23 overlapping proteins classified from Venn diagrams was subsequently studied through the STITCH database. Most show interactions with each other and with other known proteins, including with two antibiotics, clarithromycin and metronidazole. However, there are three exceptional proteins that do not interact with the substances mentioned above, i.e. iron chelatin transport ATP-binding protein HP_0888, Portal protein (Head-to-tail connector gp8) and RNA-binding protein CP29A (Figure 4.4.1).

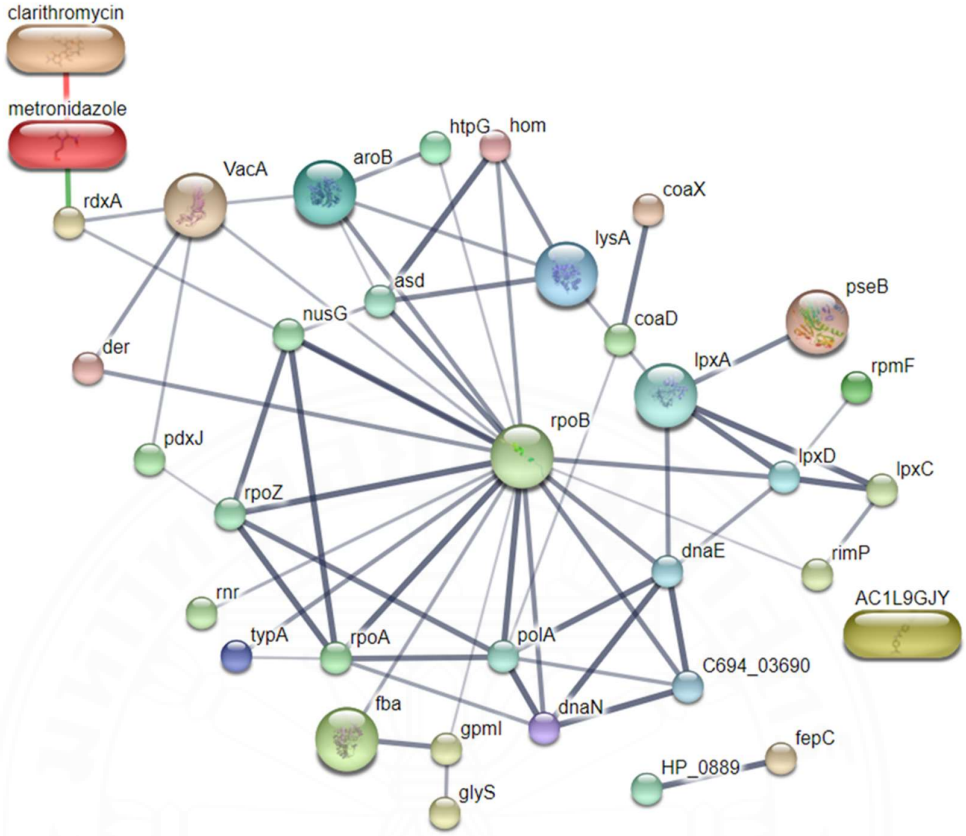

Figure 4.4.1 The interaction network between 23 secreted proteins in Table 4.3 and clarithromycin, metronidazole, and other known proteins by STITCH 4.0. The color of the lines denoting their relationship is as follows: antibiotic-antibiotic interactions are shown in red, protein-protein interactions are shown in gray, and antibiotic-protein interactions are shown in green.

To investigate the relationship of 9 secreted proteins from Sen-S strains (numbers 1 to 9 in Table 4.3) to other antibiotics and other proteins, their network was generated using the STITCH database. Based on its abundance in each strain, four STITCH interaction networks were predicted (Figure 4.4.2). They were categorized as follows: group 1 showed a predictive relationship between proteins #1-4 (the secreted protein found from Sen-S, Cla/Mtz-R, and Cla-R strains, but not from Mtz-R strain) with Cla, Mtz, and other known proteins (Figure 4.4.2(a)). Group 2 represented a predictive interaction between proteins #5-7 (the secreted protein found from Sen-S, Cla/Mtz-R,

and Mtz-R strains, but not from Cla-R strain) with the same group of antibiotics/other known proteins as mention earlier (Figure 4.4.2(b)). Group 3 and 4 present STITCH networks between Cla, Mtz and, other known proteins with protein #8, and #9, respectively (Figure 4.4.2(c) and (d)).

Based on the STITCH prediction of group 1, the bifunctional DNA-directed RNA polymerase subunit beta-beta' (*rpoB*) is the central junction between two proteins: 2,3-BPGM (2,3-bisphosphoglycerate-independent phosphoglycerate mutase) (*gpmI*), UDP-3-O-acyl-N-acetylglucosamine deacetylase (*lpxC*), and the antibiotics (Cla and Mtz). The relationship is via oxygen-insensitive NADPH nitroreductase (*rdxA*). Meanwhile, the prediction of group 2 found that all of the three proteins: chaperone proteins HtpG (*htpG*), glycine-tRNA ligase beta subunit (*glyS*), and ribosome maturation factor RimP (*rimP*), interacted with both antibiotics via *rdxA* as well. However, the central protein junction is 60-kDa chaperonin (*groL*), a protein found in the 569 secretory proteins previously mentioned (Appendix E). While neither protein-to-protein interaction nor protein-antibiotic interactions were observed from STITCH predictions of group 3 proteins (portal proteins, *AC1LGJY*). Ultimately, a unique protein from group 4: fructose-1,6 bisphosphate aldolase II (*fba*) was shown to be centrally linked to the two antibiotics via trios phosphate and *rdxA*. In summary, of all these predictive STITCH results, the protein secreted from the Sen-S strain directly interacting with the antibiotic was the bifunctional DNA-regulated RNA polymerase subunit beta-beta' (*rpoB*) and fructose-1,6 bisphosphate aldolase II (*fba*). Therefore, these two enzymes were identified for mRNA expression level via quantitative real-time reverse transcription-PCR (RT-PCR) analysis, which is shown in the next section.

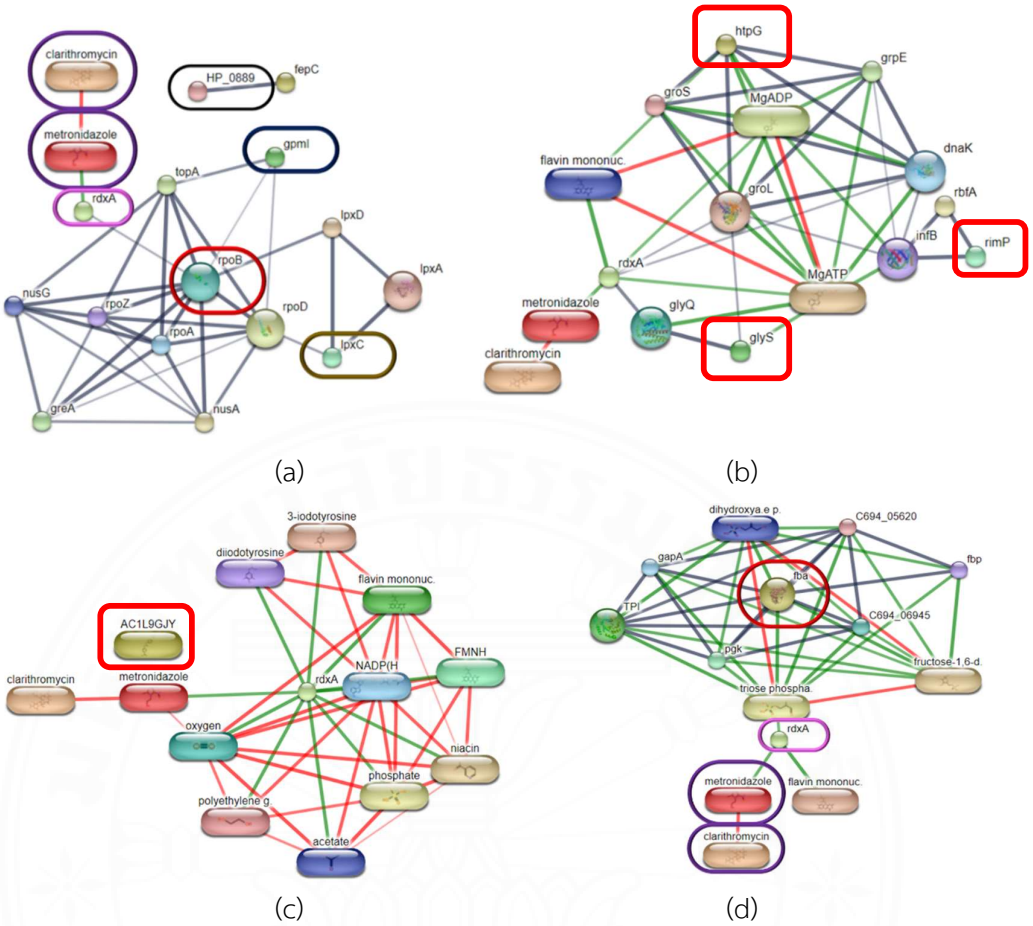

Figure 4.4.2 STITCH prediction between 9 secreted proteins found from Sen-S strains (#1-9 Table 4.3) with clarithromycin, metronidazole, and other known proteins. The color of the lines denoting their relationship is as follows: antibiotic- antibiotic interactions are shown in red, protein- protein interactions are shown in gray, and antibiotic- protein interactions are shown in green. As described in the section above, (a), (b), (c) and (d) represent the predictive networks of protein groups 1, 2, 3, and 4, respectively.

4.5 Quantitative real-time RT-PCR of *rpoB* and *fba*.

To further investigate the mRNA level expression of two proteins of interest: bifunctional DNA-regulated RNA polymerase subunit beta-beta' (*rpoB*) and fructose-1,6 bisphosphate aldolase II (*fba*), quantitative real-time reverse transcription-PCR (RT-PCR) was performed. Their forward and reverse primers are shown in table 3.10.1. By using the mRNA level of the Sen-S strain as a reference, *fba* and *rpoB* expressions derived from all three antibiotic-resistant strains (Cla/Mtz-R, Cla-R, and Mtz-R) were found to be opposite. i.e. upregulation of *fba* mRNA levels (approximately 2-fold) while downregulation of *rpoB* mRNA levels (Figure 4.5).

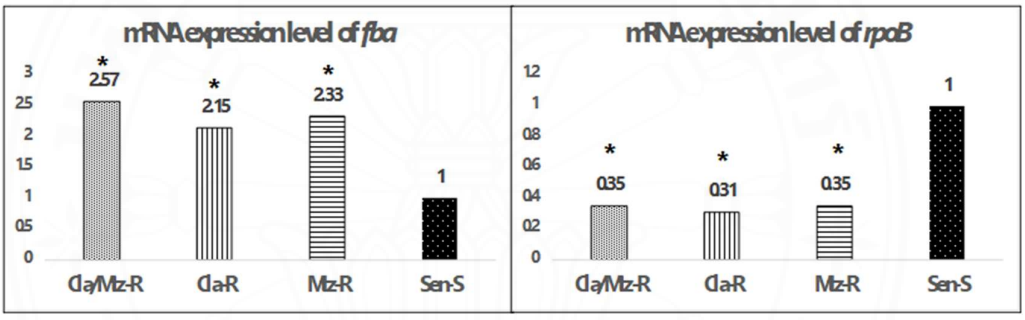

(a) (b)

Figure 4.5 Bar graphs of mRNA expression levels of two proteins of interest from Cla/Mtz-R, Cla-R, Mtz-R by quantitative real-time reverse transcription-PCR analysis compared to Sen-S strains as reference. (a) *fba*. and (b) *rpoB*. The folding change value was calculated using the expression level for which the Sen-S strain was referenced. The standard deviation from the three independent trials is represented by error bars. The significant difference (*) was at $P<0.05$.

4.6 Validation of *fba* and *rpoB* gene by DNA sequencing

The PCR products of the *fba* and *rpoB* genes from qRT- PCR were subsequently examined for their DNA sequence. In brief, after examining the size of PCR products by running on agarose gel electrophoresis, their DNA sequence was analyzed by U2 bio Inc. with the 3730xl 96- capillary DNA Analyzer (Applied Biosystems®). The nucleotide sequence of the PCR product gene was then aligned with forward primer and reverse primer on these template genes. In addition, the sequencing result had double-checked with NCBI Alignment Search Tool (BLAST) online database program (blastn). Moreover, the nucleotide sequence was validated by amino acid sequence alignment (blastx). The results from gel agarose are shown in figures 4.6 (a) and 4.6 (b). (*fba* had 161 bp and *rpoB* had 190 bp), and the result from blastn and blastx are shown in figures 4.6 (c) and 4.6 (d), respectively. When the nucleotide sequences are blasted on the nucleotide database, the alignment sequences are found to be aligned with the *fba* gene. But 1 point of silent mutation (from T to C) is found for the *rpoB* gene. Additionally, when nucleotide sequences were converted to amino acid sequences, and then blasted onto the amino acid database. Their amino acid sequences were found aligned with those of FBPAII and rpoB proteins.

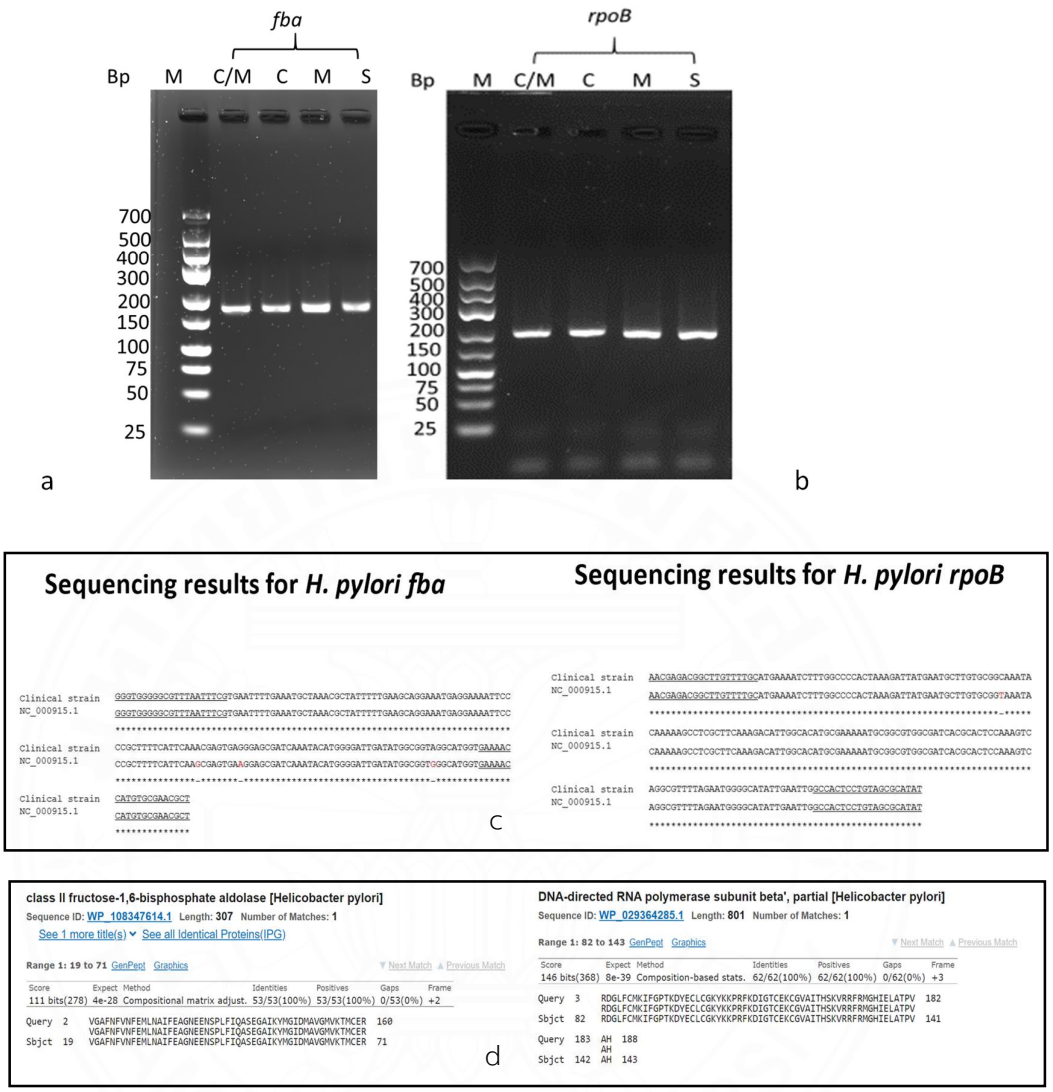

Figure 4.6 PCR product from *fba* (a) and *rpoB* (b) gene on agarose gel electrophoresis. The result from blastn (c) and blastx (d) database, respectively.

From the STITCH prediction of group 1 (Figure 4.4.2(a)), the central junction between 2,3-BPGM (*gpmI*), UDP-3-O-acyl-N-acetylglucosamine deacetylase (*lpxC*), and both of antibiotics (Cla and Mtz) is the bifunctional DNA-directed RNA polymerase subunit beta-beta' (*rpoB*). It is not surprising to found RNA polymerase in secreted proteins, as this has been reported previously (238). Additionally, *rpoB* mutations have been reported to play a major role in inducing *H. pylori* to resistant to rifampicin, an antibiotic used to eradicate *H. pylori* (239). However, *rpoB* mutations have also been reported in rifampicin-sensitive *H. pylori* clinical strains (240). Similar mutations of *rpoB* have also been reported to be associated with resistance to the two antibiotics concomitantly (241), (242). This data is consistent with our results that rpoBC was found in protein secretions from Sen-S, Cla-R, and Cla/Mtz-R *H. pylori* strains, but not from Mtz-R strains (Table 4.3). Additionally, the presence of a silent mutation of *rpoB* (Figure 4.6(c)) seems to explain the absence of rpoBC in proteins secreted by metronidazole-resistant *H. pylor*i strains used in this study. The result is likely related to these synonymous mutations. However, a poor correlation between the level of protein and mRNA level (down-regulation at the mRNA but up-regulation at the protein level) was observed (Figure 4.5(b)). This might be due to its mRNA instability, translation efficiency, rate of transcription, etc (243). Additionally, rpoBC has previously been reported to act as a MUC7 binding protein in *Streptococcus gordonii* (244), (245). It is possible that this protein's adhesin role may also be found in *H. pylori*. If this is the case, it is likely to be associated with better adhesion of *H. pylori* to the host epithelial cells. This likely promotes the pathogenesis of this bacteria. However, this issue cannot be discussed in relation to metronidazole resistance. It still requires more in-depth research. In addition, by detecting rpoBC in proteins secreted by *H. pylori* Sen-S, Cla-R and Cla/Mtz-R but not in Mtz-R strains, it is possible that this rpoBC secreted protein may associate with dual resistance or secondary antibiotic resistance mechanisms. In other words, it may be related to the mechanism by which *H. pylori* is still sensitive to metronidazole. To summarize this assumption, further studies with *rpoB* gene cloning and mutation analysis should be performed. Also, western blot analysis of this protein from all species should be done. Additionally, a re-examination of the total amino

acid sequence should be performed together with a prediction of three-dimensional structure.

Another interesting secretion protein is FBPAII. It is an enzyme that catalyzes pyruvate conversion to sugar in the *H. pylori* gluconeogenesis pathway (246). It has also been found to perform other functions including host cell adhesion and plasminogen-binding proteins in *Neisseria meningitides*, and *Paracoccidioides* respectively (247), (248). Moreover, there are many studies investigating FBPA class II as (1) a candidate protein for *Streptococcus pneumoniae* vaccine (249), (2) an immune surface target for the detection of *Listeria* genus (250), and (3) a new antibiotic promising target (251). Additionally, Ziveri et al. recently reported its function as a transcription regulator in *Francisella novicida* (252). According to our results, this protein was secreted from Sen-S only (Table 4.3). It implies that while *Helicobacter pylori* are still sensitive to antibiotics, this protein is secreted. In other words, if *Helicobacter pylori* have evolved into antibiotic-resistant pathogens, the bacteria will not secrete this protein. The results, therefore, support the work of Fonvielle et al., which investigated FBPAII inhibitors for the treatment of *Helicobacter pylori* (253). However, upregulation of the *fba* gene was found in all antibiotic-resistant strains from the qRT-PCR analysis (Figure 4.5(a)). This demonstrates that the results are inconsistent with the level of protein secreted. This inconsistency may be explained as a result of (1) delays in protein synthesis, as described by Liu et al. (254), (2) post-transcription and post-translational processes, and (3) protein degradation process as reviewed by Vogel and Marcotte (255). To explain these inconsistent results, a quantitative analysis of proteomic cell lysates should be performed using a protein expression enhancement technique such as SILAC (256). While the exact molecular mechanism linkage of FBPAII in *H. pylori*-susceptible strains remains to be explored. In conclusion, the results obtained from this research may expand knowledge about this protein in *H. pylori*-associated gastritis strains.

Finally, of the nine proteins secreted from the Sen-S strain, STITCH predictions revealed two proteins unrelated to Cla-R and Mtz-R (Figure 4.4.2(a) and (c)), i.e. iron chelation transport ATP-binding protein HP_0888 and portal protein (head-

to-tail connector gp8). The first protein was HP_0888, also known as transmembrane ABC-transporter component FecE. Studies have shown that it can induce immune responses (257). In addition, there have been studies that HP_0888 is a protein with immunogenic properties. Therefore, if further studies are conducted to determine that it is detected in the blood of patients during *H. pylori* infection, it would be useful to develop a new serological marker for antibiotic susceptibility testing (258). The last protein to be discussed is the portal protein. It is a protein that helps in the head-to-tail connection in *H. pylori* bacteriophage KHP30. Numerous studies have shown that KHP30 phages are associated with the genetic diversity of *H. pylori,* which is often found in clinically derived strains (259), (260), (261). Therefore, it may be another reason to explain the differences in the types of secreted proteins identified from different clinical *H. pylori* strains obtained from this study.

CHAPTER 5
CONCLUSIONS AND RECOMMENDATIONS

As previously mentioned, untreated *H. pylori* infection is the leading cause of chronic gastritis. This is a condition that can develop into stomach cancer. Therefore, eradication of *H. pylori* with two antibiotics (Clarithomycin and Metronidazole) and proton pump inhibitors is not only the treatment of choice but also effectively prevents the incidence of gastric cancer. However, the current treatments mentioned above are less effective due to the antibiotic resistance of *H. pylori*. The prevalence of *H. pylori*-resistant strains (Cla/Mtz-R, Cla-R, and Mtz-R) has continued to increase over the past several years (5), (262), (263). Currently, studies on protein secreted by clinical strains of *H. pylori* are of increasing interest. Because it is a group of proteins that come into direct contact with tissues. And it's because these secreted proteins play a key role in host-pathogen interactions (264), (265), (266). However, few studies have compared protein secreted by antibiotic-susceptible and antibiotic-resistant of *H. pylori* clinical strains (25), (26), (45). An important research question is; what proteins do antibiotic-susceptible *H. pylori* strains secrete? This question could be answered by studying the protein secreted from antibiotic-susceptible strains versus proteins from antibiotic-resistant strains. These findings could be useful in the development of new serological tools or new drug targets that may improve the diagnosis or treatment of *H. pylori* infection. Therefore, the aim of this study was to examine new protein candidates secreted from Sen-S strains and comparing with proteins secreted from *H. pylori*-associated with gastritis strains (Cla/Mtz-R, Cla-R, and Mtz-R) by proteomics method (in-solution digestion coupled with nano-LC-MS/MS).

Before conclusion, it is important to ensure that the methods used to separate culture supernatant from *H. pylori* cell pellet actually yield the secreted protein and does not contain the inner membrane and outer membrane proteins. Therefore, a comparison was made to examine the types of proteins previously reported for the *H. pylori*-secreted proteins and the secreted proteins found in this study. Of the 569 proteins found in this study, no specific proteins classified as markers

of inner and outer membrane proteins (i.e. UreI and HopB) were identified, indicating that this method results in no contamination of these group of proteins (267). The findings also revealed a number of *H. pylori*-secreted proteins found in our research and other studies. Examples of these are the cag-PAI protein (CAG-PAI 12, 13, and 23), plasminogen-binding protein PgbA, flavodoxin FldA, the group of flagella component proteins (flagellin A, flagellin B, etc.), and VacA (268), (220). The discovery of these proteins confirmed that the method used yielded a portion of *H. pylori*-secreted proteins.

In conclusion, this study focused on the protein profile secreted from antibiotic-susceptible and antibiotic-resistant *Helicobacter pylori*-associated with gastritis strains using proteomic techniques. The results of this study provide preliminary information that may be useful for further investigations into proteins secreted by *Helicobacter pylori,* the pathogen in the gastrointestinal tract. According to our knowledge, this report is the first to demonstrate the 9-secreted protein found in the Sen-S strain. Of these, FBPAII is the secreted proteins identified only from the Sen-S strain. Whereas rpoBC was found in the secreted protein from Sen-S, Cla/Mtz-R, and Cla-R *H. pylori* strains, but not from Mtz-R strains. Its mutation presented in previous reports implies the association with rifampicin resistance. They are therefore interesting to conduct further studies to explore new targets for the eradication of *Helicobacter pylori*. Additionally, HP_0888 itself would be useful for further study in the development of serological markers, however, its antigenic potential should be validated first.

REFERENCES

1. Peek RM, Jr., Crabtree JE. *Helicobacter* infection and gastric neoplasia. The Journal of Pathology. 2006;208(2):233-48.

2. Moss SF. The clinical evidence linking *Helicobacter pylori* to gastric cancer. Cellular and Molecular Gastroenterology and Hepatology. 2017;3(2):183-91.

3. Zhang XY, Zhang PY, Aboul-Soud MA. From inflammation to gastric cancer: Role of *Helicobacter pylori*. Oncology Letters. 2017;13(2):543-8.

4. Chiang TH, Chang WJ, Chen SL, Yen AM, Fann JC, Chiu SY, et al. Mass eradication of *Helicobacter pylori* to reduce gastric cancer incidence and mortality: a long-term cohort study on Matsu Islands. Gut. 2020.

5. Savoldi A, Carrara E, Graham DY, Conti M, Tacconelli E. Prevalence of antibiotic resistance in *Helicobacter pylori*: A systematic review and meta-analysis in World Health Organization Regions. Gastroenterology. 2018;155(5):1372-82 e17.

6. Kuo YT, Liou JM, El-Omar EM, Wu JY, Leow AHR, Goh KL, et al. Primary antibiotic resistance in *Helicobacter pylori* in the Asia-Pacific region: a systematic review and meta-analysis. Lancet Gastroenterology and Hepatology. 2017;2(10):707-15.

7. Vilaichone RK, Quach DT, Yamaoka Y, Sugano K, Mahachai V. Prevalence and pattern of antibiotic resistant strains of *Helicobacter Pylori* infection in ASEAN. Asian Pacific journal of cancer prevention. 2018;19(5):1411-3.

8. Lu HH, Lai FP, Lo HY, Sheu BS, Yang YJ. Increasing antimicrobial resistance to clarithromycin and metronidazole in pediatric *Helicobacter pylori* infection in southern Taiwan: A comparison between two decades. Helicobacter. 2019;24(5):e12633.

9. WHO. WHO Global priority list of antibiotic-resistant bacteria to guide research, discovery, and development of new antibiotics. 2017.

10. Oleastro M, Menard A, Santos A, Lamouliatte H, Monteiro L, Barthelemy P, et al. Real-time PCR assay for rapid and accurate detection of point mutations conferring resistance to clarithromycin in *Helicobacter pylori*. Journal of Clinical Microbiology. 2003;41(1):397-402.

11. Bina JE, Alm RA, Uria- Nickelsen M, Thomas SR, Trust TJ, Hancock RE. *Helicobacter pylori* uptake and efflux: basis for intrinsic susceptibility to antibiotics in vitro. Antimicrobial agents and chemotherapy. 2000;44(2):248-54.

12. Liu ZQ, Zheng PY, Yang PC. Efflux pump gene *hefA* of *Helicobacter pylori* plays an important role in multidrug resistance. World journal of gastroenterology. 2008;14(33):5217-22.

13. Marques AT, Vitor JMB, Santos A, Oleastro M, Vale FF. Trends in *Helicobacter pylori* resistance to clarithromycin: from phenotypic to genomic approaches. Microbial genomics 2020;6(3).

14. Olekhnovich IN, Goodwin A, Hoffman PS. Characterization of the NAD(P)H oxidase and metronidazole reductase activities of the RdxA nitroreductase of *Helicobacter pylori*. The FEBS Journal. 2009;276(12):3354-64.

15. Sisson G, Jeong JY, Goodwin A, Bryden L, Rossler N, Lim- Morrison S, et al. Metronidazole activation is mutagenic and causes DNA fragmentation in *Helicobacter pylori* and in *Escherichia coli* containing a cloned *H. pylori* RdxA(+) (Nitroreductase) gene. Journal of Bacteriology. 2000;182(18):5091-6.

16. Jeong JY, Mukhopadhyay AK, Akada JK, Dailidiene D, Hoffman PS, Berg DE. Roles of FrxA and RdxA nitroreductases of *Helicobacter pylori* in susceptibility and resistance to metronidazole. Journal of Bacteriology. 2001;183(17):5155-62.

17. Goodwin A, Kersulyte D, Sisson G, Veldhuyzen van Zanten SJ, Berg DE, Hoffman PS. Metronidazole resistance in *Helicobacter pylori* is due to null mutations in a gene (rdxA) that encodes an oxygen- insensitive NADPH nitroreductase. Molecular Microbiology. 1998;28(2):383-93.

18. Jenks PJ, Ferrero RL, Labigne A. The role of the *rdxA* gene in the evolution of metronidazole resistance in *Helicobacter pylori*. Journal of Antimicrobial Chemotherapy. 1999;43(6):753-8.

19. Kwon DH, Hulten K, Kato M, Kim JJ, Lee M, El- Zaatari FA, et al. DNA sequence analysis of *rdxA* and *frxA* from 12 pairs of metronidazole-sensitive and -resistant clinical *Helicobacter pylori* isolates. Antimicrobial agents and chemotherapy. 2001;45(9):2609-15.

20. Moore JM, Salama NR. Mutational analysis of metronidazole resistance in *Helicobacter pylori*. Antimicrobial agents and chemotherapy. 2005;49(3):1236-7.

21. Tsugawa H, Suzuki H, Satoh K, Hirata K, Matsuzaki J, Saito Y, et al. Two amino acids mutation of ferric uptake regulator determines *Helicobacter pylori* resistance to metronidazole. Antioxidants & Redox Signaling. 2011;14(1):15-23.

22. Albert TJ, Dailidiene D, Dailide G, Norton JE, Kalia A, Richmond TA, et al. Mutation discovery in bacterial genomes: metronidazole resistance in *Helicobacter pylori*. Nature Methods. 2005;2(12):951-3.

23. Chua EG, Debowski AW, Webberley KM, Peters F, Lamichhane B, Loke MF, et al. Analysis of core protein clusters identifies candidate variable sites conferring metronidazole resistance in *Helicobacter pylori*. Gastroenterology Report. 2019;7(1):42-9.

24. McAtee CP, Hoffman PS, Berg DE. Identification of differentially regulated proteins in metronidozole resistant *Helicobacter pylori* by proteome techniques. Proteomics. 2001;1(4):516-21.

25. Smiley R, Bailey J, Sethuraman M, Posecion N, Showkat Ali M. Comparative proteomics analysis of sarcosine insoluble outer membrane proteins from clarithromycin resistant and sensitive strains of *Helicobacter pylori*. Journal of Microbiology. 2013;51(5):612-8.

26. Hanafi A, Lee WC, Loke MF, Teh X, Shaari A, Dinarvand M, et al. Molecular and proteomic analysis of Levofloxacin and Metronidazole resistant *Helicobacter pylori*. Frontiers in Microbiology. 2016;7:2015.

27. Sugiyama N, Miyake S, Lin MH, Wakabayashi M, Marusawa H, Nishiumi S, et al. Comparative proteomics of *Helicobacter pylori* strains reveals geographical features rather than genomic variations. Genes Cells. 2019;24(2):139-50.

28. Khodadadi E, Zeinalzadeh E, Taghizadeh S, Mehramouz B, Kamounah FS, Khodadadi E, et al. Proteomic applications in antimicrobial resistance and clinical microbiology studies. Infection and Drug Resistance. 2020;13:1785-806.

29. Link AJ, Eng J, Schieltz DM, Carmack E, Mize GJ, Morris DR, et al. Direct analysis of protein complexes using mass spectrometry. Nature Biotechnology. 1999;17(7):676-82.

30. Aebersold R, Mann M. Mass spectrometry- based proteomics. Nature. 2003;422(6928):198-207.

31. Eng JK, McCormack AL, Yates JR. An approach to correlate tandem mass spectral data of peptides with amino acid sequences in a protein database. Journal of the American Society for Mass Spectrometry. 1994;5(11):976-89.

32. Perkins DN, Pappin DJ, Creasy DM, Cottrell JS. Probability- based protein identification by searching sequence databases using mass spectrometry data. Electrophoresis. 1999;20(18):3551-67.

33. Catherman AD, Skinner OS, Kelleher NL. Top Down proteomics: facts and perspectives. Biochemical and Biophysical Research Communications. 2014;445(4):683-93.

34. Zhang Y, Fonslow BR, Shan B, Baek MC, Yates JR, 3rd. Protein analysis by shotgun/bottom-up proteomics. Chemical Reviews. 2013;113(4):2343-94.

35. Li N, Shaw AR, Zhang N, Mak A, Li L. Lipid raft proteomics: analysis of in-solution digest of sodium dodecyl sulfate- solubilized lipid raft proteins by liquid chromatography- matrix- assisted laser desorption/ ionization tandem mass spectrometry. Proteomics. 2004;4(10):3156-66.

36. Kim SC, Chen Y, Mirza S, Xu Y, Lee J, Liu P, et al. A clean, more efficient method for in- solution digestion of protein mixtures without detergent or urea. Journal of Proteome Research. 2006;5(12):3446-52.

37. Choksawangkarn W, Edwards N, Wang Y, Gutierrez P, Fenselau C. Comparative study of workflows optimized for in- gel, in- solution, and on- filter proteolysis in the analysis of plasma membrane proteins. Journal of Proteome Research. 2012;11(5):3030-4.

38. Huang CH, Chiou SH. Proteomic analysis of upregulated proteins in *Helicobacter pylori* under oxidative stress induced by hydrogen peroxide. Kaohsiung Journal of Medical Sciences. 2011;27(12):544-53.

39. Muller SA, Pernitzsch SR, Haange SB, Uetz P, von Bergen M, Sharma CM, et al. Stable isotope labeling by amino acids in cell culture based proteomics reveals differences in protein abundances between spiral and coccoid forms of the gastric pathogen *Helicobacter pylori*. Journal of Proteomics. 2015;126:34-45.

40. Warren JR. Gastric pathology associated with *Helicobacter pylori*. Gastroenterology Clinics of North America. 2000;29(3):705-51.

41. Guarner J. The spectrum of gastric disease associated with *Helicobacter pylori* and other infectious gastritides. Curr Gastroenterol Rep. 2004;6(6):441-6.

42. Repetto O, Zanussi S, Casarotto M, Canzonieri V, De Paoli P, Cannizzaro R, et al. Differential proteomics of *Helicobacter pylori* associated with autoimmune atrophic gastritis. Molecular Medicine. 2014;20:57-71.

43. Zhang YN, Ding SG, Huang LH, Zhang J, Shi YY, Zhong LJ. Comparative proteome analysis of *Helicobacter pylori* clinical strains by two-dimensional gel electrophoresis. Journal of Zhejiang University Science B. 2011;12(10):820-7.

44. Govorun VM, Moshkovskii SA, Tikhonova OV, Goufman EI, Serebryakova MV, Momynaliev KT, et al. Comparative analysis of proteome maps of *Helicobacter pylori* clinical isolates. Biochemistry (Mosc). 2003;68(1):42-9.

45. Chen J, Ye L, Jin L, Xu X, Xu P, Wang X, et al. Application of next-generation sequencing to characterize novel mutations in clarithromycin-susceptible *Helicobacter pylori* strains with A2143G of 23S rRNA gene. Annals of Clinical Microbiology and Antimicrobials. 2018;17(1):10.

46. Warren JR, Marshall B. Unidentified curved bacilli on gastric epithelium in active chronic gastritis. The Lancet. 1983;1(8336):1273-5.

47. Goodwin CS, Armstrong JA, Chilvers T, Peters M, Collins MD, Sly L, et al. Transfer of *Campylobacter pylori* and *Campylobacter mustelae* to *Helicobacter* gen. nov. as *Helicobacter pylori* comb. nov. and *Helicobacter mustelae* comb. nov., Respectively. International Journal of Systematic and Evolutionary Microbiology. 1989;39(4):397-405.

48. Marshall BJ, Warren JR. Unidentified curved bacilli in the stomach of patients with gastritis and peptic ulceration. The Lancet. 1984;1(8390):1311-5.

49. Kuipers EJ, Uyterlinde AM, Peña AS, Roosendaal R, Pals G, Nelis GF, et al. Long-term sequelae of *Helicobacter pylori* gastritis. The Lancet. 1995;345(8964):1525-8.

50. Sakaki N, Momma K, Egawa N, Yamada Y, Kan T, Ishiwata J. The influence of *Helicobacter pylori* infection on the progression of gastric mucosal atrophy and occurrence of gastric cancer. European Journal of Gastroenterology & Hepatology. 1995;7 Suppl 1:S59-62.

51. Schistosomes, liver flukes and *Helicobacter pylori*. IARC Working Group on the Evaluation of Carcinogenic Risks to Humans. Lyon, 7-14 June 1994. IARC monographs on the evaluation of carcinogenic risks to humans. 1994;61:1-241.

52. Asaka M, Takeda H, Sugiyama T, Kato M. What role does *Helicobacter pylori* play in gastric cancer? Gastroenterology. 1997;113(6 Suppl):S56-60.

53. Rocco A, Nardone G. Diet, *H pylori* infection and gastric cancer: evidence and controversies. World journal of gastroenterology. 2007;13(21):2901-12.

54. Park YH, Kim N. Review of atrophic gastritis and intestinal metaplasia as a premalignant lesion of gastric cancer. Journal of Cancer Prevention. 2015;20(1):25-40.

55. Raei N, Behrouz B, Zahri S, Latifi-Navid S. *Helicobacter pylori* infection and dietary factors act synergistically to promote gastric cancer. Asian Pacific Journal of Cancer Prevention. 2016;17(3):917-21.

56. Segal I, Ally R, Mitchell H. *Helicobacter pylori*--an African perspective. QJM: An International Journal of Medicine. 2001;94(10):561-5.

57. Chong VH, Lim KC, Rajendran N. Prevalence of active *Helicobacter pylori* infection among patients referred for endoscopy in Brunei Darussalam. Singapore Medical Journal. 2008;49(1):42-6.

58. Dube C, Nkosi TC, Clarke AM, Mkwetshana N, Green E, Ndip RN. *Helicobacter pylori* antigenemia in an asymptomatic population of Eastern Cape Province, South Africa: public health implications. Reviews on Environmental Health 2009;24(3):249-55.

59. Ogihara A, Kikuchi S, Hasegawa A, Kurosawa M, Miki K, Kaneko E, et al. Relationship between *Helicobacter pylori* infection and smoking and drinking habits. Journal of Gastroenterology and Hepatology. 2000;15(3):271-6.

60. Brown LM. *Helicobacter pylori*: epidemiology and routes of transmission. Epidemiologic Reviews. 2000;22(2):283-97.

61. Kouitcheu Mabeku LB, Noundjeu Ngamga ML, Leundji H. Potential risk factors and prevalence of *Helicobacter pylori* infection among adult patients with dyspepsia symptoms in Cameroon. BMC infectious diseases. 2018;18(1):278.

62. Yokota S, Konno M, Fujiwara S, Toita N, Takahashi M, Yamamoto S, et al. Intrafamilial, preferentially mother- to- child and intraspousal, *Helicobacter pylori* infection in japan determined by mutilocus sequence typing and random amplified polymorphic dna fingerprinting. Helicobacter. 2015;20(5):334-42.

63. Hooi JKY, Lai WY, Ng WK, Suen MMY, Underwood FE, Tanyingoh D, et al. Global prevalence of *Helicobacter pylori* infection: systematic review and meta- analysis. Gastroenterology. 2017;153(2):420-9.

64. Sjomina O, Pavlova J, Niv Y, Leja M. Epidemiology of *Helicobacter pylori* infection. Helicobacter. 2018;23 Suppl 1:e12514.

65. Uchida T, Miftahussurur M, Pittayanon R, Vilaichone RK, Wisedopas N, Ratanachu-Ek T, et al. *Helicobacter pylori* infection in Thailand: A nationwide study of the CagA phenotype. PLoS One. 2015;10(9):e0136775.

66. Suchartlikitwong S, Lapumuaypol K, Rerknimitr R, Werawatganon D. Epidemiology of upper gastrointestinal bleeding and *Helicobacter pylori* infection: Review of 3,488 Thai patients. Asian Biomedicine. 2015;9:87-93.

67. O'Mahony R, Al-Khtheeri H, Weerasekera D, Fernando N, Vaira D, Holton J, et al. Bactericidal and anti- adhesive properties of culinary and medicinal plants against *Helicobacter pylori*. World Journal of Gastroenterology. 2005;11(47):7499-507.

68. Goh KL, Chan WK, Shiota S, Yamaoka Y. Epidemiology of *Helicobacter pylori* infection and public health implications. Helicobacter. 2011;16 Suppl 1:1-9.

69. Perez-Perez GI, Taylor DN, Bodhidatta L, Wongsrichanalai J, Baze WB, Dunn BE, et al. Seroprevalence of *Helicobacter pylori* infections in Thailand. The Journal of Infectious Diseases. 1990;161(6):1237-41.

70. Atherton JC. The pathogenesis of *Helicobacter pylori*-induced gastro-duodenal diseases. Annual Review of Pathology Mechanisms of Disease. 2006;1:63-96.

71. Windle HJ, Fox A, D NE, Kelleher D. The thioredoxin system of *Helicobacter pylori*. Journal of Biological Chemistry. 2000;275(7):5081-9.

72. Celli JP, Turner BS, Afdhal NH, Keates S, Ghiran I, Kelly CP, et al. *Helicobacter pylori* moves through mucus by reducing mucin viscoelasticity. Proceedings of the National Academy of Sciences of the United States of America. 2009;106(34):14321-6.

73. Schoep TD, Fulurija A, Good F, Lu W, Himbeck RP, Schwan C, et al. Surface properties of *Helicobacter pylori* urease complex are essential for persistence. PLOS ONE. 2010;5(11):e15042.

74. Bode G, Malfertheiner P, Nilius M, Lehnhardt G, Ditschuneit H. Ultrastructural localisation of urease in outer membrane and periplasm of *Campylobacter pylori*. Journal of clinical pathology. 1989;42(7):778-9.

75. Su C, Padra M, Constantino MA, Sharba S, Thorell A, Lindén SK, et al. Influence of the viscosity of healthy and diseased human mucins on the motility of *Helicobacter pylori*. Scientific Reports. 2018;8(1):9710.

76. Bansil R, Celli J, Hardcastle J, Turner B. The influence of mucus microstructure and rheology in *Helicobacter pylori* infection. Frontiers in Immunology. 2013;4(310).

77. Celli JP, Turner BS, Afdhal NH, Ewoldt RH, McKinley GH, Bansil R, et al. Rheology of gastric mucin exhibits a pH- dependent sol- gel transition. Biomacromolecules. 2007;8(5):1580-6.

78. Ansari S, Yamaoka Y. Survival of *Helicobacter pylori* in gastric acidic territory. Helicobacter. 2017;22(4).

79. Marcus EA, Moshfegh AP, Sachs G, Scott DR. The periplasmic alpha- carbonic anhydrase activity of *Helicobacter pylori* is essential for acid acclimation. Journal of Bacteriology. 2005;187(2):729-38.

80. Sachs G, Weeks DL, Wen Y, Marcus EA, Scott DR, Melchers K. Acid acclimation by *Helicobacter pylori*. Physiology (Bethesda). 2005;20:429-38.

81. Huynh KK, Grinstein S. Regulation of vacuolar pH and its modulation by some microbial species. Microbiology and molecular biology reviews : MMBR. 2007;71(3):452-62.

82. Burne RA, Chen YY. Bacterial ureases in infectious diseases. Microbes and Infection. 2000;2(5):533-42.

83. Bury-Moné S, Skouloubris S, Labigne A, De Reuse H. The *Helicobacter pylori* UreI protein: role in adaptation to acidity and identification of residues essential for its activity and for acid activation. Molecular Microbiology. 2001;42(4):1021-34.

84. Voland P, Weeks DL, Marcus EA, Prinz C, Sachs G, Scott D. Interactions among the seven *Helicobacter pylori* proteins encoded by the urease gene cluster. American Journal of Physiology-Gastrointestinal and Liver Physiology. 2003;284(1):G96-G106.

85. Marcus EA, Sachs G, Scott DR. Acid-regulated gene expression of *Helicobacter pylori*: Insight into acid protection and gastric colonization. Helicobacter. 2018;23(3):e12490-e.

86. Turbett GR, Høj PB, Horne R, Mee BJ. Purification and characterization of the urease enzymes of *Helicobacter* species from humans and animals. Infection and Immunity. 1992;60(12):5259-66.

87. Zschiedrich CP, Keidel V, Szurmant H. Molecular mechanisms of two-component signal transduction. Journal of Molecular Biology. 2016;428(19):3752-75.

88. Cheung J, Hendrickson WA. Sensor domains of two-component regulatory systems. Current Opinion in Microbiology. 2010;13(2):116-23.

89. Bekker M, Teixeira De Mattos MJ, Hellingwerf KJ. The role of two-component regulation systems in the physiology of the bacterial cell. Science Progress. 2006;89(3-4):213-42.

90. Wen Y, Scott DR, Vagin O, Tokhtaeva E, Marcus EA, Sachs G. Measurement of internal pH in *Helicobacter pylori* by using green fluorescent protein fluorimetry. Journal of Bacteriology. 2018;200(14):e00178-18.

91. Pflock M, Kennard S, Delany I, Scarlato V, Beier D. Acid-induced activation of the urease promoters is mediated directly by the ArsRS two-component system of *Helicobacter pylori*. Infection and Immunity. 2005;73(10):6437-45.

92. Marcus E.A. SDR. Gastric colonization by *H. pylori.* In: Kim N (eds) *Helicobacter pylori* Springer, 2016.

93. Ge R-G, Wang D-X, Hao M-C, Sun X-S. Nickel trafficking system responsible for urease maturation in *Helicobacter pylori*. World journal of gastroenterology. 2013;19(45):8211-8.

94. van Vliet AH, Kuipers EJ, Waidner B, Davies BJ, de Vries N, Penn CW, et al. Nickel-responsive induction of urease expression in *Helicobacter pylori* is mediated at the transcriptional level. Infection and Immunity. 2001;69(8):4891-7.

95. Ha NC, Oh ST, Sung JY, Cha KA, Lee MH, Oh BH. Supramolecular assembly and acid resistance of *Helicobacter pylori* urease. Nature Structural Biology. 2001;8(6):505-9.

96. Vollan HS, Tannæs T, Caugant DA, Vriend G, Bukholm G. Outer membrane phospholipase A' s roles in *Helicobacter pylori* acid adaptation. Gut Pathogens. 2017;9(1):36.

97. Vollan HS, Tannæs T, Vriend G, Bukholm G. *In Silico* structure and sequence analysis of bacterial porins and specific diffusion channels for hydrophilic molecules: conservation, multimericity and multifunctionality. International journal of molecular sciences. 2016;17(4):599.

98. Sachs G, Kraut JA, Wen Y, Feng J, Scott DR. Urea transport in bacteria: acid acclimation by gastric *Helicobacter* spp. The Journal of Membrane Biology. 2006;212(2):71-82.

99. Scott DR, Marcus EA, Weeks DL, Lee A, Melchers K, Sachs G. Expression of the *Helicobacter pylori ureI* gene is required for acidic pH activation of cytoplasmic urease. Infection and Immunity. 2000;68(2):470-7.

100. Mobley HL, Island MD, Hausinger RP. Molecular biology of microbial ureases. Microbiological Reviews. 1995;59(3):451-80.

101. Dunn BE, Campbell GP, Perez- Perez GI, Blaser MJ. Purification and characterization of urease from *Helicobacter pylori*. Journal of Biological Chemistry. 1990;265(16):9464-9.

102. Marcus Elizabeth A, Moshfegh Amiel P, Sachs G, Scott David R. The periplasmic α-carbonic anhydrase activity of *Helicobacter pylori* is essential for acid acclimation. Journal of Bacteriology. 2005;187(2):729-38.

103. Bury-Moné S, Mendz GL, Ball GE, Thibonnier M, Stingl K, Ecobichon C, et al. Roles of alpha and beta carbonic anhydrases of *Helicobacter pylori* in the urease-dependent response to acidity and in colonization of the murine gastric mucosa. Infection and Immunity. 2008;76(2):497-509.

104. Tomb JF, White O, Kerlavage AR, Clayton RA, Sutton GG, Fleischmann RD, et al. The complete genome sequence of the gastric pathogen *Helicobacter pylori*. Nature. 1997;388(6642):539-47.

105. Suerbaum S, Josenhans C, Sterzenbach T, Drescher B, Brandt P, Bell M, et al. The complete genome sequence of the carcinogenic bacterium *Helicobacter hepaticus*. Proceedings of the National Academy of Sciences of the United States of America. 2003;100(13):7901-6.

106. Guilloton MB, Korte JJ, Lamblin AF, Fuchs JA, Anderson PM. Carbonic anhydrase in *Escherichia coli*. a product of the cyn operon. Journal of Biological Chemistry. 1992;267(6):3731-4.

107. Buzas GM, Supuran CT. The history and rationale of using carbonic anhydrase inhibitors in the treatment of peptic ulcers. In memoriam Ioan Puscas (1932-2015). Journal of Enzyme Inhibition and Medicinal Chemistry. 2016;31(4):527-33.

108. Chirică LC, Elleby B, Jonsson BH, Lindskog S. The complete sequence, expression in *Escherichia coli*, purification and some properties of carbonic anhydrase from *Neisseria gonorrhoeae*. European Journal of Biochemistry. 1997;244(3):755-60.

109. Supuran CT. Structure-based drug discovery of carbonic anhydrase inhibitors. Journal of Enzyme Inhibition and Medicinal Chemistry. 2012;27(6):759-72.

110. Supuran CT, Capasso C. Antibacterial carbonic anhydrase inhibitors: an update on the recent literature. Expert Opinion on Therapeutic Patents. 2020;30(12):963-82.

111. Maresca A, Vullo D, Scozzafava A, Supuran CT. Inhibition of the alpha- and beta-carbonic anhydrases from the gastric pathogen *Helycobacter pylori* with anions. Journal of Enzyme Inhibition and Medicinal Chemistry. 2013;28(2):388-91.

112. Hiroaki T, Claudiu TS, Saburo O, Isao N. The alpha and beta classes carbonic anhydrases from *Helicobacter pylori* as novel drug targets. Current Pharmaceutical Design. 2008;14(7):622-30.

113. Bury-Moné S, Skouloubris S, Dauga C, Thiberge J-M, Dailidiene D, Berg Douglas E, et al. Presence of active aliphatic amidases in *Helicobacter* species able to colonize the stomach. Infection and Immunity. 2003;71(10):5613-22.

114. Skouloubris S, Labigne A, De Reuse H. The AmiE aliphatic amidase and AmiF formamidase of *Helicobacter pylori*: natural evolution of two enzyme paralogues. Molecular Microbiology. 2001;40(3):596-609.

115. Wen Y, Marcus EA, Matrubutham U, Gleeson MA, Scott DR, Sachs G. Acid-adaptive genes of *Helicobacter pylori*. Infection and Immunity. 2003;71(10):5921-39.

116. Phadnis SH, Parlow MH, Levy M, Ilver D, Caulkins CM, Connors JB, et al. Surface localization of *Helicobacter pylori* urease and a heat shock protein homolog requires bacterial autolysis. Infection and Immunity. 1996;64(3):905-12.

117. Hong W, Sano K, Morimatsu S, Scott DR, Weeks DL, Sachs G, et al. Medium pH-dependent redistribution of the urease of *Helicobacter pylori*. Journal of Medical Microbiology. 2003;52(Pt 3):211-6.

118. Chmiela M, Walczak N, Rudnicka K. *Helicobacter pylori* outer membrane vesicles involvement in the infection development and *Helicobacter pylori*-related diseases. Journal of Biomedical Science. 2018;25(1):78.

119. Olofsson A, Vallström A, Petzold K, Tegtmeyer N, Schleucher J, Carlsson S, et al. Biochemical and functional characterization of *Helicobacter pylori* vesicles. Molecular Microbiology. 2010;77(6):1539-55.

120. Gu H. Role of flagella in the pathogenesis of *Helicobacter pylori*. Current Microbiology. 2017;74(7):863-9.

121. Lertsethtakarn P, Ottemann KM, Hendrixson DR. Motility and chemotaxis in *Campylobacter* and *Helicobacter*. Annual Review of Microbiology. 2011;65:389-410.

122. Tsang J, Hoover TR. Basal body structures differentially affect transcription of RpoN- and FliA- Dependent flagellar genes in *Helicobacter pylori*. Journal of Bacteriology. 2015;197(11):1921-30.

123. Ottemann KM, Lowenthal AC. *Helicobacter pylori* uses motility for initial colonization and to attain robust infection. Infection and Immunity. 2002;70(4):1984-90.

124. Josenhans C, Labigne A, Suerbaum S. Comparative ultrastructural and functional studies of *Helicobacter pylori* and *Helicobacter mustelae* flagellin mutants: both flagellin subunits, FlaA and FlaB, are necessary for full motility in *Helicobacter* species. Journal of Bacteriology. 1995;177(11):3010-20.

125. O'Toole PW, Kostrzynska M, Trust TJ. Non-motile mutants of *Helicobacter pylori* and *Helicobacter mustelae* defective in flagellar hook production. Molecular Microbiology. 1994;14(4):691-703.

126. Van den Brink GR, Tytgat KM, Van der Hulst RW, Van der Loos CM, Einerhand AW, Büller HA, et al. *H. pylori* colocalises with MUC5AC in the human stomach. Gut. 2000;46(5):601-7.

127. Dunne C, Dolan B, Clyne M. Factors that mediate colonization of the human stomach by *Helicobacter pylori*. World journal of gastroenterology. 2014;20(19):5610-24.

128. Ilver D, Arnqvist A, Ogren J, Frick IM, Kersulyte D, Incecik ET, et al. *Helicobacter pylori* adhesin binding fucosylated histo-blood group antigens revealed by retagging. Science. 1998;279(5349):373-7.

129. Hidaka E, Ota H, Hidaka H, Hayama M, Matsuzawa K, Akamatsu T, et al. *Helicobacter pylori* and two ultrastructurally distinct layers of gastric mucous cell mucins in the surface mucous gel layer. Gut. 2001;49(4):474-80.

130. Mahdavi J, Sondén B, Hurtig M, Olfat FO, Forsberg L, Roche N, et al. *Helicobacter pylori* SabA adhesin in persistent infection and chronic inflammation. Science. 2002;297(5581):573-8.

131. Unemo M, Aspholm-Hurtig M, Ilver D, Bergström J, Borén T, Danielsson D, et al. The sialic acid binding SabA adhesin of *Helicobacter pylori* is essential for nonopsonic activation of human neutrophils. Journal of Biological Chemistry. 2005;280(15):15390-7.

132. Odenbreit S, Till M, Hofreuter D, Faller G, Haas R. Genetic and functional characterization of the alpAB gene locus essential for the adhesion of *Helicobacter pylori* to human gastric tissue. Molecular Microbiology. 1999;31(5):1537-48.

133. Foegeding NJ, Caston RR, McClain MS, Ohi MD, Cover TL. An Overview of *Helicobacter pylori* VacA Toxin Biology. Toxins. 2016;8(6).

134. Boquet P, Ricci V. Intoxication strategy of *Helicobacter pylori* VacA toxin. Trends in Microbiology. 2012;20(4):165-74.

135. Nakano M, Yahiro K, Yamasaki E, Kurazono H, Akada J, Yamaoka Y, et al. *Helicobacter pylori* VacA, acting through receptor protein tyrosine phosphatase α, is crucial for CagA phosphorylation in human duodenum carcinoma cell line AZ-521. Disease Models & Mechanisms. 2016;9(12):1473-81.

136. Nakano M, Hirayama T, Moss J, Yahiro K. *Helicobacter pylori* VacA Exhibits Pleiotropic Actions in Host Cells. In: Suzuki H, Warren R, Marshall B, editors. Helicobacter pylori. Tokyo: Springer Japan; 2016. p. 49-66.

137. Yahiro K, Wada A, Nakayama M, Kimura T, Ogushi K, Niidome T, et al. Protein-tyrosine phosphatase alpha, RPTP alpha, is a *Helicobacter pylori* VacA receptor. Journal of Biological Chemistry. 2003;278(21):19183-9.

138. Ivie SE, McClain MS, Algood HMS, Lacy DB, Cover TL. Analysis of a β-helical region in the p55 domain of *Helicobacter pylori* vacuolating toxin. BMC Microbiology. 2010;10(1):60.

139. Gangwer KA, Mushrush DJ, Stauff DL, Spiller B, McClain MS, Cover TL, et al. Crystal structure of the *Helicobacter pylori* vacuolating toxin p55 domain. Proceedings of the National Academy of Sciences of the United States of America. 2007;104(41):16293-8.

140. Genisset C, Puhar A, Calore F, De Bernard M, Dell'Antone P, Montecucco C. The concerted action of the *Helicobacter pylori* cytotoxin VacA and of the v-ATPase proton pump induces swelling of isolated endosomes. Cellular Microbiology. 2007;9(6):1481-90.

141. Necchi V, Sommi P, Vanoli A, Fiocca R, Ricci V, Solcia E. Natural history of *Helicobacter pylori* VacA toxin in human gastric epithelium in vivo: vacuoles and beyond. Scientific Reports. 2017;7(1):14526.

142. Papini E, de Bernard M, Milia E, Bugnoli M, Zerial M, Rappuoli R, et al. Cellular vacuoles induced by *Helicobacter pylori* originate from late endosomal compartments.

Proceedings of the National Academy of Sciences of the United States of America. 1994;91(21):9720-4.

143. Cover TL, Blanke SR. *Helicobacter pylori* VacA, a paradigm for toxin multifunctionality. Nature Reviews Microbiology. 2005;3(4):320-32.

144. Galmiche A, Rassow J, Doye A, Cagnol S, Chambard JC, Contamin S, et al. The N-terminal 34 kDa fragment of *Helicobacter pylori* vacuolating cytotoxin targets mitochondria and induces cytochrome c release. EMBO Journal. 2000;19(23):6361-70.

145. Alipour M. Molecular mechanism of *Helicobacter pylori*-induced gastric cancer. Journal of Gastrointestinal Cancer. 2021;52(1):23-30.

146. Beurel E, Grieco SF, Jope RS. Glycogen synthase kinase-3 (GSK3): regulation, actions, and diseases. Pharmacology & Therapeutics. 2015;148:114-31.

147. Kim I-J, Blanke SR. Remodeling the host environment: modulation of the gastric epithelium by the *Helicobacter pylori* vacuolating toxin (VacA). Frontiers in cellular and infection microbiology. 2012;2:37-.

148. Backert S, Tegtmeyer N. Type IV secretion and signal transduction of *Helicobacter pylori* CagA through interactions with host cell receptors. Toxins (Basel). 2017;9(4).

149. Backert S, Tegtmeyer N, Fischer W. Composition, structure and function of the *Helicobacter pylori cag* pathogenicity island encoded type IV secretion system. Future Microbiology. 2015;10(6):955-65.

150. Tegtmeyer N, Wessler S, Backert S. Role of the cag-pathogenicity island encoded type IV secretion system in *Helicobacter pylori* pathogenesis. The FEBS Journal. 2011;278(8):1190-202.

151. Odenbreit S, Püls J, Sedlmaier B, Gerland E, Fischer W, Haas R. Translocation of *Helicobacter pylori* CagA into gastric epithelial cells by type IV secretion. Science. 2000;287(5457):1497-500.

152. Kwok T, Zabler D, Urman S, Rohde M, Hartig R, Wessler S, et al. *Helicobacter* exploits integrin for type IV secretion and kinase activation. Nature. 2007;449(7164):862-6.

153. Jiménez-Soto LF, Kutter S, Sewald X, Ertl C, Weiss E, Kapp U, et al. *Helicobacter pylori* type IV secretion apparatus exploits beta1 integrin in a novel RGD-independent manner. PLoS Pathogens. 2009;5(12):e1000684.

154. Murata-Kamiya N, Kikuchi K, Hayashi T, Higashi H, Hatakeyama M. *Helicobacter pylori* exploits host membrane phosphatidylserine for delivery, localization, and pathophysiological action of the CagA oncoprotein. Cell Host & Microbe. 2010;7(5):399-411.

155. Murata-Kamiya N, Kurashima Y, Teishikata Y, Yamahashi Y, Saito Y, Higashi H, et al. *Helicobacter pylori* CagA interacts with E-cadherin and deregulates the beta-catenin signal that promotes intestinal transdifferentiation in gastric epithelial cells. Oncogene. 2007;26(32):4617-26.

156. Bolós V, Gasent JM, López-Tarruella S, Grande E. The dual kinase complex FAK-Src as a promising therapeutic target in cancer. OncoTargets and Therapy. 2010;3:83-97.

157. Mitra SK, Schlaepfer DD. Integrin-regulated FAK-Src signaling in normal and cancer cells. Current Opinion in Cell Biology. 2006;18(5):516-23.

158. Hatakeyama M. Structure and function of *Helicobacter pylori* CagA, the first-identified bacterial protein involved in human cancer. Proceedings of the Japan Academy Series B, Physical and biological sciences. 2017;93(4):196-219.

159. Chey WD, Leontiadis GI, Howden CW, Moss SF. ACG clinical guideline: treatment of *Helicobacter pylori* infection. The American Journal of Gastroenterology. 2017;112(2):212-39.

160. Gisbert JP, González L, Calvet X, García N, López T, Roqué M, et al. Proton pump inhibitor, clarithromycin and either amoxycillin or nitroimidazole: a meta-analysis of eradication of *Helicobacter pylori*. Alimentary Pharmacology & Therapeutics. 2000;14(10):1319-28.

161. Scott D, Weeks D, Melchers K, Sachs G. The life and death of *Helicobacter pylori*. Gut. 1998;43(suppl 1):S56.

162. Whitman MS, Tunkel AR. Azithromycin and clarithromycin: overview and comparison with erythromycin. Infection Control & Hospital Epidemiology. 1992;13(6):357-68.

163. Amsden GW. Erythromycin, clarithromycin, and azithromycin: are the differences real? Clinical Therapeutics. 1996;18(1):56-72; discussion 55.

164. Clemons WM, Jr. , May JL, Wimberly BT, McCutcheon JP, Capel MS, Ramakrishnan V. Structure of a bacterial 30S ribosomal subunit at 5.5 A resolution. Nature. 1999;400(6747):833-40.

165. Ban N, Nissen P, Hansen J, Capel M, Moore PB, Steitz TA. Placement of protein and RNA structures into a 5 A-resolution map of the 50S ribosomal subunit. Nature. 1999;400(6747):841-7.

166. Menninger JR. Functional consequences of binding macrolides to ribosomes. Journal of Antimicrobial Chemotherapy. 1985;16 Suppl A:23-34.

167. Noller HF. Structure of ribosomal RNA. Annual Review of Biochemistry. 1984;53:119-62.

168. Chittum HS, Champney WS. Erythromycin inhibits the assembly of the large ribosomal subunit in growing *Escherichia coli* cells. Current Microbiology. 1995;30(5):273-9.

169. Hansen LH, Mauvais P, Douthwaite S. The macrolide-ketolide antibiotic binding site is formed by structures in domains II and V of 23S ribosomal RNA. Molecular Microbiology. 1999;31(2):623-31.

170. Xiong L, Shah S, Mauvais P, Mankin AS. A ketolide resistance mutation in domain II of 23S rRNA reveals the proximity of hairpin 35 to the peptidyl transferase centre. Molecular Microbiology. 1999;31(2):633-9.

171. Vester B, Douthwaite S. Macrolide resistance conferred by base substitutions in 23S rRNA. Antimicrobial agents and chemotherapy. 2001;45(1):1-12.

172. Vazquez D. Inhibitors of protein synthesis. FEBS Letters. 1974;40(0):suppl:S63-84.

173. Sturgill MG, Rapp RP. Clarithromycin: review of a new macrolide antibiotic with improved microbiologic spectrum and favorable pharmacokinetic and adverse effect profiles. FEMS Microbiology Letters. 1992;26(9):1099-108.

174. Kim BJ, Lee H, Lee YC, Jeon SW, Kim GH, Kim HS, et al. Ten-Day concomitant, 10-Day sequential, and 7-Day triple therapy as First-Line treatment for *Helicobacter pylori* Infection: a nationwide randomized trial in Korea. Gut Liver. 2019;13(5):531-40.

175. Kim SY, Chung J-W. Best *Helicobacter pylori* eradication strategy in the era of antibiotic resistance. Antibiotics (Basel, Switzerland). 2020;9(8):436.

176. Gómez C, Marchat L, Lopez-Canovas L, Ishiwara D, Rodriguez M, Orozco E. Drug resistance mechanisms in *Entamoeba histolytica*, *Giardia lamblia*, *Trichomonas vaginalis*, and opportunistic anaerobic protozoa. 2017. p. 613-28.

177. Sisson G, Jeong JY, Goodwin A, Bryden L, Rossler N, Lim-Morrison S, et al. Metronidazole activation is mutagenic and causes DNA fragmentation in *Helicobacter pylori* and in *Escherichia coli* containing a cloned *H. pylori* RdxA(+) (Nitroreductase) gene. Journal of Bacteriology. 2000;182(18):5091-6.

178. Smith MA, Edwards DI. Redox potential and oxygen concentration as factors in the susceptibility of *Helicobacter pylori* to nitroheterocyclic drugs. Journal of Antimicrobial Chemotherapy. 1995;35(6):751-64.

179. Goodwin CS, Marshall BJ, Blincow ED, Wilson DH, Blackbourn S, Phillips M. Prevention of nitroimidazole resistance in *Campylobacter pylori* by coadministration of colloidal bismuth subcitrate: clinical and in vitro studies. Journal of Clinical Pathology. 1988;41(2):207-10.

180. Bell GD, Powell KU, Burridge SM, Spencer G, Bolton G, Purser K, et al. Short report: omeprazole plus antibiotic combinations for the eradication of metronidazole-resistant *Helicobacter pylori*. Alimentary Pharmacology & Therapeutics. 1992;6(6):751-8.

181. Raymond J, Kalach N, Bergeret M, Benhamou PH, Barbet JP, Gendrel D, et al. Effect of metronidazole resistance on bacterial eradication of *Helicobacter pylori* in infected children. Antimicrobial agents and chemotherapy. 1998;42(6):1334-5.

182. Selgrad M, Meissle J, Bornschein J, Kandulski A, Langner C, Varbanova M, et al. Antibiotic susceptibility of *Helicobacter pylori* in central Germany and its relationship with the number of eradication therapies. European Journal of Gastroenterology & Hepatology. 2013;25(11):1257-60.

183. Mégraud F, Lehours P. *Helicobacter pylori* detection and antimicrobial susceptibility testing. Clin Microbiol Rev. 2007;20(2):280-322.

184. Francesco VD, Zullo A, Hassan C, Giorgio F, Rosania R, Ierardi E. Mechanisms of *Helicobacter pylori* antibiotic resistance: An updated appraisal. World Journal of Gastrointestinal Pathophysiology. 2011;2(3):35-41.

185. Salcedo JA, Al-Kawas F. Treatment of *Helicobacter pylori* Infection. Archives of Internal Medicine. 1998;158(8):842-51.

186. Oderda G, Vaira D, Holton J, Ainley C, Altare F, Ansaldi N. Amoxycillin plus tinidazole for *Campylobacter pylori* gastritis in children: assessment by serum IgG antibody, pepsinogen I, and gastrin levels. The Lancet. 1989;1(8640):690-2.

187. Rauws EA, Langenberg W, Houthoff HJ, Zanen HC, Tytgat GN. *Campylobacter pyloridis*-associated chronic active antral gastritis. A prospective study of its prevalence and the effects of antibacterial and antiulcer treatment. Gastroenterology. 1988;94(1):33-40.

188. Qarah NAS, Abdulrahman SAM, Algethami FK, Basavaiah K, El-Maaiden E. New applications for amoxicillin determination in pure form and pharmaceuticals based on iodate-iodide mixture: titrimetry and spectroscopy studies. Química Nova. 2020;43:44-9.

189. Malfertheiner P, Megraud F, O'Morain CA, Gisbert JP, Kuipers EJ, Axon AT, et al. Management of *Helicobacter pylori* infection-the Maastricht V/Florence consensus report. Gut. 2017;66(1):6-30.

190. Vilaichone RK, Mahachai V, Graham DY. *Helicobacter pylori* diagnosis and management. Gastroenterology Clinics of North America. 2006;35(2):229-47.

191. Vilaichone RK, Prapitpaiboon H, Gamnarai P, Namtanee J, Wongcha-um A, Chaithongrat S, et al. Seven-Day Bismuth-based Quadruple Therapy as an initial

treatment for *Helicobacter pylori* infection in a high metronidazole resistant area. Asian Pacific Journal of Cancer Prevention. 2015;16(14):6089-92.

192. Mégraud F. *H. pylori* antibiotic resistance: prevalence, importance, and advances in testing. Gut. 2004;53(9):1374-84.

193. Nash KA, Inderlied CB. Genetic basis of macrolide resistance in *Mycobacterium avium* isolated from patients with disseminated disease. Antimicrobial agents and chemotherapy. 1995;39(12):2625-30.

194. Occhialini A, Urdaci M, Doucet-Populaire F, Bébéar C, Lamouliatte H, Megraud F. Macrolide resistance in *Helicobacter pylori*: Rapid detection of point mutations and assays of macrolide binding to ribosomes. Antimicrobial agents and chemotherapy. 1997;41:2724-8.

195. Pernodet JL, Boccard F, Alegre MT, Blondelet-Rouault MH, Guérineau M. Resistance to macrolides, lincosamides and streptogramin type B antibiotics due to a mutation in an rRNA operon of *Streptomyces ambofaciens*. The EMBO Journal. 1988;7(1):277-82.

196. Versalovic J, Shortridge D, Kibler K, Griffy MV, Beyer J, Flamm RK, et al. Mutations in 23S rRNA are associated with clarithromycin resistance in *Helicobacter pylori*. Antimicrobial agents and chemotherapy. 1996;40(2):477-80.

197. Verdier L, Gharbi-Benarous J, Bertho G, Mauvais P, Girault JP. Antibiotic resistance peptides: interaction of peptides conferring macrolide and ketolide resistance with *Staphylococcus aureus* ribosomes: conformation of bound peptides as determined by transferred NOE experiments. Biochemistry. 2002;41(13):4218-29.

198. Liu Z-Q, Zheng P-Y, Yang P-C. Efflux pump gene *hefA* of *Helicobacter pylori* plays an important role in multidrug resistance. World journal of gastroenterology. 2008;14(33):5217-22.

199. Marques AT, Vítor JMB, Santos A, Oleastro M, Vale FF. Trends in *Helicobacter pylori* resistance to clarithromycin: from phenotypic to genomic approaches. Microbial genomics. 2020;6(3):e000344.

200. Kwon DH, Kato M, El-Zaatari FA, Osato MS, Graham DY. Frame-shift mutations in NAD(P)H flavin oxidoreductase encoding gene (*frxA*) from metronidazole resistant

Helicobacter pylori ATCC43504 and its involvement in metronidazole resistance. FEMS Microbiology Letters. 2000;188(2):197-202.

201. Anderson NL, Anderson NG. Proteome and proteomics: new technologies, new concepts, and new words. Electrophoresis. 1998;19(11):1853-61.

202. Raijmakers R, van Beers JJBC, El-Azzouny M, Visser NFC, Božič B, Pruijn GJM, et al. Elevated levels of fibrinogen-derived endogenous citrullinated peptides in synovial fluid of rheumatoid arthritis patients. Arthritis Research & Therapy. 2012;14(3):R114.

203. O'Farrell PH. High resolution two-dimensional electrophoresis of proteins. The Journal of biological chemistry. 1975;250(10):4007-21.

204. Klose J. Protein mapping by combined isoelectric focusing and electrophoresis of mouse tissues. A novel approach to testing for induced point mutations in mammals. Humangenetik. 1975;26:231-43.

205. Laemmli UK. Cleavage of structural proteins during the assembly of the head of bacteriophage T4. Nature. 1970;227(5259):680-5.

206. Carrette O, Burkhard PR, Sanchez JC, Hochstrasser DF. State-of-the-art two-dimensional gel electrophoresis: a key tool of proteomics research. Nature Protocols. 2006;1(2):812-23.

207. Afeyan NB, Gordon NF, Fulton SP, Regnier FE. Perfusion chromatography: a novel tool for protein purification and analysis. In: Angeletti RH, editor. Techniques in Protein Chemistry III: Academic Press; 1992. p. 135-49.

208. Tuli L, Ressom HW. LC-MS based detection of differential protein expression. Journal of proteomics & bioinformatics. 2009;2:416-38.

209. Pitt JJ. Principles and applications of liquid chromatography-mass spectrometry in clinical biochemistry. Clinical Biochemist Reviews. 2009;30(1):19-34.

210. Coskun O. Separation techniques: Chromatography. Northern Clinics of Istanbul. 2016;3(2):156-60.

211. Theodoridis GA, Gika HG, Plumb R, Wilson ID. Chapter 9 - Liquid chromatographic methods combined with mass spectrometry in metabolomics. In: Issaq HJ, Veenstra TD, editors. Proteomic and Metabolomic Approaches to Biomarker Discovery (Second Edition). Boston: Academic Press; 2020. p. 149-69.

212. Rubakhin SS, Sweedler JV. A mass spectrometry primer for mass spectrometry imaging. Methods in molecular biology (Clifton, NJ). 2010;656:21-49.

213. Agnieszka KaS, J. (eds.) Proteomics: introduction to methods and applications. John Wiley & Sons. 2008.

214. Arevalo R, Jr., Ni Z, Danell RM. Mass spectrometry and planetary exploration: a brief review and future projection. Journal of mass spectrometry. 2020;55(1):e4454-e.

215. Mellon FA. Mass spectrometry | Principles and Instrumentation. In: Caballero B, editor. Encyclopedia of Food Sciences and Nutrition (Second Edition). Oxford: Academic Press; 2003. p. 3739-49.

216. Thomas SN. Chapter 10 - Mass spectrometry. In: Clarke W, Marzinke MA, editors. Contemporary Practice in Clinical Chemistry (Fourth Edition): Academic Press; 2019. p. 171-85.

217. March RE. Ion trap mass spectrometers. In: Lindon JC, editor. Encyclopedia of Spectroscopy and Spectrometry (Second Edition). Oxford: Academic Press; 2010. p. 1165-73.

218. Burlingame AL. Methods in enzymology: biological mass spectrometry. Elsevier Academic Press. 2005.

219. Jungblut PR, Bumann D, Haas G, Zimny-Arndt U, Holland P, Lamer S, et al. Comparative proteome analysis of *Helicobacter pylori*. Molecular Microbiology. 2000;36(3):710-25.

220. Bumann D, Aksu S, Wendland M, Janek K, Zimny-Arndt U, Sabarth N, et al. Proteome analysis of secreted proteins of the gastric pathogen *Helicobacter pylori*. Infection and Immunity. 2002;70(7):3396-403.

221. Chiu KH, Wang LH, Tsai TT, Lei HY, Liao PC. Secretomic analysis of host-pathogen interactions reveals that elongation factor-tu is a potential adherence factor of *Helicobacter pylori* during pathogenesis. Journal of Proteome Research. 2017;16(1):264-73.

222. Vilaichone RK, Mahacahai V, Tumwasorn S, Kachintorn U. CagA genotype and metronidazole resistant strain of *Helicobacter pylori* in functional dyspepsia in Thailand. Journal of Gastroenterology and Hepatology. 2011;26 Suppl 3:46-8.

223. Vilaichone RK, Ratanachu-Ek T, Gamnarai P, Chaithongrat S, Uchida T, Yamaoka Y, et al. Extremely high prevalence of metronidazole-resistant *Helicobacter pylori* strains in mountain people (Karen and Hmong) in Thailand. American Journal of Tropical Medicine and Hygiene. 2016;94(4):717-20.

224. EUCAST. EUCAST (The European Committee on Antimicrobial Susceptibility Testing) Breakpoint Tables for Interpretation of MICs and Zone Diameters. The European Committee on Antimicrobial Susceptibility Testing. 2015(Version 5.0).

225. Smith SM, O'Morain C, McNamara D. Antimicrobial susceptibility testing for *Helicobacter pylori* in times of increasing antibiotic resistance. World Journal of Gastroenterology. 2014;20(29):9912-21.

226. Lowry OH, Rosebrough NJ, Farr AL, Randall RJ. Protein measurement with the Folin phenol reagent. Journal of Biological Chemistry. 1951;193(1):265-75.

227. Losuwannarak N, Maiuthed A, Kitkumthorn N, Leelahavanichkul A, Roytrakul S, Chanvorachote P. Gigantol targets cancer stem cells and destabilizes tumors via the suppression of the PI3K/AKT and JAK/STAT pathways in ectopic lung cancer xenografts. Cancers (Basel). 2019;11(12).

228. Wongin S, Narkbunnam R, Waikakul S, Chotiyarnwong P, Aresanasuwan T, Roytrakul S, et al. Construction and evaluation of osteochondral-like tissue using chondrocyte sheet and cancellous bone. Tissue Engineering - Part A. 2020.

229. Johansson C, Samskog J, Sundström L, Wadensten H, Björkesten L, Flensburg J. Differential expression analysis of *Escherichia coli* proteins using a novel software for relative quantitation of LC-MS/MS data. Proteomics. 2006;6(16):4475-85.

230. Thorsell A, Portelius E, Blennow K, Westman-Brinkmalm A. Evaluation of sample fractionation using micro-scale liquid-phase isoelectric focusing on mass spectrometric identification and quantitation of proteins in a SILAC experiment. Rapid Communications in Mass Spectrometry. 2007;21(5):771-8.

231. Perkins DN, Pappin DJ, Creasy DM, Cottrell JS. Probability-based protein identification by searching sequence databases using mass spectrometry data. Electrophoresis. 1999;20(18):3551-67.

232. Saeed AI, Bhagabati NK, Braisted JC, Liang W, Sharov V, Howe EA, et al. TM4 microarray software suite. Methods in Enzymology. 2006;411:134-93.

233. Livak KJ, Schmittgen TD. Analysis of relative gene expression data using real-time quantitative PCR and the 2(-Delta Delta C(T)) Method. Methods. 2001;25(4):402-8.

234. Leon IR, Schwammle V, Jensen ON, Sprenger RR. Quantitative assessment of in-solution digestion efficiency identifies optimal protocols for unbiased protein analysis. Molecular & Cellular Proteomics. 2013;12(10):2992-3005.

235. Blaser MJ, Berg DE. *Helicobacter pylori* genetic diversity and risk of human disease. Journal of Clinical Investigation. 2001;107(7):767-73.

236. Lekmeechai S, Su YC, Brant M, Alvarado-Kristensson M, Vallstrom A, Obi I, et al. *Helicobacter pylori* outer membrane vesicles protect the pathogen from reactive oxygen species of the respiratory burst. Frontiers in Microbiology. 2018;9:1837.

237. Ebner P, Gotz F. Bacterial Excretion of Cytoplasmic Proteins (ECP): Occurrence, Mechanism, and Function. Trends in Microbiology. 2019;27(2):176-87.

238. Lasserre JP, Beyne E, Pyndiah S, Lapaillerie D, Claverol S, Bonneu M. A complexomic study of *Escherichia coli* using two- dimensional blue native/ SDS polyacrylamide gel electrophoresis. Electrophoresis. 2006;27(16):3306-21.

239. Hays C, Burucoa C, Lehours P, Tran CT, Leleu A, Raymond J. Molecular characterization of *Helicobacter pylori* resistance to rifamycins. Helicobacter. 2018;23(1).

240. Nishizawa T, Suzuki H, Matsuzaki J, Muraoka H, Tsugawa H, Hirata K, et al. *Helicobacter pylori* resistance to rifabutin in the last 7 years. Antimicrob Agents Chemother. 2011;55(11):5374-5.

241. Hoeksema M, Jonker MJ, Brul S, Ter Kuile BH. Effects of a previously selected antibiotic resistance on mutations acquired during development of a second resistance in *Escherichia coli*. BMC Genomics. 2019;20(1):284.

242. Lai CC, Chen CC, Lu YC, Chuang YC, Tang HJ. The clinical significance of silent mutations with respect to ciprofloxacin resistance in MRSA. Infection and Drug Resistance. 2018;11:681-7.

243. Greenbaum D, Colangelo C, Williams K, Gerstein M. Comparing protein abundance and mRNA expression levels on a genomic scale. Genome Biology. 2003;4(9):117.

244. Beckmann C, Waggoner JD, Harris TO, Tamura GS, Rubens CE. Identification of novel adhesins from group B S*treptococci* by use of phage display reveals that C5a peptidase mediates fibronectin binding. Infection and Immunity. 2002;70(6):2869-76.

245. Kesimer M, Kilic N, Mehrotra R, Thornton DJ, Sheehan JK. Identification of salivary mucin MUC7 binding proteins from *Streptococcus gordonii*. BMC Microbiology. 2009;9:163.

246. Doig P, de Jonge BL, Alm RA, Brown ED, Uria-Nickelsen M, Noonan B, et al. *Helicobacter pylori* physiology predicted from genomic comparison of two strains. Microbiology and Molecular Biology Reviews. 1999;63(3):675-707.

247. Chaves EG, Weber SS, Bao SN, Pereira LA, Bailao AM, Borges CL, et al. Analysis of *Paracoccidioides* secreted proteins reveals fructose 1,6-bisphosphate aldolase as a plasminogen-binding protein. BMC Microbiology. 2015;15:53.

248. Tunio SA, Oldfield NJ, Berry A, Ala'Aldeen DA, Wooldridge KG, Turner DP. The moonlighting protein fructose-1, 6-bisphosphate aldolase of *Neisseria meningitidis*: surface localization and role in host cell adhesion. Molecular Microbiology. 2010;76(3):605-15.

249. Elhaik Goldman S, Dotan S, Talias A, Lilo A, Azriel S, Malka I, et al. *Streptococcus pneumoniae* fructose-1,6-bisphosphate aldolase, a protein vaccine candidate, elicits Th1/Th2/Th17-type cytokine responses in mice. International Journal of Molecular Medicine. 2016;37(4):1127-38.

250. Mendonca M, Moreira GM, Conceicao FR, Hust M, Mendonca KS, Moreira AN, et al. Fructose 1,6-bisphosphate aldolase, a novel immunogenic surface protein on *Listeria* species. PLoS One. 2016;11(8):e0160544.

251. Daher R, Coincon M, Fonvielle M, Gest PM, Guerin ME, Jackson M, et al. Rational design, synthesis, and evaluation of new selective inhibitors of microbial class II (zinc dependent) fructose bis-phosphate aldolases. Journal of Medicinal Chemistry. 2010;53(21):7836-42.

252. Ziveri J, Tros F, Guerrera IC, Chhuon C, Audry M, Dupuis M, et al. The metabolic enzyme fructose- 1,6- bisphosphate aldolase acts as a transcriptional regulator in pathogenic *Francisella*. Nature Communications. 2017;8(1):853.

253. Fonvielle M, Coincon M, Daher R, Desbenoit N, Kosieradzka K, Barilone N, et al. Synthesis and biochemical evaluation of selective inhibitors of class II fructose bisphosphate aldolases: towards new synthetic antibiotics. Chemistry. 2008;14(28):8521-9.

254. Liu Y, Beyer A, Aebersold R. On the dependency of cellular protein levels on mRNA abundance. Cell. 2016;165(3):535-50.

255. Vogel C, Marcotte EM. Insights into the regulation of protein abundance from proteomic and transcriptomic analyses. Nature Reviews Genetics. 2012;13(4):227-32.

256. Ong SE, Blagoev B, Kratchmarova I, Kristensen DB, Steen H, Pandey A, et al. Stable isotope labeling by amino acids in cell culture, SILAC, as a simple and accurate approach to expression proteomics. Molecular & Cellular Proteomics. 2002;1(5):376-86.

257. Spreng S, Gentschev I, Goebel W, Mollenkopf H, Eck M, Muller- Hermelink HK, et al. Identification of immunogenic antigens of *Helicobacter pylori* via the *Escherichia coli* hemolysin secretion system. FEMS Microbiology Letters. 2000;186(2):251-6.

258. Kimmel B, Bosserhoff A, Frank R, Gross R, Goebel W, Beier D. Identification of immunodominant antigens from *Helicobacter pylori* and evaluation of their reactivities with sera from patients with different gastroduodenal pathologies. Infection and Immunity. 2000;68(2):915-20.

259. Takeuchi H, Kira M, Konishi S, Uchiyama J, Matsuzaki S, Matsumura Y. Polymorphisms in the *Helicobacter pylori* NY43 strain and its prophage- cured derivatives. Microbiology (Reading). 2018;164(6):877-82.

260. Vale FF, Lehours P. Relating phage genomes to *Helicobacter pylori* population structure: General steps using Whole-Genome sequencing data. International Journal of Molecular Sciences. 2018;19(7).

261. Uchiyama J, Takeuchi H, Kato S, Gamoh K, Takemura-Uchiyama I, Ujihara T, et al. Characterization of *Helicobacter pylori* bacteriophage KHP30. Applied and Environmental Microbiology. 2013;79(10):3176-84.

262. Suzuki S, Esaki M, Kusano C, Ikehara H, Gotoda T. Development of *Helicobacter pylori* treatment: How do we manage antimicrobial resistance? World Journal of Gastroenterology. 2019;25(16):1907-12.

263. Yousefi-Avarvand A, Vaez H, Tafaghodi M, Sahebkar AH, Arzanlou M, Khademi F. Antibiotic resistance of *Helicobacter pylori* in iranian children: a systematic review and meta-analysis. Microbial Drug Resistance. 2018;24(7):980-6.

264. Tavares R, Pathak SK. *Helicobacter pylori* secreted protein HP1286 triggers apoptosis in macrophages via TNF-Independent and ERK MAPK-Dependent pathways. Frontiers in Cellular and Infection Microbiology. 2017;7:58.

265. Kao JY, Rathinavelu S, Eaton KA, Bai L, Zavros Y, Takami M, et al. *Helicobacter pylori*-secreted factors inhibit dendritic cell IL-12 secretion: a mechanism of ineffective host defense. American Journal of Physiology-Gastrointestinal and Liver Physiology. 2006;291(1):G73-81.

266. Carlsohn E, Nystrom J, Karlsson H, Svennerholm AM, Nilsson CL. Characterization of the outer membrane protein profile from disease- related *Helicobacter pylori* isolates by subcellular fractionation and nano- LC FT- ICR MS analysis. Journal of Proteome Research. 2006;5(11):3197-204.

267. Kim N, Weeks DL, Shin JM, Scott DR, Young MK, Sachs G. Proteins released by *Helicobacter pylori* in vitro. Journal of Bacteriology. 2002;184(22):6155-62.

268. Zanotti G, Cendron L. Structural and functional aspects of the *Helicobacter pylori* secretome. World Journal of Gastroenterology. 2014;20(6):1402-23.

APPENDICES

APPENDIX A

CHEMICAL REAGENTS PREPARATION

1. Protein determination reagents

1.1. Lowry method

1.1.1 Solution A

0.4% $CuSO_4.7H_20$	5	ml
20% sodium carbonate	5	ml
0.8 N NaOH	10	ml
5% SDS	20	ml

1.1.2 Solution B

20% Folin-Ciocalteu phenol	2	ml
Deionized water	10	ml

2. In-solution digestion reagents

2.1	10 mM Ammonium bicarbonate			
	Ammonium bicarbonate		39.8	mg
	Deionized water	add to	50	ml
2.2	Reducing solution			
	DTT		15.425	mg
	10 mM Ammonium bicarbonate		10	ml
2.3	Alkylating solution			
	Iodoacetamide		185	mg
	10 mM Ammonium bicarbonate		10	ml
2.4	10 ng/µl Trypsin solution			
	Trypsin		20	µg
	10 mM Ammonium bicarbonate		2	ml

3. Chemical lists

Water (LC grade)	(Labscan, Thailand)
Absolute Ethanol (AR grade)	(Labscan, Thailand)
Agarose	(Vivantis, USA)
Ammonium bicarbonate	(Sigma, USA)
Bovine serum albumin (BSA)	(Sigma, USA)
Copper sulfate ($CuSo_4.7H_2O$)	(Fisher scientific, USA)
Chloroform	(Labscan, Thailand)
DEPC treat-water	(USB corporation, USA)
Dithiotheritol (DTT)	(GE Healthcare, UK)
Folin-Ciocalteu phenol	(Merck, Germany)
Formic acid	(Merck, Germany)
Iodoacetamide (IAA)	(GE Healthcare, UK)
Isopropanol	(Labscan, Thailand)
Sodium Carbonate	(Sigma, USA)
Sodium dodecyl sulfate (SDS)	(USB corporation, USA)
TBE buffer	(Bio basic, Canada)
Trypsin	(Promega, USA)

APPENDIX B

THE GUIDELINES AND REGULATIONS FOR STANDARD AND SPECIAL MICROBIOLOGICAL PRACTICES FOR BIOSAFETY LEVEL II.

This study was initiated after approval from Thammasat University' s Institution Biosafety Committee (IBC 126/2019).

ลับ

งานบริหารการวิจัย คณะแพทยศาสตร์
รับที่ 1910
วันที่ 15 พ.ย. 2562
เวลา 16.00

บันทึกข้อความ

ส่วนราชการ คณะกรรมการควบคุมความปลอดภัยทางชีวภาพ มธ. กองบริหารการวิจัย (สิริลักษณ์) โทร.1805
ที่ อว 67.04.2/ 1486 **วันที่** 6 พฤศจิกายน 2562
เรื่อง ขอแจ้งผลการพิจารณาของคณะกรรมการควบคุมความปลอดภัยทางชีวภาพ มหาวิทยาลัยธรรมศาสตร์

เรียน นางสาว สุธาทิพย์ กิตติเสนาชัย

ตามที่ท่านได้เสนอโครงการวิจัย เรื่อง "การศึกษาเบื้องต้นของโปรตีนที่หลั่งออกมาจากเชื้อ Helicobacter pylori ชนิดดื้อต่อยาคลาริโธรมัยซิน และเมโทรนิดาโซล" (รหัสโครงการ 119/2562) โดยมี นางสาว สุธาทิพย์ กิตติเสนาชัย คณะแพทยศาสตร์ เป็นหัวหน้าโครงการวิจัย และมี รองศาสตราจารย์ ปนัดดา โรจน์พิบูลย์สถิตย์ คณะแพทยศาสตร์ เป็นที่ปรึกษาโครงการวิจัย เพื่อขอรับการพิจารณาจาก คณะกรรมการควบคุมความปลอดภัยทางชีวภาพ มหาวิทยาลัยธรรมศาสตร์ นั้น

ในการนี้ คณะกรรมการควบคุมความปลอดภัยทางชีวภาพ มหาวิทยาลัยธรรมศาสตร์ ได้พิจารณา **อนุมัติด้านความปลอดภัยทางชีวภาพให้กับโครงการวิจัยดังกล่าวเรียบร้อยแล้ว** สรุปได้ดังนี้ (ตามหนังสือรับรองเลขที่ 126/2562 ที่ได้แนบมาพร้อมนี้)

ประเภทของโครงการ ประเภทที่ 2
ระดับความปลอดภัยของห้องปฏิบัติการ ความปลอดภัยระดับที่ 2 (Biosafety Level 2)

ทั้งนี้ข้อปฏิบัติของการดำเนินงานด้านความปลอดภัยทางชีวภาพ ผู้วิจัยต้องแจ้งรายงานความก้าวหน้าและปิดโครงการเมื่อแล้วเสร็จตามแบบแบบฟอร์ม TU-IBC_E (Amendment/ Extension/ Termination Form version 1.0) ดาวน์โหลดแบบฟอร์มได้ที่ลิ้งก์ http://research.tu.ac.th/process-biosafety ***ส่งมาที่ คณะกรรมการควบคุมความปลอดภัยทางชีวภาพ มหาวิทยาลัยธรรมศาสตร์ งานวางแผนและบริหารงานวิจัย กองบริหารการวิจัย อาคารสำนักงานออิการบดี ชั้น 2 มหาวิทยาลัยธรรมศาสตร์ ศูนย์รังสิต***

จึงเรียนมาเพื่อโปรดทราบ และโปรดดำเนินการตามข้อกำหนดดังกล่าวด้วย จักขอบคุณยิ่ง

(ผู้ช่วยศาสตราจารย์ ดร. พจนีย์ ศรีมาโนชญ์)
ประธานคณะกรรมการควบคุมความปลอดภัยทางชีวภาพ
มหาวิทยาลัยธรรมศาสตร์

สำเนาเรียน 1. คณบดีคณะแพทยศาสตร์
2. รองศาสตราจารย์ ปนัดดา โรจน์พิบูลย์สถิต (ที่ปรึกษาโครงการ)

APPENDIX C

THE GUIDELINES AND REGULATIONS FOR STANDARD AND SPECIAL MICROBIOLOGICAL PRACTICES FOR BIOSAFETY LEVEL II.

This study was initiated after approval from National Center for Genetic Engineering and Biotechnology Biosafety Committee (BT-IBC 62-056).

BIOTEC
a member of NSTDA

ศูนย์พันธุวิศวกรรมและเทคโนโลยีชีวภาพแห่งชาติ

113 อุทยานวิทยาศาสตร์ประเทศไทย ถนนพหลโยธิน ตำบลคลองหนึ่ง อำเภอคลองหลวง ปทุมธานี 12120

โทรศัพท์ 0 2564 6700 โทรสาร 0 2564 6580

บันทึกข้อความ

ที่ อว 6002.0106/28/2563 วันที่ 15 มกราคม 2563

เรื่อง ผลการพิจารณาโครงการวิจัยทางพันธุวิศวกรรม รหัสโครงการ BT-IBC-62-056

เรียน หัวหน้าโครงการ (นางสาวสุธาทิพย์ กิตติเสนาชัย)

ตามที่ มีการประชุมคณะกรรมการด้านความปลอดภัยทางชีวภาพ ศช. เมื่อวันที่ 12 ธันวาคม 2562 โดยข้อเสนอโครงการวิจัยเรื่อง **การศึกษาเบื้องต้นของโปรตีนที่หลั่งออกมาจากเชื้อ *Helicobacter pylori* ชนิดดื้อต่อยาคลาริโธรมัยซิน และเมโทรนิดาโซล** ได้ผ่านการพิจารณาจากคณะกรรมการฯ แล้วมี**มติให้เป็นโครงการวิจัยประเภทที่ 1 (C1) ควรต้องใช้ระดับห้องปฏิบัติการ 1 (BSL1) กรณีที่นำ supernatant ผ่านการกรองด้วยกระดาษกรองขนาด 0.2 µm จากห้องปฏิบัติการ BSL2 ของ มธ. มาแล้ว**

ทั้งนี้ ขอให้มีการรายงานความก้าวหน้าโครงการวิจัยที่เกี่ยวข้องกับโครงการทางพันธุวิศวกรรม เชื้อโรคและพิษจากสัตว์ ในเดือน**กันยายนของทุกปี** ดังรายละเอียดตามเอกสาร F-BT-SHE-BS03 Rev.0 ที่แนบมาพร้อมนี้ ในการนี้คณะกรรมการฯ มีความเห็นและข้อเสนอแนะเพิ่มเติม ดังนี้ **ขอใบอนุญาตจาก IBC ของ มธ. และแจ้ง IBC-ศช. เพื่อรับทราบด้วย**

จึงเรียนมาเพื่อทราบ**และโปรดเก็บใบแจ้งผลการพิจารณาโครงการวิจัยทางพันธุวิศวกรรมโดยมิให้สูญหาย เนื่องจากคณะกรรมการฯ จะไม่ดำเนินการออกใบแจ้งผลการพิจารณาโครงการฯ ย้อนหลังให้**

นงนพร จันทร์วราสุทธิ์

(นางนงนพร จันทร์วราสุทธิ์)
ประธานคณะกรรมการ
ด้านความปลอดภัยทางชีวภาพ ศช.

ฝ่ายศึกษานโยบายและความปลอดภัยทางชีวภาพ
โทร. 0 2564 6700 ต่อ 3312 (วิภาพร)
โทรสาร 0 2564 6703
สำเนาส่ง ฝ่ายสนับสนุนการวิจัย ศช.

APPENDIX D

ETHICS APPROVAL FROM THE RESEARCH ETHICS SUBCOMMITTEE IN PEOPLE THAMMASAT UNIVERSITY SERIES 1 (APPROVAL NUMBER 236/2019)

Certificate of Approval

Human Research Ethics Committee of Thammasat University No.1 (Faculty of Medicine)

99/209 Moo 18, Paholyotin Road, Auphur Klongluang, Pathumthani, Thailand 12120,

Tel 662-9269704 and Fax 662-5644444 ext. 7535

Number of COA	236/2019
Title of Project	Preliminary study of secretome analysis from Helicobacter pylori dual resistance to clarithromycin and metronidazole strain
Project No	MTU-EC-ES-0-247/62
Principal Investigator	Miss Suthathip Kittisenachai Associate. Professor Panadda Rojpibulstit Professor Ratha Korn Vilaichone Associate. Professor Dr. Sasichai Kangsaldalamphai Miss Pornpen Kamnarai
Responsible Department	Graduate Studies, Faculty of Medicine, Thammasat University, Pathumthani, Thailand 12120 Tel. 083-242-6592

Document Reviewed

1. Protocol No 1: dated January 14, 2020

The Human Research Ethics Committee of Thammasat University No. I (Faculty of Medicine) is in full compliance with International Regulations such as Declaration of Helsinki, The Belmont Report, CIOMS Guidelines and the International Practice (ICH-GCP).

The Human Research Ethics Committee of Thammasat University No.1 (Faculty of Medicine) decided to exempt the above study on January 14, 2019 these decision has been reported in 1/2020 meeting.

Signed: .....

(Associate Professor Thana Khawcharoenporn,M.D.)

Secretary and Committee of the Human Research Ethics Committee of Thammasat University No.1

(Faculty of Medicine)

Signed: .....

(Associate Professor Waipoj Chanvimalueng,M.D.)

Chairman of the Human Research Ethics Committee of Thammasat University No.1

(Faculty of Medicine)

Note 1. No Continuing review required.

2. The protocol will be kept for 3 years after the date of exempt decision.

APPENDIX E

Quantitative analysis by LC-MS/MS showed 592 differentials expressed proteins.

#	Accession No.	Protein Name	Peptide	MOWSE Score	Cla/Mtz-R	Cla-R	Mtz-R	Sen-S
1	gi|226701775	10 kDa chaperonin	VVSHK	3.33	16.85	16.29	16.43	16.38
2	gi|12230506	1-acyl-sn-glycerol-3-phosphate acyltransferase	NNNARSSR	7.94	18.08	16.43	16.86	16.01
3	gi|226697591	1-deoxy-D-xylulose 5-phosphate reductoisomerase	ITIDSASMVNK	1.29	15.52	14.80	15.02	14.91
4	gi|226801559	1-deoxy-D-xylulose-5-phosphate synthase	IAEGR	3.56	15.60	15.70	15.11	15.11
5	gi|81555811	2,3,4,5-tetrahydropyridine-2,6-dicarboxylate N-succinyltransferase	VDIAPISK	6.45	16.90	17.32	18.37	17.31
6	gi|123373726	2,3-bisphosphoglycerate-independent phosphoglycerate mutase	VLIPSPK	2.62	18.11	16.56	0	15.87
7	gi|133247	28 kDa ribonucleoprotein, chloroplastic	ETDRSR	4.22	18.14	17.48	16.98	17.33
8	gi|30316379	29 kDa ribonucleoprotein, chloroplastic	SSYGSGSGSGSGSGSGNR	4.11	0	19.37	18.80	0
9	gi|9789774	2-amino-4-hydroxy-6-hydroxymethyldihydropteridine pyrophosphokinase	NPLKILK	5.05	17.78	16.13	16.82	15.71
10	gi|123373868	2-dehydro-3-deoxyphosphooctonate aldolase	QTDLIVEVSQTNAIINIK	2.03	14.59	14.67	15.79	15.15
11	gi|8928319	3,4-dihydroxy-2-butanone 4-phosphate synthase	NGEMLIVMDDEDR	2.46	14.80	14.76	13.50	13.65
12	gi|81341571	3',5'-cyclic-nucleotide phosphodiesterase	NYKLK	5.54	15.74	16.44	15.40	16.53
13	gi|1350820	30 kDa ribonucleoprotein, chloroplastic	ENSSFRGGSR	2.70	16.51	16.01	16.13	15.55
14	gi|75275079	30S ribosomal protein 2, chloroplastic	TVTNELLKDFFSEK	3.70	20.24	16.19	19.51	16.08
15	gi|12230557	30S ribosomal protein S1	NDANHIGK	4.43	15.46	16.64	15.95	16.20
16	gi|226705577	30S ribosomal protein S10	MEKIR	1.03	16.45	16.25	16.52	16.00

#	Accession No.	Protein Name	Peptide	MOWSE Score	Cla/Mtz-R	Cla-R	Mtz-R	Sen-S
17	gi|226708376	30S ribosomal protein S11	ETAIKSVGATEGVK	2.19	15.39	16.38	16.39	15.78
18	gi|226708511	30S ribosomal protein S12	VYTTTPK	1.46	18.98	18.68	19.35	18.43
19	gi|226712745	30S ribosomal protein S13	MARIAGVDLPK	2.45	18.72	18.33	17.35	22.28
20	gi|226725251	30S ribosomal protein S14 type Z	KPKFQVR	1.38	15.80	15.98	16.60	16.47
21	gi|2500462	30S ribosomal protein S15	LVAQRR	2.36	16.35	15.28	15.60	15.17
22	gi|226697841	30S ribosomal protein S16	GVGAK	14.11	15.37	15.99	15.66	15.95
23	gi|226697984	30S ribosomal protein S17	VVHEKYR	11.74	16.22	16.51	17.66	16.82
24	gi|229559989	30S ribosomal protein S18	VEVAIKR	1.02	20.20	20.57	20.88	19.54
25	gi|226735201	30S ribosomal protein S19	MSRSIK	7.92	12.99	14.36	14.09	15.55
26	gi|123246861	30S ribosomal protein S2	LDKYLGGVR	6.93	16.78	16.73	16.57	12.96
27	gi|226736504	30S ribosomal protein S20	NTASRK	2.58	14.78	15.96	16.34	16.33
28	gi|226697719	30S ribosomal protein S3	GIQFEKK	3.37	16.61	16.55	15.93	16.54
29	gi|226699073	30S ribosomal protein S4	AKMMYGISEK	3.08	21.10	19.73	20.08	18.13
30	gi|152031680	30S ribosomal protein S5	VTKVVK	12.76	17.07	14.68	14.37	15.11
31	gi|226703475	30S ribosomal protein S6	KPSHAKEK	8.10	15.21	14.84	15.31	15.10
32	gi|123073738	30S ribosomal protein S7	MMVDRLANELMDAASDK	1.20	21.87	17.15	18.15	17.97
33	gi|226708537	30S ribosomal protein S8	RLSKPGR	4.45	18.91	15.91	15.28	15.56
34	gi|54041994	30S ribosomal protein S9	IYATGK	8.16	16.19	16.06	15.90	15.77
35	gi|464662	31 kDa ribonucleoprotein, chloroplastic	AAPRGSRPER	9.21	15.62	15.35	15.11	15.74
36	gi|133249	33 kDa ribonucleoprotein, chloroplastic	AHFPISSLYR	6.80	15.16	11.69	14.59	13.53
37	gi|12229681	36 kDa antigen	LAQAEAGHK	3.22	17.89	17.10	18.37	18.23
38	gi|2492962	3-dehydroquinate synthase	MQEILIPLKEK	23.44	17.76	17.74	18.26	0

#	Accession No.	Protein Name	Peptide	MOWSE Score	Cla/Mtz-R	Cla-R	Mtz-R	Sen-S
39	gi|238056511	3-deoxy-manno-octulosonate cytidylyltransferase	MIIIPAR	4.32	14.96	14.46	14.49	15.28
40	gi|226700474	3-hydroxyacyl-[acyl-carrier-protein] dehydratase FabZ	VVELEANKK	6.16	21.92	19.13	18.18	17.97
41	gi|226700739	3-methyl-2-oxobutanoate hydroxymethyltransferase	SMQTAPIK	2.68	15.64	15.37	16.60	15.42
42	gi|254783805	3-oxoacyl-[acyl-carrier-protein] synthase 3	TLLRDVEMILEK	9.49	19.28	18.77	18.87	16.39
43	gi|123073753	3-phosphoshikimate 1-carboxyvinyltransferase	IIEPLKAFGAR	8.63	17.64	17.76	16.24	18.41
44	gi|6919918	4-diphosphocytidyl-2-C-methyl-D-erythritol kinase	LEIYAPNHVFCSTK	9.88	16.94	14.72	16.74	16.14
45	gi|226741014	4-hydroxy-3-methylbut-2-en-1-yl diphosphate synthase (flavodoxin)	ISLKASDVMR	1.27	16.57	14.25	13.38	12.91
46	gi|54041395	4-hydroxy-3-methylbut-2-enyl diphosphate reductase	RAIQIAEK	8.48	17.13	17.51	16.29	16.68
47	gi|226696355	4-hydroxy-tetrahydrodipicolinate reductase	GYDEK	5.52	23.70	22.11	20.29	19.02
48	gi|226722431	4-hydroxy-tetrahydrodipicolinate synthase	TGVSIEVSTALK	1.75	15.95	11.05	7.80	11.91
49	gi|122386074	4-hydroxythreonine-4-phosphate dehydrogenase	ACELADDK	1.63	17.03	15.60	15.86	15.97
50	gi|2500218	50S ribosomal protein L1	ENMLELVK	6.96	13.72	15.55	13.73	15.31
51	gi|226699960	50S ribosomal protein L10	ESVSVAHVEAVSK	2.90	19.89	18.12	16.22	14.81
52	gi|226702700	50S ribosomal protein L11	LQIPAGK	2.62	16.25	16.00	15.78	15.19
53	gi|226702868	50S ribosomal protein L13	TAKVNEIVR	1.28	16.66	15.15	15.48	15.74
54	gi|7674191	50S ribosomal protein L14	FGLVVK	4.36	17.29	17.90	17.17	17.72
55	gi|115502664	50S ribosomal protein L15	MIMGLENLKPAKGSVK	9.34	20.70	20.86	20.78	20.86
56	gi|226710734	50S ribosomal protein L16	GSVEK	3.36	16.61	15.83	15.83	16.42
57	gi|226712163	50S ribosomal protein L17	IQRTTFR	3.84	16.31	15.13	15.99	15.21
58	gi|226723335	50S ribosomal protein L18	KMGFK	1.14	16.60	15.72	16.16	14.09
59	gi|7674218	50S ribosomal protein L19	SMPTFK	1.42	20.02	18.68	17.61	17.17

#	Accession No.	Protein Name	Peptide	MOWSE Score	Cla/Mtz-R	Cla-R	Mtz-R	Sen-S
60	gi|226702945	50S ribosomal protein L2	RFMSVLDSK	1.59	14.53	14.52	14.05	15.24
61	gi|226730408	50S ribosomal protein L20	VAGVELDR	3.91	15.43	15.94	15.64	15.76
62	gi|226733244	50S ribosomal protein L21	MDKEPK	1.21	15.67	15.75	16.08	15.88
63	gi|226733472	50S ribosomal protein L22	EMKSSK	9.08	16.09	15.92	16.08	16.31
64	gi|226734814	50S ribosomal protein L23	MADIMDIK	2.83	15.17	14.65	14.59	15.21
65	gi|123246889	50S ribosomal protein L24	NDMVKVIAGDDK	1.36	13.88	14.46	13.36	13.90
66	gi|7674253	50S ribosomal protein L25	DGYLIANIYGK	2.69	15.43	15.26	18.71	15.17
67	gi|226737937	50S ribosomal protein L27	AGNIIVR	15.25	21.32	21.70	19.35	22.93
68	gi|226694946	50S ribosomal protein L28	LLPNLR	9.62	16.13	15.12	14.08	14.77
69	gi|123246888	50S ribosomal protein L29	KYTELK	2.89	17.55	18.01	17.62	17.49
70	gi|7674309	50S ribosomal protein L3	ALVAYAMHKK	6.88	18.26	17.39	18.20	16.30
71	gi|2500328	50S ribosomal protein L32	MAVPDRR	3.47	14.12	15.71	15.67	0
72	gi|226725019	50S ribosomal protein L35	GSAFK	2.11	17.59	17.34	17.24	17.17
73	gi|2500340	50S ribosomal protein L36	KMCDNCK	4.61	15.74	15.42	16.39	16.16
74	gi|7674310	50S ribosomal protein L4	DTLFVCLNMDEYTELAFSNLKK	1.39	11.19	11.02	10.17	14.80
75	gi|226731292	50S ribosomal protein L5	IREGMAVGAK	2.16	15.20	16.09	14.85	15.02
76	gi|226733547	50S ribosomal protein L6	VGQVAAEIR	7.47	16.18	16.59	16.13	15.63
77	gi|7388074	50S ribosomal protein L7/L12	VVREITGLGLK	2.94	16.92	16.64	16.13	17.35
78	gi|226734574	50S ribosomal protein L9	AEKEALEK	4.36	14.43	14.71	14.51	13.17
79	gi|226709104	5'-nucleotidase SurE	AEKIK	2.99	15.18	15.22	14.96	15.68
80	gi|226738661	6,7-dimethyl-8-ribityllumazine synthase	VAILTSR	5.15	19.20	15.98	15.82	15.93
81	gi|2506272	60 kDa chaperonin	AAPAMPDMGGMGGMGGMGGMM	1.84	14.44	14.33	12.30	11.96

#	Accession No.	Protein Name	Peptide	MOWSE Score	Cla/Mtz-R	Cla-R	Mtz-R	Sen-S
82	gi|6647977	6-carboxy-5,6,7,8-tetrahydropterin synthase	RLYQFCASHVVR	7.80	17.45	17.32	15.92	15.70
83	gi|7387521	6-phosphogluconolactonase	ENIVLTKPTNAPYER	10.52	24.39	23.73	23.29	23.29
84	gi|254764352	7-cyano-7-deazaguanine synthase	AQEFQMAKDLGVLDLVIK	3.49	14.27	15.50	15.70	15.15
85	gi|6685217	Acetate kinase	FKLFDMK	3.58	14.42	14.75	14.91	14.51
86	gi|226706949	Acetyl-coenzyme A carboxylase carboxyl transferase subunit alpha	VPTISVIIGEGGSGGALAIAVADK	1.81	17.11	14.92	16.07	14.73
87	gi|226709492	Acetyl-coenzyme A synthetase	INDAQAKLVITADGTFR	4.83	14.40	14.31	15.41	14.97
88	gi|9789850	Aconitate hydratase B	SAAACVVRLNK	14.23	17.10	13.16	13.28	14.63
89	gi|3023239	Acyl carrier protein	IINVGDVVK	3.25	18.10	17.04	17.60	18.47
90	gi|14285529	Acyl-[acyl-carrier-protein]--UDP-N-acetylglucosamine O-acyltransferase	RLFRPIPSLR	2.10	21.76	19.97	20.47	18.97
91	gi|6176568	Acyl-CoA thioesterase YbgC	ARSEFFFK	1.05	17.22	17.38	17.79	17.25
92	gi|48428272	Adenine DNA glycosylase	RDLPWR	12.89	18.37	20.77	21.42	21.08
93	gi|81341163	Adenosine deaminase	IALLGATR	4.76	18.96	19.32	17.39	17.26
94	gi|3182925	Adenosylmethionine-8-amino-7-oxononanoate aminotransferase	LCQLTHMDK	5.82	18.09	17.32	17.29	16.54
95	gi|238055697	Adenylate kinase	MKQLFLIIGAPGSGK	4.89	18.89	15.42	16.82	15.40
96	gi|6685830	Adenylosuccinate lyase	YLNESEIR	6.86	15.71	13.86	14.96	14.64
97	gi|226709081	Adenylosuccinate synthetase	EQSQNIGTTKK	1.91	12.87	16.78	14.63	13.79
98	gi|410516865	Adhesion G protein-coupled receptor B1	SGATIPLVGQDIIDLQTEV	1.54	14.49	14.04	12.77	13.20
99	gi|9789719	Alanine racemase	NIVPKDACVMAVVK	2.08	15.81	15.40	14.60	16.20
100	gi|3024653	Alanine--tRNA ligase	GDFASAGGK	4.11	14.58	14.58	14.24	14.16

#	Accession No.	Protein Name	Peptide	MOWSE Score	Cla/Mtz-R	Cla-R	Mtz-R	Sen-S
101	gi|31339951	Aliphatic amidase	TWVNDPKK	2.53	16.36	15.69	14.37	15.52
102	gi|7387493	Alkyl hydroperoxide reductase C	LAPDFK	3.64	16.13	16.85	17.14	17.20
103	gi|75340762	Alpha-(1,3)-fucosyltransferase FucT	YLHTHK	4.53	17.69	15.82	16.09	14.87
104	gi|308153632	Alpha-protein kinase 1	QARISVNSGK	2.47	16.57	15.33	14.92	15.12
105	gi|3183121	Aminodeoxyfutalosine nucleosidase	MVQKIGILGAMR	1.26	15.79	15.21	18.39	17.34
106	gi|745998051	Aminopyrimidine aminohydrolase	ELQITQK	6.17	15.60	14.93	15.59	15.08
107	gi|3914982	aminotransferase HP_0736	KAALATQK	1.52	16.61	16.64	16.84	15.95
108	gi|8134817	aminotransferase jhp_0673	RVALASQK	5.20	15.55	16.12	15.32	15.75
109	gi|3913428	Anaerobic C4-dicarboxylate transporter DcuA	ISPPK	1.59	16.47	15.24	15.01	15.52
110	gi|238057714	Anthranilate phosphoribosyltransferase	ILEYDLSAK	3.37	14.67	12.92	14.98	15.61
111	gi|6647867	Anthranilate synthase component 1	ISAIR	6.32	16.73	17.21	17.64	17.18
112	gi|46576681	Apolipoprotein N-acyltransferase	VGNIELVSTK	8.61	16.00	16.89	15.91	16.11
113	gi|2501046	Arginine--tRNA ligase	ISARD	5.91	16.02	14.42	13.98	14.34
114	gi|2494615	Aspartate ammonia-lyase	ELNLGGTAIGTGINSHPDYR	2.14	15.41	17.17	15.87	17.67
115	gi|226710810	Aspartate carbamoyltransferase	DIDIESAVLEDK	3.23	18.25	16.52	16.54	16.04
116	gi|9789750	Aspartate-semialdehyde dehydrogenase	GLENSFFPIKK	4.38	15.04	13.41	12.37	11.78
117	gi|238691926	Aspartate--tRNA(Asp/Asn) ligase	SSSIR	4.45	16.43	16.42	16.08	16.38
118	gi|11131019	Aspartokinase	LGHQVVVVVSAMSGETDR	1.00	17.08	14.28	14.85	14.64
119	gi|7994574	Aspartyl/glutamyl-tRNA(Asn/Gln) amidotransferase subunit B	INELPSAK	2.60	15.40	18.37	18.83	16.05
120	gi|226740262	ATP synthase epsilon chain	DDAISRAK	2.07	16.17	16.74	16.36	17.21
121	gi|226698261	ATP synthase gamma chain	TLTISYNKAR	2.32	15.61	16.32	16.33	16.87

#	Accession No.	Protein Name	Peptide	MOWSE Score	Cla/Mtz-R	Cla-R	Mtz-R	Sen-S
122	gi|226739894	ATP synthase subunit alpha	VGGAAQIKATK	3.46	15.37	17.22	16.91	14.96
123	gi|2493068	ATP synthase subunit b	AELIVSDANK	3.53	15.35	16.59	15.39	14.75
124	gi|2493023	ATP synthase subunit beta	NRIAFTGLTMAEYFR	2.84	15.27	14.60	15.08	15.57
125	gi|2493073	ATP synthase subunit c	NPGVGGK	4.16	16.34	16.12	16.12	15.29
126	gi|81815262	ATP/GTP phosphatase	VPNFPPIPNQSGYNRQFK	6.54	15.54	15.85	15.29	15.15
127	gi|2495581	ATP-dependent Clp protease adapter protein ClpS	AAWVRDK	2.26	14.50	15.61	16.14	14.73
128	gi|8134369	ATP-dependent Clp protease ATP-binding subunit ClpX	MESSAYEEEFLLSRIPAPK	2.92	15.05	13.21	13.28	14.56
129	gi|226706454	ATP-dependent Clp protease proteolytic subunit	EYGLIDKVLQK	22.74	23.11	22.44	21.91	21.92
130	gi|11131453	ATP-dependent dethiobiotin synthetase BioD	MLFISATNTNAGK	10.49	21.10	21.01	20.76	20.21
131	gi|10720254	ATP-dependent DNA helicase RecG	MASSK	1.29	15.22	16.46	15.20	15.58
132	gi|238065799	ATP-dependent protease ATPase subunit HslU	QDPSK	2.16	17.69	17.56	17.55	16.98
133	gi|11132781	ATP-dependent protease subunit HslV	GELNHK	3.80	16.76	16.33	16.82	15.99
134	gi|2492508	ATP-dependent zinc metalloprotease FtsH	MKPTNEPK	8.32	15.90	16.16	15.36	16.43
135	gi|2506399	Bacterial non-heme ferritin	DILDK	2.64	21.52	21.69	21.08	19.20
136	gi|3913505	Beta sliding clamp	RELAGILMQFDQK	2.89	17.44	18.71	18.67	0
137	gi|12643339	Beta-lactamase HcpA	KASQYYSK	3.98	16.65	15.08	15.46	15.86
138	gi|34098776	beta-lactamase HcpC	SYKEQDFTQAK	2.54	15.15	13.99	15.54	13.95
139	gi|34098373	beta-lactamase HcpD	SDDLQDDAQNDTQDDMQ	2.49	16.34	14.57	14.61	16.38
140	gi|34098374	beta-lactamase HcpE	GFLEVK	1.15	16.33	15.99	15.82	15.90
141	gi|81555856	Bifunctional dihydropteroate synthase/dihydropteroate reductase	KALEEIYQWLEK	2.95	19.78	19.78	19.74	19.51

#	Accession No.	Protein Name	Peptide	MOWSE Score	Cla/Mtz-R	Cla-R	Mtz-R	Sen-S
142	gi|41017590	Bifunctional DNA-directed RNA polymerase subunit beta-beta'	VGAGQIIADGPSMDR	4.60	19.98	19.66	0	18.75
143	gi|226711673	Bifunctional enzyme IspD/IspF	FSQTIKK	1.88	15.58	15.93	15.88	15.41
144	gi|11387374	Bifunctional NAD(P)H-hydrate repair enzyme Nnr	ADTTISMGAIKSCLLSDK	1.60	13.97	15.57	14.45	14.67
145	gi|119369798	Bifunctional protein FolD	HIDSKMVLEAIDPSK	6.13	16.08	16.14	15.38	15.64
146	gi|119370573	Bifunctional protein GlmU	DANDEEKTIQSVNAGVYGFER	2.94	14.87	15.02	13.31	10.19
147	gi|6093961	Bifunctional protein HldE	ARGIDASGILIDK	1.69	13.55	12.67	12.19	14.65
148	gi|9910670	Biopolymer transport protein ExbB	GGFSMAMLK	1.98	20.02	19.01	19.11	19.95
149	gi|9910671	biopolymer transport protein ExbB-like 1	VYDLSVYVQMQVDILSSKK	2.71	15.36	14.23	13.05	16.47
150	gi|9910672	biopolymer transport protein ExbD-like 1	VIEIRMDK	13.09	15.44	14.89	15.60	14.99
151	gi|254810716	Biotin synthase	VVLQEARALK	2.98	16.48	15.62	17.10	14.62
152	gi|9789770	Branched-chain-amino-acid aminotransferase	SYSFEAPGNITK	2.97	14.58	14.04	14.37	13.61
153	gi|9973363	Cadmium, zinc and cobalt-transporting ATPase	SKVLGGSLNLK	1.82	12.84	15.19	14.08	10.95
154	gi|2498202	CAG pathogenicity island protein 12	QVINEVAR	6.69	16.63	16.23	15.86	15.78
155	gi|2498201	CAG pathogenicity island protein 13	FDRSILGIFLPFFSKPIMFK	1.13	15.47	11.05	11.78	13.74
156	gi|12229774	CAG pathogenicity island protein 23	IELIEELLSKYHPTR	1.02	13.90	15.31	13.44	15.07
157	gi|22095480	Carbamoyl-phosphate synthase large chain	NIVGYSK	1.71	15.34	15.77	15.11	15.75
158	gi|21759011	Carbamoyl-phosphate synthase small chain	TSHKIIAVLDFGAK	1.78	15.79	17.27	17.03	18.03
159	gi|11131942	Carbonic anhydrase	ISHENF	5.41	16.29	15.83	15.98	15.57
160	gi|226706619	Carboxy-S-adenosyl-L-methionine synthase	EALENVLVPYSLK	1.95	15.83	14.90	14.34	13.03
161	gi|2493545	Catalase	GSADAVR	1.33	18.62	15.20	14.71	16.72
162	gi|75344431	Cbb3-type cytochrome c oxidase subunit CcoP	NPQLIDKGK	2.41	17.61	17.03	18.29	17.51

#	Accession No.	Protein Name	Peptide	MOWSE Score	Cla/Mtz-R	Cla-R	Mtz-R	Sen-S
163	gi|46396012	CD209 antigen	SKLQEIYQELTWLK	2.35	18.71	19.32	20.84	21.53
164	gi|13124013	CDP-diacylglycerol pyrophosphatase	QLDNNLK	3.25	16.95	16.76	16.13	16.89
165	gi|2493570	CDP-diacylglycerol--serine O-phosphatidyltransferase	IIFNK	5.07	20.93	20.53	20.28	19.55
166	gi|11132643	Cell division protein FtsA	IIGTAHQDSKEINSK	3.09	24.71	20.89	21.81	22.90
167	gi|2494599	Cell division protein FtsZ	GAKIVVIGVGGGGSNMIK	2.61	19.37	19.29	19.10	19.02
168	gi|238058282	Cell division topological specificity factor	SSDIHFK	7.83	21.95	19.58	20.61	20.76
169	gi|2493732	Chaperone protein ClpB	LDPVIGRDEEIIR	2.62	17.28	13.75	13.61	14.42
170	gi|9789749	Chaperone protein DnaJ	HPESSYR	2.19	14.96	15.70	16.21	16.96
171	gi|2495351	Chaperone protein DnaK	NNAEQPKK	7.29	16.47	16.36	16.55	16.71
172	gi|118575192	Chaperone protein HtpG	KTLELNPNHAILQK	1.24	18.03	0	17.04	18.08
173	gi|2500738	Chemotaxis protein CheY homolog	MKLLVVDDSSTMR	7.85	23.58	22.93	22.49	22.39
174	gi|2492947	Chorismate synthase	GFLSNR	5.62	15.80	13.08	12.17	10.73
175	gi|123246872	Chromosomal replication initiator protein DnaA	EILALAK	2.92	17.33	16.34	15.71	15.26
176	gi|12230507	chromosome-partitioning protein ParB	HGFKQTQTLIAEDELER	6.88	16.24	17.93	14.86	16.96
177	gi|11131939	Citrate synthase	YEFETIECTR	2.47	19.05	19.44	18.34	18.78
178	gi|425936525	Coiled-coil domain-containing protein ORF29	KTPSTPESEDK	6.01	17.42	16.03	18.44	15.36
179	gi|464924	Conjugal transfer protein TraG	MDFENGRPVAHYKHR	3.52	15.96	14.77	15.93	15.81
180	gi|9789743	COP-associated protein	KVTFQVPSITCNHCVDK	6.76	15.04	14.73	13.43	15.37
181	gi|2493006	Copper-transporting ATPase	EHIAQIK	1.35	15.27	15.48	14.59	15.06
182	gi|226698757	Crossover junction endodeoxyribonuclease RuvC	MRILGIDPGSR	1.53	13.51	16.06	15.92	13.74
183	gi|11387047	CTP synthase	NVLGLKGANSTEFNQR	5.38	15.39	15.17	15.09	15.31
184	gi|2497961	Cyclic pyranopterin monophosphate synthase	MVDIGDK	3.09	16.04	16.57	15.77	16.20

#	Accession No.	Protein Name	Peptide	MOWSE Score	Cla/Mtz-R	Cla-R	Mtz-R	Sen-S
185	gi|380876964	Cystathionine gamma-synthase	VLVKNGLSCTIIDTSDLSQIK	2.49	14.04	15.96	12.90	15.20
186	gi|13431579	Cysteine desulfurase IscS	IPVDVLK	2.57	18.53	17.38	16.70	17.44
187	gi|2493890	Cysteine synthase	KNGLLVGSSSGAAFVAALK	5.63	15.05	14.73	14.36	14.89
188	gi|226710844	Cysteine--tRNA ligase	IALMDTPQGTIWEKLF	10.60	16.31	15.68	15.18	15.43
189	gi|20137594	Cytochrome c-553	NPVMTAQAKK	2.23	15.49	15.67	15.54	15.80
190	gi|3182910	Cytosol aminopeptidase	MNAFLAVNKASLSVNPPR	4.14	22.68	22.45	22.10	21.48
191	gi|122980522	cytosol aminopeptidase	AECGLVFIVNKDFSHAWVK	5.64	14.71	14.07	14.11	12.67
192	gi|1705562	Cytotoxicity-associated immunodominant antigen	DLLDER	6.37	19.27	14.86	14.87	15.17
193	gi|226696388	D-alanine--D-alanine ligase	KLPPLILAHNGLLK	8.46	16.90	20.40	16.54	19.58
194	gi|704000327	D-amino acid dehydrogenase	EDGLLMIYTLEESFEKK	1.45	13.97	12.91	12.83	14.51
195	gi|238057997	dCTP deaminase	STYAR	1.54	15.89	14.98	14.82	14.94
196	gi|81815103	DEAD-box ATP-dependent RNA helicase RhpA	SSIMAFKK	4.28	16.36	16.20	16.78	15.96
197	gi|85687556	Deleted in malignant brain tumors 1 protein	LVNGGDRCR	14.34	16.14	15.31	15.33	16.34
198	gi|11133273	Delta-aminolevulinic acid dehydratase	AVLLFGIPK	16.78	15.99	16.41	16.11	16.04
199	gi|122980489	Deoxyuridine 5'-triphosphate nucleotidohydrolase	GSGGFGSTGVSKA	1.95	16.52	13.66	15.41	12.96
200	gi|14194488	Dephospho-CoA kinase	STTIKILESQGYK	1.42	16.14	16.16	16.03	15.83
201	gi|52782807	D-glycero-beta-D-manno-heptose-1,7-bisphosphate 7-phosphatase	MNTNK	6.34	15.48	16.46	16.27	16.02
202	gi|8134398	Diaminopimelate decarboxylase	FGVEEK	1.40	20.33	17.22	17.36	0
203	gi|229807494	Diaminopimelate epimerase	LFYNAPK	5.99	14.89	13.95	13.08	14.61
204	gi|226710828	Dihydroorotase	AHEKGIR	2.75	18.87	15.52	15.01	16.06
205	gi|9087191	dihydroorotase-like protein	LNAGEVK	4.84	19.01	15.23	15.30	15.59

#	Accession No.	Protein Name	Peptide	MOWSE Score	Cla/Mtz-R	Cla-R	Mtz-R	Sen-S
206	gi|226710765	Dihydroorotate dehydrogenase (quinone)	FAPYKTPIGINLGK	6.18	22.97	17.04	17.23	21.50
207	gi|2507466	DNA gyrase subunit A	QTLAEAYR	2.02	15.63	15.08	15.71	14.92
208	gi|6647533	DNA gyrase subunit B	AREASK	2.13	15.14	14.67	14.72	13.51
209	gi|123246990	DNA ligase	GNGLEGELVSANAK	15.51	16.97	14.92	14.66	15.52
210	gi|9789748	DNA polymerase I	EDLIPHEK	5.91	14.13	14.46	14.57	11.88
211	gi|11132624	DNA polymerase III subunit alpha	SVSVTDHGNMFGAIDFYTSMK	1.46	14.29	14.10	13.84	13.91
212	gi|9789776	DNA primase	SASFSVNQVK	3.42	13.91	16.58	15.29	15.23
213	gi|2506370	DNA protection during starvation protein	SIWMLQAHLA	4.83	14.30	15.73	14.94	13.67
214	gi|11134859	DNA repair protein RecN	MIGGSENIESAISFAKEK	1.85	19.15	20.63	19.84	20.33
215	gi|7531219	DNA topoisomerase 1	KNIISQK	1.37	16.70	15.84	16.26	16.18
216	gi|34395611	DNA translocase FtsK	FDDLTNPTNPPLK	5.88	15.39	15.22	15.58	14.54
217	gi|3913400	DNA-binding protein HU	EAGKYNSK	6.34	17.18	16.52	15.85	17.08
218	gi|7388104	DNA-directed RNA polymerase subunit alpha	GMGYVPSENTR	7.80	16.40	16.34	16.17	15.16
219	gi|123073782	DNA-directed RNA polymerase subunit omega	QLNAGAKTLVNMDPK	1.42	14.95	16.65	14.61	14.96
220	gi|123246875	Dual-specificity RNA methyltransferase RlmN	ITVSTSGVADK	1.01	15.85	16.51	13.69	15.65
221	gi|238057744	Elongation factor 4	ELIPR	5.18	16.26	15.90	15.43	16.52
222	gi|238058908	Elongation factor G	YLGGEELSVEEIK	1.97	20.15	20.51	20.14	18.63
223	gi|238058895	Elongation factor P	MAIGMSELKK	2.92	15.53	16.09	15.55	15.65
224	gi|226740480	Elongation factor Ts	IVPGKMER	1.26	15.53	16.49	16.18	16.34
225	gi|238054410	Elongation factor Tu	TTLSAAISAVLSLKGLAEMK	2.45	14.44	14.43	13.89	15.22
226	gi|20139868	Endolytic peptidoglycan transglycosylase RlpA	SVSGGKFSLQMGAFR	9.58	15.64	15.19	15.33	15.58
227	gi|3914057	Endonuclease MutS2	DTSSMHK	2.53	13.99	13.54	11.50	13.02

#	Accession No.	Protein Name	Peptide	MOWSE Score	Cla/Mtz-R	Cla-R	Mtz-R	Sen-S
228	gi|6136166	Endoribonuclease VapD homolog	VYSDIR	5.67	17.25	18.03	17.69	16.48
229	gi|2506387	Enolase	TGSTARSER	1.14	22.10	22.37	22.43	21.96
230	gi|81341088	Epoxyqueuosine reductase QueH	SVFQEEK	2.18	15.57	15.27	15.51	15.60
231	gi|122386734	Exodeoxyribonuclease 7 large subunit	GYFDKENK	3.66	13.61	15.59	13.82	12.66
232	gi|259646312	Exodeoxyribonuclease 7 small subunit	MQDELFETEKIPPK	2.73	15.79	14.95	16.57	14.71
233	gi|13431987	Fe(2+) transport protein A	KATLSVK	3.18	17.38	15.52	15.68	15.66
234	gi|76364190	Fe(2+) transporter FeoB	MLLALNMWDEAQKEGIK	1.35	14.34	14.64	13.39	14.93
235	gi|3913690	Ferric uptake regulation protein	YQAKLISHDMK	5.80	20.85	18.53	18.44	17.92
236	gi|123246933	Ferrochelatase	FIIGLVKNLK	27.51	20.51	19.03	20.37	18.90
237	gi|81341617	Flagellar assembly factor FliW 1	IDSLFSR	14.22	16.71	16.54	16.99	15.51
238	gi|81555083	Flagellar assembly factor FliW 2	QLMGQVVLDSK	9.53	15.07	15.29	15.19	15.38
239	gi|9910701	Flagellar biosynthesis protein FlhA	LKGIVIGEGMVMPDK	2.15	19.63	20.26	20.20	18.62
240	gi|12230112	Flagellar biosynthesis protein FlhF	ILMLVGPTGVGKTTTLAK	12.12	16.22	14.41	12.15	14.34
241	gi|12230110	Flagellar biosynthetic protein FlhB	MTKQEVK	5.56	17.25	16.31	15.51	16.92
242	gi|60392295	Flagellar biosynthetic protein FliQ	LAIETYK	3.42	18.12	16.05	14.99	14.47
243	gi|2506418	Flagellar hook protein FlgE	ISMRANLNAGR	1.17	15.55	12.33	14.56	14.66
244	gi|13124751	Flagellar hook-associated protein 2	RGGNIEVK	2.60	15.10	15.88	14.57	14.56
245	gi|226704234	Flagellar hook-basal body complex protein FliE	MQAIHNDK	2.65	17.37	17.05	16.66	16.54
246	gi|14548056	Flagellar L-ring protein	GGGSQKK	4.43	15.47	15.95	15.65	15.90
247	gi|81341211	Flagellar motor switch protein FliG	FLNNMSSR	1.08	18.36	17.99	20.23	20.00
248	gi|226701950	Flagellar P-ring protein	NAMVLSLK	4.04	15.18	17.17	16.01	15.51
249	gi|1706820	Flagellin A	KGDADGR	4.38	21.42	22.05	20.51	23.02

#	Accession No.	Protein Name	Peptide	MOWSE Score	Cla/Mtz-R	Cla-R	Mtz-R	Sen-S
250	gi|2506428	Flagellin B	ASIGSTSSDK	4.15	15.38	14.70	16.41	16.81
251	gi|81341569	Flagellum site-determining protein YlxH	NNQASR	4.82	20.17	18.82	18.52	17.25
252	gi|2493149	Flagellum-specific ATP synthase	STLMGMITR	5.79	16.58	16.22	17.02	16.05
253	gi|14916856	Flavin-dependent thymidylate synthase	YAMPESYK	4.98	16.19	16.17	14.88	14.94
254	gi|8134462	Flavodoxin (ferredoxin--NADP reductase)	MGKIGIFFGTDSGNAEAIAEK	3.30	15.45	13.86	15.95	15.06
255	gi|226709251	fluoride ion transporter CrcB	MMPSK	8.22	15.75	15.96	16.42	16.61
256	gi|31339952	Formamidase	ETELYAK	5.09	15.32	15.35	15.90	15.25
257	gi|224472926	Fructose-1,6-bisphosphatase class 1	YAFYQNKFHFIETIVLENK	2.02	14.95	11.97	14.23	14.30
258	gi|9789722	Fructose-bisphosphate aldolase	KFFSPAQLALK	5.23	0	0	0	22.40
259	gi|6016064	Fumarate hydratase class II	FVVPEKMIGPK	2.57	19.57	17.81	22.88	22.70
260	gi|12230113	Fumarate reductase cytochrome b subunit	DNGIKTMQEAIEADGK	3.77	14.76	15.91	13.33	14.63
261	gi|2494617	Fumarate reductase flavoprotein subunit	MKEVMDEK	1.39	16.36	15.69	15.11	15.02
262	gi|2494621	Fumarate reductase iron-sulfur subunit	VGKSR	2.19	17.38	17.12	17.01	16.78
263	gi|1730125	Galactoside 2-alpha-L-fucosyltransferase 2	GVVADRR	4.60	17.27	18.00	19.39	16.62
264	gi|20138139	Glucokinase	GRMGAFLASIPVHVVMK	1.44	14.24	13.42	14.18	14.33
265	gi|3023889	glucose/galactose transporter	MGDNASLIDK	3.26	17.57	17.63	16.91	16.24
266	gi|11386867	Glucose-6-phosphate 1-dehydrogenase	ESQTETFVAIK	4.66	14.70	15.62	15.84	15.82
267	gi|226706756	Glucose-6-phosphate isomerase	EKIEAMFK	9.31	16.58	17.14	15.89	15.13
268	gi|2492984	Glutamate racemase	DKNAPILVLGTK	2.78	16.66	15.89	15.72	14.61
269	gi|226738302	Glutamate-1-semialdehyde 2,1-aminomutase	NIINTLK	22.37	18.94	18.85	18.51	18.80
270	gi|238064677	Glutamate--tRNA ligase 1	DFKGTPPK	1.51	17.65	17.37	17.61	19.58
271	gi|238064683	Glutamate--tRNA ligase 2	LSQLKGK	6.34	14.60	13.10	12.68	12.07

#	Accession No.	Protein Name	Peptide	MOWSE Score	Cla/Mtz-R	Cla-R	Mtz-R	Sen-S
272	gi|2494748	Glutamine synthetase	IDPGEAMDINLFK	1.71	13.66	13.08	14.19	14.83
273	gi|8134479	Glutamine--fructose-6-phosphate aminotransferase [isomerizing]	HLLFDKTK	11.43	14.40	14.46	15.20	13.53
274	gi|226706273	Glutamyl-tRNA reductase	NLFNLDK	5.77	16.87	17.45	18.51	17.54
275	gi|7674048	Glutamyl-tRNA(Gln) amidotransferase subunit A	YGVIAYR	3.91	16.56	16.50	16.54	16.58
276	gi|11386770	Glyceraldehyde-3-phosphate dehydrogenase	LIDLAHPLDKR	2.59	16.86	16.28	18.01	16.76
277	gi|115311979	Glycerol-3-phosphate acyltransferase	EVDTQTPMVLIFIFTLIK	6.38	14.91	14.48	15.85	14.16
278	gi|118595407	Glycerol-3-phosphate dehydrogenase [NAD(P)+]	DLNEPLK	13.35	19.47	18.79	19.51	18.33
279	gi|1346180	Glycine-rich RNA-binding protein GRP1A	SMKDAIEGMNGQDLDGR	3.22	14.35	15.65	17.35	15.43
280	gi|11135461	Glycine--tRNA ligase alpha subunit	VENILEIEWAKK	3.89	16.70	16.19	16.38	15.93
281	gi|238064852	Glycine--tRNA ligase beta subunit	YFATFCQK	2.18	15.22	0	13.04	13.23
282	gi|226739788	GMP reductase	IENGIAYK	1.78	15.92	17.32	15.38	15.58
283	gi|226739631	GMP synthase [glutamine-hydrolyzing]	IFGLQFHPEVVQSEEGGK	4.02	14.56	15.59	14.91	14.67
284	gi|7674140	GTP 3',8-cyclase	DAGLSR	3.71	14.96	15.12	18.70	15.54
285	gi|229487969	GTP cyclohydrolase 1	GVIVVCEAKHLCMSMQGVQK	2.51	14.28	14.63	11.97	13.50
286	gi|20978799	GTP cyclohydrolase 1 type 2	HFAHALLEFDGLVEK	1.63	21.04	19.30	19.05	18.24
287	gi|8928121	GTP cyclohydrolase-2	LLTNNPLKIAALEK	1.65	15.34	16.64	13.43	14.19
288	gi|238058975	GTPase Der	NTSPKTLK	3.29	17.01	0	17.50	0
289	gi|12643474	GTPase Era	LGYIHR	1.16	21.35	21.35	20.53	19.66
290	gi|10720359	GTPase Obg	LDLGIKEQYK	1.62	14.62	15.65	18.05	16.14
291	gi|238058985	GTP-binding protein EngB	NEQHR	3.05	15.64	15.64	15.70	15.93
292	gi|8134781	GTP-binding protein TypA/BipA homolog	CEEMGEGK	5.80	22.84	0	0	0

#	Accession No.	Protein Name	Peptide	MOWSE Score	Cla/Mtz-R	Cla-R	Mtz-R	Sen-S
293	gi|11133267	Guanylate kinase	IPVEKALK	1.71	16.24	16.39	16.20	15.98
294	gi|7387772	Heat-inducible transcription repressor HrcA	IKVGSNLNK	3.55	15.50	18.25	13.22	16.99
295	gi|81341192	Heme oxygenase HugZ	QYYIYVSEVAEHFAGLK	1.55	15.18	14.78	14.31	15.85
296	gi|229558685	Histidine--tRNA ligase	IGLDGVEEELKK	2.96	11.78	14.40	12.23	12.27
297	gi|226698733	Holliday junction ATP-dependent DNA helicase RuvA	EALQQLR	3.31	16.65	16.35	15.22	15.89
298	gi|226698779	Holliday junction ATP-dependent DNA helicase RuvB	LDIIIGSGPAAQTIK	3.60	15.36	15.06	14.82	15.27
299	gi|7531025	Holo-[acyl-carrier-protein] synthase	MKFLER	1.85	19.85	16.00	16.26	16.20
300	gi|11132649	Homoserine dehydrogenase	AMLAYHRYELEQIAK	8.18	14.32	14.02	15.55	0
301	gi|14194909	Homoserine kinase	VISTKQSR	1.58	14.75	14.80	15.86	15.36
302	gi|60392429	Hydrogenase/urease maturation factor HypA	IERVVVGIGER	5.03	15.23	15.77	16.10	16.03
303	gi|14285478	Hydrogenase/urease maturation factor HypB	TTMLENLADFK	8.94	21.91	21.58	21.07	19.92
304	gi|9910903	Hydroxyethylthiazole kinase	GLDSK	2.05	16.93	17.26	16.69	17.67
305	gi|7388317	Hydroxymethylpyrimidine/phosphomethylpyrimidine kinase	AMGVLR	2.27	15.80	15.21	15.21	15.05
306	gi|8134520	Inorganic pyrophosphatase	VKGFENK	3.49	16.10	15.17	15.60	15.71
307	gi|12230202	Inosine-5'-monophosphate dehydrogenase	LRVGAAIGVGQLDR	1.67	15.58	16.60	15.34	15.68
308	gi|124474	Interferon gamma receptor 1	MNGSEIQYK	1.09	15.74	16.54	16.70	16.17
309	gi|2492572	iron chelatin transport ATP-binding protein HP_0888	QMVLLAR	4.54	14.89	14.29	0	14.47
310	gi|12230996	Iron-sulfur cluster carrier protein	LADNK	5.63	16.59	14.87	14.84	15.26
311	gi|2497255	Isocitrate dehydrogenase [NADP]	ILQKPK	2.25	14.81	15.10	14.39	15.62
312	gi|254782410	Isoleucine--tRNA ligase	GCYNEGIIHKK	4.91	14.01	13.70	13.51	13.80
313	gi|2501567	Isoprenyl transferase	SEVDFLMK	1.81	14.53	14.73	14.85	15.85
314	gi|14195414	Ketoisovalerate oxidoreductase subunit VorB	EDIEVLQK	7.29	15.34	14.59	14.93	15.52

#	Accession No.	Protein Name	Peptide	MOWSE Score	Cla/Mtz-R	Cla-R	Mtz-R	Sen-S
315	gi|6225546	Ketol-acid reductoisomerase (NADP(+))	IQNGSFAK	6.38	14.44	14.67	17.19	16.02
316	gi|6919983	Leucine--tRNA ligase	YLENASVKK	3.39	20.41	19.31	18.56	18.59
317	gi|81554995	Lipid A 4'-phosphatase	FLPIFVGTVSLAMR	6.10	19.64	19.99	19.79	17.27
318	gi|7387929	lipid II flippase MurJ	GLLGFK	16.34	16.45	15.91	16.25	16.31
319	gi|118573581	Lipid-A-disaccharide synthase	QNLPKDYR	10.75	15.57	16.92	17.05	15.19
320	gi|1351500	lipoprotein MG149	TGGHR	5.14	22.08	20.46	20.95	20.86
321	gi|238058052	Lipoprotein signal peptidase	MLKTTQK	3.83	16.44	17.12	17.41	18.20
322	gi|12230210	Lon protease	GRILEPAK	3.55	14.96	14.91	15.68	15.47
323	gi|2501151	L-serine dehydratase	GILEQVVR	6.81	18.93	16.92	18.24	17.15
324	gi|15214299	L-seryl-tRNA(Sec) selenium transferase	IEPYLK	3.67	17.77	16.22	16.05	16.23
325	gi|226710889	Lysine--tRNA ligase	SLIVSSVR	1.19	16.14	16.98	15.53	18.11
326	gi|81341686	Magnesium transport protein CorA	MVNVFFK	3.28	14.14	15.84	13.35	12.62
327	gi|425936522	Major structural protein ORF14	EIQNASWIK	2.82	16.67	16.70	18.06	17.03
328	gi|8472786	Malate:quinone oxidoreductase	LSAYKTR	5.45	16.35	15.39	15.56	15.40
329	gi|3123102	membrane protein HP_1331	EGVSEK	8.78	22.50	21.73	20.53	20.52
330	gi|38503266	Membrane protein insertase YidC	LKELAPK	4.33	18.08	17.82	18.15	16.52
331	gi|116256135	membrane protein insertion efficiency factor	ILSCNPFCSGGIAYPTTRLK	1.75	15.34	15.07	16.27	16.12
332	gi|13878898	metallophosphoesterase jhp_0380	IILLTDMHVGSLLQK	11.03	20.03	18.05	18.18	18.22
333	gi|10719887	Methionine aminopeptidase	MAISIKSPK	4.29	17.96	15.59	16.40	15.91
334	gi|81815354	Methionine import ATP-binding protein MetN	GDILGVIGYSGAGK	1.86	16.15	16.35	17.78	17.45
335	gi|7388283	Methionine--tRNA ligase	EAQRIEK	1.55	17.58	18.64	18.43	16.72
336	gi|123073743	Methionyl-tRNA formyltransferase	NFSSITR	2.09	16.03	15.23	16.40	13.57

#	Accession No.	Protein Name	Peptide	MOWSE Score	Cla/Mtz-R	Cla-R	Mtz-R	Sen-S
337	gi|11387381	methylthiotransferase jhp_0270	DTPSSLMR	3.94	17.75	17.94	15.87	17.82
338	gi|259495889	Molybdenum cofactor guanylyltransferase	NFSVVYAK	7.84	15.38	14.65	14.40	14.64
339	gi|11133335	Molybdopterin adenylyltransferase	DITPEATK	2.54	18.39	18.08	17.48	20.08
340	gi|9789772	Molybdopterin synthase catalytic subunit	DYQEEACTK	1.68	19.65	19.55	19.94	19.71
341	gi|54041481	Motility protein A	DGVLSLEGRVAQIEDDFTR	2.42	13.28	16.73	16.12	14.64
342	gi|6136524	MscS family protein HP_0415	GYGEALVTNMATKSTHNFR	2.41	13.75	14.88	15.32	12.46
343	gi|11136007	MscS family protein jhp_0969	EDVMLKIMGIVEK	1.67	16.83	14.92	15.58	16.60
344	gi|803341928	Mucin-5AC	MQCVATCPTPPLPPR	5.08	18.31	15.94	17.14	17.81
345	gi|332278200	Mucin-6	QAQHAR	1.25	15.94	16.57	15.48	15.76
346	gi|254767350	Na(+)/H(+) antiporter NhaA	RVPTALK	6.06	20.70	16.20	16.12	15.73
347	gi|226704907	NAD kinase	KALGVLDIQAYVGHTPFNTYK	1.34	18.72	17.81	16.31	17.85
348	gi|38257810	NAD-dependent protein deacylase	LIEMAS	9.09	16.41	15.75	15.98	16.02
349	gi|238065159	NADH-quinone oxidoreductase subunit B	HAEFMR	4.70	15.61	16.03	16.37	16.49
350	gi|229891397	NADH-quinone oxidoreductase subunit D	LENVGVVTPKMAQSWGMSGIMLR	8.15	14.14	13.26	11.96	15.19
351	gi|226737395	NADH-quinone oxidoreductase subunit I	GEDNR	5.79	16.98	16.18	16.25	15.87
352	gi|81625861	NADPH-dependent 7-cyano-7-deazaguanine reductase	MTPESNLK	4.83	14.02	14.23	15.06	13.74
353	gi|11132638	NADP-specific glutamate dehydrogenase	KVASAMIAQGV	8.08	14.86	14.57	16.06	16.15
354	gi|17433253	NCK-interacting protein with SH3 domain	LLLLLNR	1.64	15.23	18.12	15.68	15.64
355	gi|2497718	Neuraminyllactose-binding hemagglutinin	GTDNSNDAIKSALNK	2.93	17.49	17.28	16.47	17.04
356	gi|6093467	NH(3)-dependent NAD(+) synthetase	TDALNLCEK	8.97	15.37	15.21	14.98	14.99
357	gi|226732789	nickel-responsive regulator	DTPNK	5.63	19.30	20.70	19.36	19.25
358	gi|10720117	nicotinate-nucleotide adenylyltransferase	GRYHPLK	9.52	22.03	19.39	19.83	18.84

#	Accession No.	Protein Name	Peptide	MOWSE Score	Cla/Mtz-R	Cla-R	Mtz-R	Sen-S
359	gi|11387010	nicotinate-nucleotide pyrophosphorylase [carboxylating]	DTHLK	6.05	16.50	17.25	16.92	16.87
360	gi|6093533	Nuclear factor erythroid 2-related factor 2	APFTKDK	2.40	17.99	17.42	17.76	18.04
361	gi|12644594	Nucleoid-associated protein HP_0035	MDFSQLGGLLDGMKK	5.79	21.17	20.22	20.16	20.16
362	gi|226729822	Nucleoside diphosphate kinase	DAENFYAIHR	3.57	14.10	12.73	14.13	13.88
363	gi|81341630	Nucleoside permease NupC	AINYR	3.82	16.36	16.53	16.97	16.34
364	gi|20140423	Nucleoside triphosphate pyrophosphatase	ELILGSQSSTR	1.01	15.46	14.93	16.25	15.71
365	gi|12230845	ORFX	VSNAY	10.00	15.59	16.39	15.82	16.03
366	gi|2499948	Orotate phosphoribosyltransferase	VDNTMALR	5.35	17.67	17.75	17.84	17.80
367	gi|7387626	Orotidine 5'-phosphate decarboxylase	GFLTLTPGIR	1.41	13.16	13.39	14.50	16.05
368	gi|81341376	Outer membrane protein assembly factor BamA	IRVGDIVDSK	4.65	15.22	15.09	15.68	15.35
369	gi|81341698	Outer membrane protein assembly factor BamD	TFLFITMAIIVIGTGCANKK	1.84	12.65	15.47	14.43	14.48
370	gi|122386457	Outer-membrane lipoprotein carrier protein	EEEVLQHLQSFSAHFK	2.76	21.41	22.28	22.21	21.54
371	gi|123524295	Oxalate oxidoreductase subunit beta	LSVKVDK	9.77	20.28	19.47	19.53	19.80
372	gi|11386870	Oxygen-independent coproporphyrinogen III oxidase	LEILESLISFLEK	13.00	23.49	20.08	22.49	19.32
373	gi|81341521	Oxygen-insensitive NADPH nitroreductase	LSPSSYNTQPWHFVMVTDK	1.73	14.41	15.61	14.92	14.71
374	gi|2498743	Pantothenate synthetase	LKLYAPK	1.72	18.13	16.08	16.21	16.25
375	gi|238058715	Peptide chain release factor 1	DPNDDK	5.74	15.12	15.78	14.85	14.85
376	gi|238054481	Peptide chain release factor 2	ASGAGGQHVNK	1.43	16.81	17.20	16.99	15.82
377	gi|238691921	Peptide deformylase	FIETKGTIMYK	6.19	15.42	15.08	15.14	15.04
378	gi|3914383	Peptide methionine sulfoxide reductase MsrA/MsrB	GELKK	5.95	17.09	16.76	16.22	16.53
379	gi|9789739	Peptide transporter CstA	NIGESSILSR	2.62	14.86	14.83	15.13	16.68
380	gi|11387122	Peptidoglycan glycosyltransferase MrdB	SKEACTQTK	2.33	14.80	15.31	15.17	15.97

#	Accession No.	Protein Name	Peptide	MOWSE Score	Cla/Mtz-R	Cla-R	Mtz-R	Sen-S
381	gi|81341474	Peptidoglycan O-acetyltransferase	NSSHLYQSNQMDWIK	4.90	16.40	16.02	14.32	15.42
382	gi|25090943	Peptidyl-prolyl cis-trans isomerase	RGSISMAHAGR	3.56	17.52	18.66	18.61	16.35
383	gi|2499779	peptidyl-prolyl cis-trans isomerase HP_0175	KTTDSSAGVLATVDGRPITK	2.61	15.38	14.15	14.13	13.67
384	gi|10720360	peptidyl-prolyl cis-trans isomerase jhp_0161	LFQERMNQR	2.99	15.22	15.53	15.15	16.32
385	gi|226694256	Peptidyl-tRNA hydrolase	MTLLVGLGNPTLRYAHTR	1.64	15.73	14.19	13.73	14.41
386	gi|7387552	peroxiredoxin bcp	LEVGQLAPDFR	1.86	15.28	15.70	15.47	15.70
387	gi|226710876	Phenylalanine--tRNA ligase alpha subunit	GVFADK	1.80	21.74	21.74	21.34	21.78
388	gi|11135454	Phenylalanine--tRNA ligase beta subunit	AWDFYSFAECVSR	2.31	18.49	18.50	17.67	20.26
389	gi|226701058	Phosphate acyltransferase	SVIISHGK	2.19	16.99	16.45	16.20	16.13
390	gi|7388495	phosphate permease HP_1491	MEIKNIK	3.19	14.73	15.25	18.60	12.57
391	gi|7388501	phosphate permease jhp_1384	EIRNIK	2.36	17.49	15.86	16.43	16.68
392	gi|7673969	Phosphatidate cytidylyltransferase	MKEELFK	2.59	15.38	15.84	15.58	16.27
393	gi|32469611	Phosphatidylserine decarboxylase proenzyme	GINALYVK	1.23	16.90	17.03	17.03	18.19
394	gi|6685766	Phosphoenolpyruvate synthase	GKTELIHYIK	3.17	15.86	14.78	14.39	14.76
395	gi|81555770	Phosphoethanolamine transferase EptA	VSALK	17.65	20.87	20.33	20.92	19.86
396	gi|6685394	Phosphogluconate dehydratase	VALVTDGR	6.05	16.64	16.23	16.85	16.76
397	gi|123247055	Phosphoglucosamine mutase	NALSSQAIVATNMSNLALK	1.59	14.46	14.46	14.44	15.60
398	gi|8134612	Phosphoglycerate kinase	MSFMQNVKNIQEVDVNHK	1.74	15.59	15.24	15.36	14.40
399	gi|7387837	Phosphoheptose isomerase	MIDNLIK	5.19	20.52	18.82	17.64	17.02
400	gi|6225716	Phospho-N-acetylmuramoyl-pentapeptide-transferase	AGLGFFIAFFLTLFLMPK	1.76	12.99	15.27	13.49	12.97
401	gi|226709008	Phosphopantetheine adenylyltransferase	MMQLATKSFK	1.25	13.71	0	15.61	0
402	gi|2829464	Phosphopentomutase	EILDEIVR	8.08	20.71	16.96	17.24	17.47

#	Accession No.	Protein Name	Peptide	MOWSE Score	Cla/Mtz-R	Cla-R	Mtz-R	Sen-S
403	gi|7994658	Phosphoribosylamine--glycine ligase	ILEDAFK	1.87	16.13	17.65	16.02	17.18
404	gi|57012993	Plasminogen-binding protein PgbA	NYQKAER	2.49	20.96	18.63	17.46	18.37
405	gi|57012994	Plasminogen-binding protein PgbB	EVPKPNSK	2.51	15.71	16.75	15.72	15.60
406	gi|45477242	Polyamine aminopropyltransferase	NMGGVFSVAMPFVAPLR	2.90	15.02	15.22	15.33	15.11
407	gi|13878635	Polyphosphate kinase	VELLIPATNPKIANK	3.23	16.23	16.00	16.69	16.13
408	gi|257096696	Polyribonucleotide nucleotidyltransferase	LNALEEPLMLK	9.31	20.34	20.33	22.13	23.03
409	gi|11133270	Porphobilinogen deaminase	EVIAKEK	1.34	16.10	16.76	16.42	17.17
410	gi|426021105	Portal protein	QLLRLLAGLNDESLGMAVNR	2.34	15.95	0	0	14.74
411	gi|32130008	pre-16S rRNA nuclease	YCQKVLK	1.34	15.55	15.45	14.95	15.02
412	gi|8928280	Primosomal protein N'	NKTPPLTYFSK	1.93	17.14	16.86	18.03	16.42
413	gi|11135064	Proline--tRNA ligase	EANEEDLNK	2.16	16.07	14.99	15.50	14.98
414	gi|8039786	Protease HtpX homolog	EIDKNSTR	1.77	14.56	14.65	14.29	14.38
415	gi|12230795	protease jhp_0155	NPDNGVMMR	6.43	15.33	15.18	14.28	14.68
416	gi|226737141	Protein GrpE	IVQVLQQGYK	2.76	15.44	15.24	15.18	14.83
417	gi|54042421	protein HP_0245	EQTDSFEALLLK	2.82	16.51	15.45	15.90	15.84
418	gi|12231042	protein HP_0262	DKPKG	2.89	16.27	15.48	16.36	15.84
419	gi|6686081	protein HP_0396	DLIIK	5.08	16.48	15.60	15.94	15.84
420	gi|13431976	protein HP_0495	VVQTL	4.47	18.94	17.71	17.78	18.05
421	gi|7674418	Protein HP_1247	SALDIYDYLLKEGK	6.41	19.19	18.25	18.60	18.19
422	gi|7388494	protein HP_1429	IITFTK	1.85	18.70	17.33	17.71	16.89
423	gi|12230794	protein jhp_0176	ELLNAANR	10.40	21.07	19.84	20.16	19.25
424	gi|15214381	protein jhp_0854	MALYDR	1.42	22.36	22.27	23.22	22.92

#	Accession No.	Protein Name	Peptide	MOWSE Score	Cla/Mtz-R	Cla-R	Mtz-R	Sen-S
425	gi|6686112	protein jhp_0985	KPNGGKALLFTQPIR	4.31	17.51	16.69	16.16	16.81
426	gi|7674428	Protein jhp_1168	YTSEIIVKFFQK	15.17	19.43	19.07	20.83	20.95
427	gi|11387375	protein jhp_1250	ALSCSVIGMLVVYCFK	3.10	16.40	15.22	18.62	15.89
428	gi|7388502	protein jhp_1324	LILKSQEK	6.93	16.29	16.75	17.39	17.63
429	gi|10720255	Protein RecA	IGMTGYGSPETTTGGNALK	9.54	13.94	14.08	14.96	13.23
430	gi|11135450	Protein TonB	MKISPSPR	3.43	19.76	17.52	17.68	16.32
431	gi|226732208	Protein translocase subunit SecA	VENLHFESR	3.70	19.33	19.26	18.71	19.06
432	gi|347595706	Protein translocase subunit SecD	IFGDFSGANVGK	1.08	13.66	13.37	16.01	12.13
433	gi|6647833	Protein translocase subunit SecF	ELFKR	1.37	15.11	14.54	14.76	15.02
434	gi|10720277	Protein translocase subunit SecY	DIADNLR	10.49	16.46	16.75	15.98	17.66
435	gi|13431940	Protein trl	SGGVTKIK	3.59	21.94	18.84	17.48	16.26
436	gi|60416206	Protein VdlD	VLSEDIKTR	2.52	15.29	16.02	14.73	14.40
437	gi|10720400	Protein-export membrane protein SecG	ENGIKGVEK	5.17	17.67	16.60	16.27	16.25
438	gi|7388015	Protein-L-isoaspartate O-methyltransferase	EAMESIEREVFVPAPFK	10.81	13.28	15.03	14.50	15.63
439	gi|81341195	Pseudaminic acid cytidylyltransferase and UDP-2,4-diacetamido-2,4,6-trideoxy-beta-L-altropyranose hydrolase	SFSLENGVQMAFK	2.23	16.31	15.66	15.33	15.14
440	gi|81341127	Pseudaminic acid synthase	LQPPK	9.86	16.14	16.13	15.68	15.68
441	gi|7388415	PSEUDOGENE: protein HP_0451	QALENHMK	1.92	15.39	15.59	13.48	13.37
442	gi|13431978	PSEUDOGENE: protein HP_0945	VYLPTIPKK	5.20	17.39	15.12	14.82	13.89
443	gi|3023633	Purine nucleoside phosphorylase DeoD-type	DIIMATGASTDSK	8.31	15.63	15.07	15.91	15.64
444	gi|11136004	Pyridoxal phosphate homeostasis protein	MLDYR	8.93	17.59	16.92	17.63	17.49
445	gi|226700973	Pyridoxine 5'-phosphate synthase	RHIQNEDVLR	6.69	18.71	13.73	16.99	0

#	Accession No.	Protein Name	Peptide	MOWSE Score	Cla/Mtz-R	Cla-R	Mtz-R	Sen-S
446	gi|11387012	Pyrroline-5-carboxylate reductase	SVAPSISEK	1.28	15.30	14.71	16.56	16.05
447	gi|313104159	Pyruvate synthase subunit PorB	ESFGEDRPK	1.99	16.50	15.25	15.91	15.89
448	gi|226726619	Queuine tRNA-ribosyltransferase	SLDAMDMQEILGAK	3.94	19.86	18.48	18.91	18.67
449	gi|24418574	Quinolinate synthase A	DDGVVCTSR	2.33	15.70	15.70	15.91	15.34
450	gi|238058666	Recombination protein RecR	DFLGR	3.69	16.39	15.38	15.84	16.00
451	gi|10719989	Replicative DNA helicase	GYIYQMR	7.62	14.51	14.46	16.54	12.90
452	gi|238691923	Ribonuclease 3	IYATAKGK	16.34	14.90	14.80	15.24	15.19
453	gi|123246975	Ribonuclease H	NVDLWKEFLK	6.88	18.15	17.96	18.17	17.31
454	gi|6685895	Ribonuclease HI	VKTTT	5.09	17.36	17.41	17.08	16.79
455	gi|238056779	Ribonuclease HII	ILNPK	8.07	17.59	18.52	18.31	17.59
456	gi|677995745	Ribonuclease J	GTLGFHK	1.65	19.01	16.46	16.18	16.29
457	gi|123073716	Ribonuclease P protein component	SFQSKPYDSLK	2.50	15.41	15.76	16.00	14.28
458	gi|7674337	Ribonuclease R	EALQSNKDR	6.11	19.16	20.50	0	0
459	gi|13431977	Ribonuclease Y	KSDEEYAK	4.78	15.76	15.66	15.35	15.05
460	gi|7388069	Ribonucleoside-diphosphate reductase subunit alpha	IEPLDITK	4.10	15.23	15.58	15.40	15.98
461	gi|254783307	Ribosomal protein L11 methyltransferase	VIHGSTQK	2.67	14.73	15.42	14.64	15.14
462	gi|238066301	Ribosomal protein S12 methylthiotransferase RimO	NSSQAHHLKLLNAMK	5.62	15.84	14.47	14.38	14.64
463	gi|238056559	Ribosomal RNA large subunit methyltransferase H	CVVYSIAK	1.87	15.82	16.26	15.79	16.82
464	gi|226732586	Ribosomal RNA small subunit methyltransferase A	SVSYR	5.96	15.29	15.83	15.54	15.61
465	gi|6226368	Ribosomal RNA small subunit methyltransferase E	LLEVMASK	3.61	18.66	18.40	18.40	18.24
466	gi|7387704	Ribosomal RNA small subunit methyltransferase G	RVYFYK	10.63	13.92	14.04	14.23	14.91
467	gi|8134818	Ribosomal RNA small subunit methyltransferase H	GFNFRSHALDMR	2.17	15.99	16.81	16.78	17.38

#	Accession No.	Protein Name	Peptide	MOWSE Score	Cla/Mtz-R	Cla-R	Mtz-R	Sen-S
468	gi|11387380	Ribosomal RNA small subunit methyltransferase I	AKMEAAMTQK	7.69	16.02	15.55	15.49	15.28
469	gi|172045867	Ribosome maturation factor RimM	SVGLNGGLK	3.42	18.35	17.36	17.18	17.78
470	gi|6648012	Ribosome maturation factor RimP	VEVKLINK	2.08	15.32	0	16.10	14.67
471	gi|20978667	Ribosome-binding factor A	GKDND	5.15	15.59	15.41	15.37	15.40
472	gi|226749932	Ribosome-recycling factor	EDAILKV	1.65	16.82	15.82	16.86	15.47
473	gi|11387124	RNA polymerase sigma factor RpoD	HIQETGK	4.62	19.25	17.26	16.39	15.29
474	gi|11387123	RNA polymerase sigma-54 factor	DLIDALNLR	6.71	17.01	16.47	18.24	17.38
475	gi|3915350	RNA pseudouridine synthase HP_0347	ALFMQK	4.50	15.63	15.29	15.38	16.25
476	gi|3915378	RNA pseudouridine synthase HP_0745	ENLDEVLDEEK	2.92	19.79	19.53	18.44	16.79
477	gi|3915400	RNA pseudouridine synthase HP_0956	NTHFSVQK	8.50	15.05	15.33	15.01	14.71
478	gi|2501526	RNA pseudouridine synthase HP_1459	VIINEGKNR	1.12	16.79	16.98	14.89	14.86
479	gi|11136019	RNA pseudouridine synthase jhp_0321	FMPFLKD	1.08	14.98	17.36	16.04	15.94
480	gi|11136009	RNA pseudouridine synthase jhp_0890	ETSGVILLVK	12.25	19.29	19.86	18.94	18.14
481	gi|238057834	RNA pyrophosphohydrolase	FYAFDGQKQR	1.11	19.01	20.13	18.30	17.38
482	gi|12230623	RNA-binding protein CP29B, chloroplastic	ITGRSR	2.20	16.88	15.24	14.95	15.79
483	gi|75319438	RNA-binding protein CP33, chloroplastic	VNFPEVPR	6.59	15.39	14.30	12.76	12.42
484	gi|81818528	RNA-binding protein RbpD	GSWGKK	10.53	16.29	19.42	15.36	15.24
485	gi|81859084	RNA-binding protein RbpE	VQLPTDR	3.89	16.29	17.05	15.59	16.02
486	gi|226699037	S-adenosylmethionine synthase	TSVYAPMQEIAREVVK	4.32	15.88	15.88	15.34	13.83
487	gi|226713842	S-adenosylmethionine:tRNA ribosyltransferase-isomerase	SSLLMLVSAMIGLEKTK	2.75	16.23	11.54	13.88	12.80
488	gi|6648025	Sec translocon accessory complex subunit YajC	LSGAK	3.93	15.59	15.95	15.76	16.04
489	gi|122386697	Sec-independent protein translocase protein TatA	IPELAK	10.16	14.90	15.37	15.48	15.17

#	Accession No.	Protein Name	Peptide	MOWSE Score	Cla/Mtz-R	Cla-R	Mtz-R	Sen-S
490	gi|122386662	Sec-independent protein translocase protein TatB	ITAENEIK	3.25	15.86	16.78	16.29	16.44
491	gi|9979054	Sec-independent protein translocase protein TatC	MFEDLKPHLQELR	10.06	23.13	22.31	21.43	21.40
492	gi|238058281	septum site-determining protein MinC	IITKNDDILDIK	1.95	17.46	17.52	17.53	17.37
493	gi|8928171	Septum site-determining protein MinD	KGMEVHK	7.25	18.65	18.21	18.42	18.50
494	gi|12230022	Serine acetyltransferase	VLQEDPAAR	2.36	15.83	15.65	16.00	15.99
495	gi|238057970	Serine hydroxymethyltransferase	EELKAMASQFPVYQQPIF	1.23	14.75	13.85	14.35	12.77
496	gi|81555228	Serine/threonine-protein kinase CtkA	SKIIDVAHTR	2.36	11.17	15.04	12.69	15.82
497	gi|62510922	Serine/threonine-protein kinase MARK2	RTELMVSMGYTR	7.97	20.34	19.12	16.74	16.18
498	gi|238065103	Serine--tRNA ligase	FKEDIFK	10.18	23.34	23.33	23.82	22.78
499	gi|122980457	Shikimate dehydrogenase (NADP(+))	TPFQDGKDMLIYQASLSFEK	1.44	12.94	13.46	14.27	10.28
500	gi|254806776	Shikimate kinase	TLKTPHIISTGGGIVMHDNLK	2.23	15.65	16.12	14.89	14.98
501	gi|2492758	short-chain type dehydrogenase/reductase VdlC	EVFSNISAK	4.72	15.63	15.09	14.26	14.10
502	gi|6225606	Signal peptidase I	HYPNAMTKEFMGK	2.22	20.72	16.68	16.00	16.18
503	gi|11387213	Signal recognition particle protein	IVGRLMGAGDIISLAEK	10.68	15.59	16.62	17.05	15.87
504	gi|11386869	Signal recognition particle receptor FtsY	ALLGAGDTFR	2.00	17.21	14.96	14.57	15.03
505	gi|83288342	Small-conductance mechanosensitive channel	IIVIPNGK	1.54	14.73	15.02	15.10	14.40
506	gi|122386820	S-ribosylhomocysteine lyase	KGANGDVIVK	14.24	19.61	19.86	17.24	19.06
507	gi|3334331	SsrA-binding protein	WQIEASK	5.32	14.83	16.52	15.13	15.51
508	gi|2492992	Succinyl-CoA:3-ketoacid coenzyme A transferase subunit A	ITTRSTK	8.55	15.34	16.30	15.11	16.77
509	gi|2492996	Succinyl-CoA:3-ketoacid coenzyme A transferase subunit B	YGESKVK	6.25	17.34	17.95	17.69	18.51
510	gi|238064752	Succinyl-diaminopimelate desuccinylase	IFNPPKEHIK	1.85	14.61	14.35	9.99	13.95
511	gi|226732517	sugar efflux transporter	IIGQMLDWR	1.29	16.49	13.77	16.18	14.60

#	Accession No.	Protein Name	Peptide	MOWSE Score	Cla/Mtz-R	Cla-R	Mtz-R	Sen-S
512	gi|1174379	Superoxide dismutase [Fe]	FKEDFIK	3.89	16.09	15.01	16.45	15.55
513	gi|14423756	Tetraacyldisaccharide 4'-kinase	ITSITNPTK	4.11	16.80	16.53	16.41	16.48
514	gi|7388293	Thiamine-phosphate synthase	ALAVGKLLNNA	1.06	15.31	15.09	15.88	16.11
515	gi|11135057	Thiol peroxidase	MQKVTFK	8.96	18.95	17.14	19.49	17.74
516	gi|7388343	Thioredoxin reductase	GGVKNAVLFEK	2.61	14.74	15.67	13.51	13.89
517	gi|8928478	Threonine synthase	QTFSPAMDILKSSNVER	1.24	15.36	17.27	14.34	16.12
518	gi|238065115	Threonine--tRNA ligase	MPLKEFLSMVESK	2.71	23.03	22.56	20.60	19.26
519	gi|8134530	Thymidylate kinase	IILLLINK	2.62	17.59	17.49	16.28	16.38
520	gi|118574582	Tol-Pal system protein TolB	ISRLK	1.83	15.01	15.27	16.63	16.16
521	gi|74751795	TRAF-interacting protein with FHA domain-containing protein A	LPSSEVVK	4.25	16.03	15.64	16.26	16.08
522	gi|226703494	Transaldolase	ASIPVNATLVFSPKIAR	1.40	15.84	14.45	15.26	15.69
523	gi|238055475	Transcription antitermination protein NusB	KIASSMLEEK	3.95	16.44	15.84	12.77	15.83
524	gi|238058235	Transcription elongation factor GreA	FIEAR	5.07	15.06	14.69	14.93	15.14
525	gi|11387014	Transcription termination factor Rho	ALIVAPPR	3.99	17.45	15.59	15.36	15.33
526	gi|11387009	Transcription termination/antitermination protein NusA	KGLLLELSR	3.06	17.80	17.01	13.15	13.78
527	gi|11387011	Transcription termination/antitermination protein NusG	IQEIIVPTEDIIEVSK	1.29	17.10	18.34	19.25	16.14
528	gi|226734880	transcriptional regulatory protein HPG27_148	WDKMSK	8.30	19.46	16.77	16.43	15.83
529	gi|11136025	transcriptional regulatory protein jhp_0149	IIIRGDYNSFK	2.28	15.61	16.48	16.52	14.22
530	gi|3914010	Transcription-repair-coupling factor	EIIYR	8.17	16.03	16.04	15.84	15.94
531	gi|119371068	Translation initiation factor IF-1	IALGDRVK	1.67	17.79	17.97	17.52	16.87
532	gi|123247016	Translation initiation factor IF-2	DDLNMVQTPKPLNK	5.61	21.04	19.96	19.68	19.88

#	Accession No.	Protein Name	Peptide	MOWSE Score	Cla/Mtz-R	Cla-R	Mtz-R	Sen-S
533	gi|7387798	Translation initiation factor IF-3	INLMKGENHAK	4.22	15.63	15.27	16.08	16.01
534	gi|238056551	Translational regulator CsrA	EAIVSENQK	17.26	23.92	23.67	22.76	22.05
535	gi|3024733	Trigger factor	IVFDLPK	6.07	16.92	17.24	16.83	17.10
536	gi|2501318	Triosephosphate isomerase	ESPSFLK	2.77	14.82	15.70	14.97	16.75
537	gi|226707835	tRNA (guanine-N(1)-)-methyltransferase	IPAPLEYSKGNHAR	7.99	19.35	19.05	19.38	18.01
538	gi|14194955	tRNA (guanine-N(7)-)-methyltransferase	AHLLLQNILSQK	12.80	17.18	17.34	18.93	17.55
539	gi|122386172	tRNA dimethylallyltransferase	HAILNHSK	4.09	17.73	16.26	17.31	17.74
540	gi|123073715	tRNA modification GTPase MnmE	TALENAITELQNAK	2.00	15.25	16.07	14.95	15.12
541	gi|238057732	tRNA pseudouridine synthase A	YLLTKNLK	4.20	17.56	17.43	17.55	16.99
542	gi|226708692	tRNA pseudouridine synthase D	GSYASALLKK	4.69	13.60	15.09	14.37	13.99
543	gi|257096308	tRNA U34 carboxymethyltransferase	SPLEALK	2.00	17.47	15.98	17.15	16.27
544	gi|226700964	tRNA uridine 5-carboxymethylaminomethyl modification enzyme MnmG	APLFSGQIEGIGPR	18.70	25.36	21.07	24.06	20.47
545	gi|61216760	tRNA (Ile)-lysidine synthase	QSLMDL	4.69	15.80	15.46	14.35	14.88
546	gi|229890642	tRNA-2-methylthio-N(6)-dimethylallyladenosine synthase	FTSPHPLHMNDGFLER	1.68	15.29	16.20	13.98	14.47
547	gi|39930913	tRNA-dihydrouridine synthase	NLHAYAKGEMQASAFR	4.48	15.74	14.87	15.43	16.26
548	gi|205371769	tRNA-specific 2-thiouridylase MnmA	NELVVGKK	7.37	18.29	19.34	18.62	16.60
549	gi|7227944	Tryptophan biosynthesis protein TrpCF	DAKAVYK	4.79	16.88	16.87	16.09	16.69
550	gi|7674400	Tryptophan synthase alpha chain	SGVTGASHTLENDASAIIK	2.27	16.98	14.99	14.76	16.29
551	gi|7674399	Tryptophan synthase beta chain	LYLKR	5.74	15.93	16.23	16.00	15.36
552	gi|8039806	Tryptophan--tRNA ligase	VPEPLIAKVGAR	2.69	15.05	15.73	15.01	15.26
553	gi|81555831	Type III pantothenate kinase	SAKILEQPFK	4.63	15.47	0	0	0

#	Accession No.	Protein Name	Peptide	MOWSE Score	Cla/Mtz-R	Cla-R	Mtz-R	Sen-S
554	gi|81341387	Tyrosine recombinase XerH	IYTHFDK	4.35	15.77	16.87	16.77	17.12
555	gi|3024675	Tyrosine--tRNA ligase	MEQKIAIALK	7.51	15.10	14.15	15.38	14.25
556	gi|119371939	UDP-3-O-acylglucosamine N-acyltransferase	ESSKVPK	5.17	16.40	15.70	15.83	16.07
557	gi|14285572	UDP-3-O-acyl-N-acetylglucosamine deacetylase	EFALQK	7.23	14.66	16.19	0	15.14
558	gi|81341218	UDP-4-amino-4,6-dideoxy-N-acetyl-beta-L-altrosamine transaminase	DNPYFTPLHPLLK	25.80	23.84	23.60	23.14	23.25
559	gi|6707717	UDP-N-acetylenolpyruvoylglucosamine reductase	NYDYICDK	15.80	21.07	21.70	21.11	19.68
560	gi|226706308	UDP-N-acetylglucosamine 1-carboxyvinyltransferase	INALGAK	1.66	15.56	15.72	16.12	16.20
561	gi|81341467	UDP-N-acetylglucosamine 4,6-dehydratase (inverting)	VLDTTNAK	3.65	16.41	15.47	16.01	0
562	gi|226694291	UDP-N-acetylglucosamine--N-acetylmuramyl-(pentapeptide) pyrophosphoryl-undecaprenol N-acetylglucosamine transferase	LFEVIRK	9.37	18.79	18.19	18.28	18.52
563	gi|122980513	UDP-N-acetylmuramate--L-alanine ligase	IHFIGIGGIGISGLAK	2.74	15.06	15.00	15.42	16.00
564	gi|118595659	UDP-N-acetylmuramoylalanine--D-glutamate ligase	NQKIHLIVGGDIK	2.35	15.17	15.13	14.84	16.15
565	gi|8134585	UDP-N-acetylmuramoyl-L-alanyl-D-glutamate--2,6-diaminopimelate ligase	KTALLGTR	11.23	15.07	15.63	15.41	15.49
566	gi|54042417	Universal stress protein HP_0031	QFEDAFKK	1.15	18.70	18.94	19.24	18.96
567	gi|11387383	UPF0026 protein jhp_0109	AKENLPIVFGPVLSR	8.72	15.26	15.69	15.26	14.54
568	gi|6686220	UPF0093 membrane protein jhp_1377	LALVVLLLIYHFYCKK	1.28	15.60	15.97	16.80	14.02
569	gi|238058884	UPF0102 protein HPG27_782	FFNNK	6.62	16.66	16.01	16.52	16.12
570	gi|18201987	UPF0174 protein HP_1587	QTLGHXACYVVGKVALK	3.20	16.87	15.58	18.36	16.06
571	gi|18201988	UPF0174 protein HP_1588	KSLQIESI	1.14	18.66	18.65	17.72	17.98

#	Accession No.	Protein Name	Peptide	MOWSE Score	Cla/Mtz-R	Cla-R	Mtz-R	Sen-S
572	gi|122386748	UPF0323 lipoprotein HPAG1_0235	VLSDEEIQKLIK	4.01	23.26	19.93	19.90	21.60
573	gi|226701181	UPF0323 lipoprotein HPG27_212	SQNSFSKSAPSASSMGGASK	2.54	17.13	14.26	14.92	14.97
574	gi|298351989	UPF0763 protein HPG27_626	KISANEMLLELEK	21.36	22.96	23.10	23.38	23.24
575	gi|298352037	UPF0763 protein HPKB_0680	LINSLTTQK	4.52	17.03	16.63	16.45	16.85
576	gi|238058170	Uracil-DNA glycosylase	EQELPVAMGLSFSVEK	1.04	16.68	15.81	18.41	18.01
577	gi|2507525	Urease accessory protein UreE	LGVQNR	5.45	16.21	15.71	16.03	16.67
578	gi|226731432	Urease accessory protein UreF	SVGIPPK	12.90	18.52	17.39	18.81	17.56
579	gi|2507528	Urease accessory protein UreG	RNALLED	3.62	17.02	17.23	16.03	16.68
580	gi|2507530	Urease accessory protein UreH	MNTYAQESKLR	8.15	17.10	17.21	16.96	17.13
581	gi|254790718	Urease subunit alpha	SVELIDIGGSR	12.00	15.54	13.80	13.81	14.38
582	gi|81529053	Urease subunit beta	IKISR	2.18	19.52	18.64	17.88	17.16
583	gi|8928320	Uridylate kinase	DPNKFK	3.36	16.70	16.14	16.32	16.42
584	gi|8928083	Uroporphyrinogen decarboxylase	VGVYK	5.56	16.40	15.82	16.10	16.86
585	gi|7388356	UvrABC system protein A	IERPK	4.08	16.64	16.01	16.05	16.01
586	gi|8134789	UvrABC system protein B	TTQSMQK	3.85	15.77	15.22	15.39	15.52
587	gi|226698353	UvrABC system protein C	AVLVK	1.33	21.92	18.79	20.35	17.34
588	gi|2499107	Vacuolating cytotoxin autotransporter	NDKNESAK	9.96	18.00	17.19	0	0
589	gi|11135055	Valine--tRNA ligase	VWEWK	4.20	15.64	15.69	15.03	14.65
590	gi|2499906	Zinc metalloprotease	SSGGLR	19.88	19.96	19.68	18.05	18.72
591	gi|2495696	zinc metalloprotease HP_0258	LIMGSSSVK	2.84	15.79	16.45	16.23	16.05
592	gi|12230846	zinc metalloprotease jhp_0242	EIVAR	17.08	22.47	22.09	21.01	20.09

BIOGRAPHY

Name	Miss Suthathip Kittisenachai
Date of Birth	June 9, 1979
Educational Attainment	Academic Year 1999: Bachelor of Science (Biology), Faculty of Science, Mahidol University.
Work Position	2008-Present: Assistant Researcher in Biotechnology of NSTDA.

Publications

1. Manochan S., Puthong S., Gamnarai P., Roytrakul S., **Kittisenachai S.**, Kangsadalampai S., Rojpibulstit P. Hep 88 mAb induced ultrastructure alteration through apoptosis like programme cell death in hepatocellular carcinoma. Journal of Medical Association of Thailand. 2011; 94(7): 109-16.

2. Aroonluk S., Roytrakul S., Yingchutrakul Y., **Kittisenachai S.**, Jantasuriyarat C. Identification and characterization of glycoproteins during oil palm somatic embryogenesis. Agriculture and Natural Resources. 2018; 52(5): 430-438.

3. Talakhun W., Roytrakul S., Phaonakrop N., **Kittisenachai S.**, Khamnamtong B., Klinbunga S., Menasveta P. 2012. Identification of reproduction-related proteins and characterization of the protein disulfide isomerase A6 cDNA in ovaries of the giant tiger shrimp *Penaeus monodon*. Comparative Biochemistry and Physiology - Part D: Genomics and Proteomics. 2012; 7(2): 180-90.

4. Abere B., Wikan N., Ubol S., Auewarakul P., Paemanee A., **Kittisenachai S.**, Roytrakul S., Smith D. R. 2012. Proteomic analysis of chikungunya virus infected microglial cells. PLoS ONE. 2012; 7(4): e34800.

5. Wintachai P., Wikan N., Kuadkitkan A., Jaimipuk T., Ubol S., Pulmanausahakul R., Auewarakul P., Kasinrerk W., Weng W. Y., Panyasrivanit M., Paemanee A., **Kittisenachai S.**, Roytrakul S., Smith D.R. Identification of prohibitin as a Chikungunya virus receptor protein. Journal of Medical Virology. 2012; 84: 1757-1770.

6. Klinbunga S., Petkorn S., **Kittisenachai S.**, Phaonakrop N., Roytrakul S., Bavornlak Khamnamtong B., Menasveta P. Identification of reproduction-related proteins and characterization of proteasome alpha 3 and proteasome beta 6 cDNAs in testes of the giant tiger shrimp *Penaeus monodon*. Molecular and Cellular Endocrinology. 355(2012): 143-152.

7. Rojpibulstit P., **Kittisenachai S.**, Puthong S., Manochantr S., Gamnarai P., Jitrapakdee S., Roytrakul S. Hep88 mAb-initiated paraptosis-like PCD pathway in hepatocellular carcinoma cell line through the binding of mortalin (HSPA9) and alpha-enolase. Cancer Cell International. 2014; 14: 69.

8. Wikan N., Khongwichit S., Phuklia W., Ubol S., Thonsakulprasert T., Thannagith M., Tanramluk D., Paemanee A., **Kittisenachai S.**, Roytrakul S., Duncan R S. Comprehensive proteomic analysis of white blood cells from chikungunya fever patients of different severities. Journal of Translational Medicine. 2014; 12: 96.

9. Panichakul T., Ponnikorn S., Roytrakul S., Paemanee A., **Kittisenachai S.**, Hongeng S., Udomsangpetch R. *Plasmodium vivax* inhibits erythroid cell growth through altered phosphorylation of the cytoskeletal protein ezrin. Malaria Journal. 2015; 14:138.

10. Mitupatum T., Aree K., **Kittisenachai S.**, Roytrakul S., Puthong S., Kangsadalampai S., Rojpibulstit P. Hep88 mAb-mediated paraptosis-like apoptosis in HepG2 cells via downstream upregulation and activation of Caspase-3, Caspase-8, and Caspase-9. Asian Pacific Journal of Cancer Prevention. 2015; 16(5): 1771-1779.

11. Akekawatchai C., Roytrakul S., **Kittisenachai S.**, Isarankura-Na-Ayudhya P., Jitrapakdee S. Protein profiles associated with anoikis resistance of metastatic MDA-MB-231 breast cancer cells. Asian Pacific Journal of Cancer Prevention. 2016; 17(2): 581-590.

12. Mitupatum T., Aree K., **Kittisenachai S.**, Roytrakul S., Puthong S., Kangsadalampai S., Rojpibulstit P. mRNA Expression of Bax, Bcl-2, p53, Cathepsin B, Caspase-3 and Caspase-9 in the HepG2 cell line following induction by a novel monoclonal Ab Hep88 mAb: cross-talk for paraptosis and apoptosis. Asian Pacific Journal of Cancer Prevention. 2016; 17(2): 703-12.

13. Likitpruekpaisarn T., Roytrakul S., **Kittisenachai S.**, Temviriyanukul P., Butryee C. Shortgun proteomics analysis of mouse colon treated with *Eryngium fotidum Linn*. extracts. Thai Journal of Toxicology. 2016; 31(2): 70-83.

14. Sornlake W., Rattanaphanjak P., Champreda V., Eurwilaichitr L., **Kittisenachai S.**, Roytrakul S., Fujii T., Inoue H. Characterization of cellulolytic enzyme system of *Schizophyllum commune* mutant and evaluation of its efficiency on biomass hydrolysis. Bioscience, Biotechnology, and Biochemistry. 2017; 81(7):1289–1299.

15. Paemanee A., Sornjai W., **Kittisenachai S.**, Sirinonthanawech N., Roytrakul S., Wongtrakul J., Duncan R. S. Nevirapine induced mitochondrial dysfunction in HepG2 cells. Scientific reports. 2017; 7: 9194.

16. Jirakkakul J., Roytrakul S., Srisuksam C., Swangmaneecharern P., **Kittisenachai S.**, Jaresitthikunchai J., Punya J., Prommeenate P., Senachak J., So L., Tachaleat A., Tanticharoen M., Cheevadhanarak S., Wattanachaisaereekul S., Amnuaykanjanasin A. Culture degeneration in conidia of *Beauveria bassiana* and virulence determinants by proteomics. Fungal Biology. 2018; 122(2-3): 156-171.

17. Aksorn N., Roytrakul S., **Kittisenachai S.**, Leelawat K., Chanvorachote P., Topanurak S., Hamano S., Lek-Uthai U. Novel potential biomarkers for *Opisthorchis viverrini* infection and associated cholangiocarcinoma. In Vivo. 2018: 32(4): 871–878.

18 Singrang N., **Kittisenachai S.**, Roytrakul S., Svasti J., Kangsamaksin T. NOTCH1 regulates the viability of cholangiocarcinoma cells via 14-3-3 theta. Journal of Cell Communication and Signaling. 2019; 13(2): 245-254.

19. Sanguansermsri P., Jenkinson H.F., Thanasak J, Chairatvit K., Roytrakul S., **Kittisenachai S.**, Puengsurin D., Surarit R. Comparative proteomic study of dog and human saliva. PLoS One. 2018; 4: 13(12).

20. Mano C., Jariyapan N., Sor-Suwan S., Roytrakul S., **Kittisenachai S.**, Tippawangkosol P., Somboon P. Protein expression in female salivary glands of pyrethroid-susceptible and resistant strains of *Aedes aegypti* mosquitoes. Parasites Vectors. 2019; 12:111.

21. Stress. Li R., Chaicherdsakul T., Kunathigan V., Roytrakul S., Paemanee A., **Kittisenachai S**. Shotgun proteomic analysis of germinated rice (*Oryza sativa L.*) under salt stress. Applied Science and Engineering Progress. 2020; 13(1): 76–85.

22. Ploypetch S., Roytrakul S., Phaonakrop N., **Kittisenachai S.**, Leetanasaksakul K., Pisamai S., Kalpravidh C., Rungsipipat A., Suriyaphol G. In-gel digestion coupled with mass spectrometry (GeLC-MS/MS)-based salivary proteomic profiling of canine oral tumors. BMC Veterinary Research. 2020; 16(1):335.

23. **Kittisenachai S.**, Rojpibulstit P., Vilaichone R., Gamnarai P., Phaonakrop N., Suealek N. FBPAII and rpoBC, the Two Novel Secreted Proteins Identified by the Proteomic Approach from a comparative study between antibiotic-sensitive and antibiotic-resistant *Helicobacter pylori*-associated gastritis strains. Infection and Immunity. 2021; 89(6): e00053-21.